11-7-2015

Advanced Organic Ligands for Protecting Metal Nanoparticles

Jonathan Yu
University of Windsor

Advanced Organic Ligands for Protecting Metal Nanoparticles

By

Jonathan Ka-Wing Yu

A Thesis
Submitted to the Faculty of Graduate Studies
through the Department of Chemistry and Biochemistry
in Partial Fulfillment of the Requirements for
the Degree of Master of Science
at the University of Windsor

Windsor, Ontario, Canada

2015

Advanced Organic Ligands for Protecting Metal Nanoparticles

by

Jonathan Yu

APPROVED BY:

_____

C. Weisener
Great Lakes Institute for Environmental Research

_____

T. Carmichael
Department of Chemistry & Biochemistry

_____

S.H. Eichhorn, Advisor
Department of Chemistry & Biochemistry

July 30, 2015

DECLARATION OF CO-AUTHORSHIP

The project design in Chapter 2 was created by Dr. S. Holger Eichhorn. The synthetic experiments were performed by the author. All experiments and characterization of compounds were performed by the author with the exception of mass spectrometry experiments. Synthesis of the aniline derivatives in section 2.3 and 2.4 were reported previously in the Eichhorn Group (J. Yu-410 Thesis) by the author. Dr. Janeen Auld conducted MALDI mass spectrometry experiments. The synthesis of section 2.8 was designed by Dr. S. Holger Eichhorn and Omar Zghal (O. Zghal-410 Thesis). The synthesis and optimization was performed by the author.

I hereby certify that I am the sole author of this thesis and that no part of this thesis has been published or submitted for publication.

I certify that, to the best of my knowledge, my thesis does not infringe upon anyone's copyright nor violate any proprietary rights and that any ideas, techniques, quotations, or any other material from the work of other people included in my thesis, published or otherwise, are fully acknowledged in accordance with the standard referencing practices. Furthermore, to the extent that I have included copyrighted material that surpasses the bounds of fair dealing within the meaning of the Canada Copyright Act, I certify that I have obtained a written permission from the copyright owner(s) to include such material(s) in my thesis and have included copies of such copyright clearances to my appendix.

I declare that this is a true copy of my thesis, including any final revisions, as approved by my thesis committee and the Graduate Studies office, and that this thesis has not been submitted for a higher degree to any other University or Institution.

ABSTRACT

Organic monolayer protected metal nanoparticles have been utilized in many different fields such as catalysis, drug delivery, and sensor chemistry. However, these nanomaterials are prone to increase in size consequently losing its function at the nanoscale. The stability these nanoparticles have been a great interest of research.

This thesis focuses on the synthesis of a novel cross-linkable ligand for the protection of metal nanoparticles.

Chapter 1 reviews key concepts of nanoparticles, its usefulness in applications, some of the stabilizing strategies employed, and the scope of the thesis project.

Chapter 2 describes the synthetic attempts and optimization of the novel cross-linkable ligand. In addition, its characterization data is also included. Section 2.8 also highlights another fully synthesized novel hydrophobic ligand.

Chapter 3 contains the summary of the work and closing remarks. Future works is also included to describe the prospects of the synthesis of the novel ligand.

Chapter 4 entails the experimental data and supplementary information.

ACKNOWLEDGEMENTS

I would like to thank Dr. S. Holger Eichhorn for this great opportunity in learning new organic synthesis skills and conducting research in his group. His ongoing support, positive attitude, and strive for excellence has motivated me greatly during my masters studies.

I would like to acknowledge Dr. Janeen Auld for performing mass spectrometry experiments.

I would like to thank Dr. Carmichael for being my departmental examiner and spending the time to read my thesis. I would like to extend my gratitude to Dr. Weisener for being my external examiner and reviewing my thesis.

I would like to thank some members of the Eichhorn Group: Ayodele Gbadamosi and Sarah Salloum for being great lab mates. I would like to acknowledge Hi Taing for his leadership in the group, synthetic help, and demonstrating how to use polarized optical microscopy. I would like to also thank past and present group members: Sam, Esmaeil, El-Mahdy, Jake, Andre, Vanessa, Serxho, Rocky, Michael, and Mayce.

I would like to thank my parents and siblings for their continuous support during my two-year study period.

TABLE OF CONTENTS

LIST OF TABLES

LIST OF FIGURES

LIST OF SCHEMES

LIST OF APPENDICES

APPENDIX A: ^{1}H and ^{13}C NMR Assignments and MALDI MS Spectra

APPENDIX B: Polarized Optical Microscopy Images

LIST OF ABBREVIATIONS/SYMBOLS/TERMS

^{1}H NMR= Proton Nuclear Magnetic Resonance Spectroscopy

^{13}C NMR= Carbon Nuclear Magnetic Resonance Spectroscopy

AFM = Atomic Force Microscopy

Å = angstrom

AcCl = acetyl chloride

Ac_2O = acetic anhydride

Al_2O_3 = activated aluminum oxide

AuNPs = gold nanoparticles

br = broad

$CDCl_3$ = deuterated chloroform

$CHCl_3$ = chloroform

CD_3OD = deuterated methanol

°C = degrees Celsius

d = doublet

dd = doublet of doublets

Δ= heat

Deprotection = removal of protecting group to retrieve the pre-existing functional group

DCC = N, N'-dicyclohexylcarbodiimide

DCM = dichloromethane

DHLA = dihydrolipoic acid

DMAP = dimethyl aminopyridine

DMF = dimethylsulfoxide

DTT = dithiothreitol

DSC = differential scanning calorimetry

δ = chemical shift

eq = equivalent

EtoAc = ethyl acetate

EtOH = ethanol

Et_2O = diethyl ether

g = grams

GSH = glutathione

h = hours

HCl = hydrochloric acid

Hex = hexanes

HNO_3 = nitric acid

Hz = hertz

IR = infrared spectroscopy

J = coupling constant

K_2CO_3 = potassium carbonate

K = kelvin

m = multiplet

MALDI = matrix-assisted laser desorption/ionization

Min = minutes

mg = milligram

mL = milliliter

MNPs = metal nanoparticles

MS = mass spectrometry

m/z = mass-to-charge ratio

NPs = nanoparticles

POM = polarizing optical microscopy

ppm = parts per million

Protection = to mask a functional group which may interfere with the chemical selectivity.

q = quartet

r.t. = room temperature

rb = round bottom

s = singlet

SAM = self-assembled monolayer

SAXS = small angle x-ray scattering

t = triplet

TEA = trimethylamine

TEM = transmission electron microscopy

TGA = thermal gravimetric analysis

THF = tetrahydrofuran

TLC = thin-layer chromatography

UV-vis = ultraviolet-visible

XRD = x-ray diffraction

CHAPTER 1: INTRODUCTION

1.1. Introduction to Nanoparticles

Nanoparticles (NPs) are close to spherical nanomaterials typically 100 nm or less in diameter. In comparison to bulk materials, NPs possess a higher fraction of atoms on the surface than the interior volume and has a much smaller volume.[1] As outlined in Whiteside's review[2], the percentage of surface atoms drastically increases when the particles progressively reach smaller sizes. For instance, a 1000 nm diameter particle has 0.2% of the atoms residing on the surface while 88% of the atoms makeup the interface for a 1.3 nm diameter NP. Consequently, the high surface area to volume ratio of NPs alters its electronic, optical, and physical properties.

The electronic structure of NPs is different from bulk materials. As shown in Rao's review[3], the electrons of NPs become confined resulting in quantized (discrete) energy levels rather than having continuous energy levels for bulk materials (**Figure 1**). The lower energy valence band and the higher energy conductance levels also become discrete. The electronic transition from the highest valence level to the lowest conductance level is known as the band gap.[4] Larger band gaps are observed for smaller NPs. In addition, the difference in energy levels between successive energy levels is the Kubo gap (δ).[3] For metal nanoparticles, electrons reside in the conductance bands as the thermal energy exceeds the Kubo energy gap.[5]

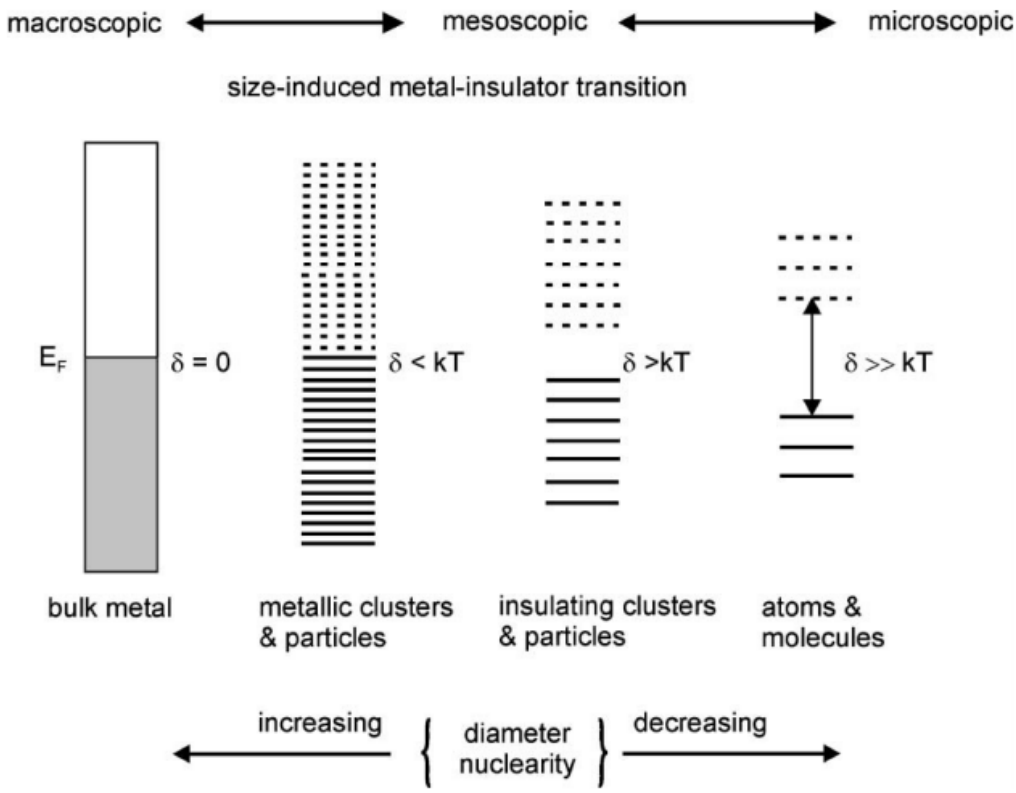

Figure 1. Electronic transition states become quantized as particle size decreases. Solid line = valence bands; dotted lines = conductance bands. Reproduced from [5] from The Royal Society of Chemistry. Original source: [On the Size Induced Metal-Insulator Transition in Clusters and Small Particles/ P. P. Edwards, R. L. Johnston and C. N. R. Rao ed. P. Braunstein, L. A. Oro, P. R. Raithby /Metal Clusters in Chemistry, Vol. 3, Copyright © 1999 Wiley, Weinheim].[6]

A consequence of quantized energy levels of NPs is the existence of new optical properties. Metal NPs smaller than the de Broglie wavelength have free “d” electrons in the conductance band residing on the surface of the core.[1] The electric field of visible light interacts with the free electrons inducing oscillation on the surface (**Figure 2**) which is known as the surface plasmon resonance (SPR). Upon relaxation, these NPs exhibit bright colours in the visible region. As the size of NPs increases, the Kubo gap decreases which causes a red-shift in the absorption spectrum, emitting wavelengths near the blue region and eventually the infrared regime like that of bulk materials.

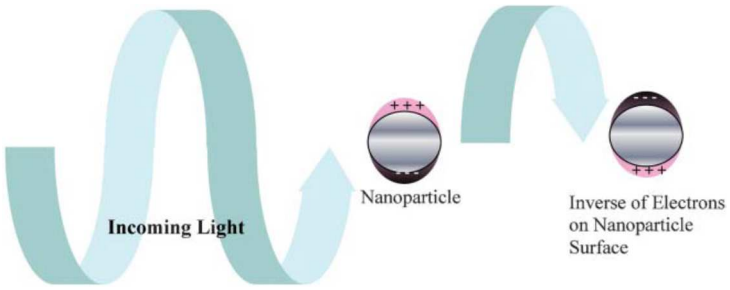

Figure 2. Visible light interacts with the electrons on the surface of the NPs, causing it to resonate and produce its surface plasmon resonance. Reproduced from [1] with permission of The Royal Society of Chemistry.

In addition, NPs display differences in physical properties compared to bulk materials. The melting point of gold NPs decreases as it size diminishes.[5,6] Buffat[7] and Sambles demonstrated the correlation between the size of gold NPs and its melting point (**Figure 3**).[8] NPs between 0-10 nm have decreasing melting points for smaller particle sizes while the melting point gradually plateaus when its diameter is greater than 10 nm. This is mainly due to the increase in surface atoms which are much more unstable with higher surface energy than bulk atoms.[5] The poorer stability on the surface will lead to decreased melting temperatures.

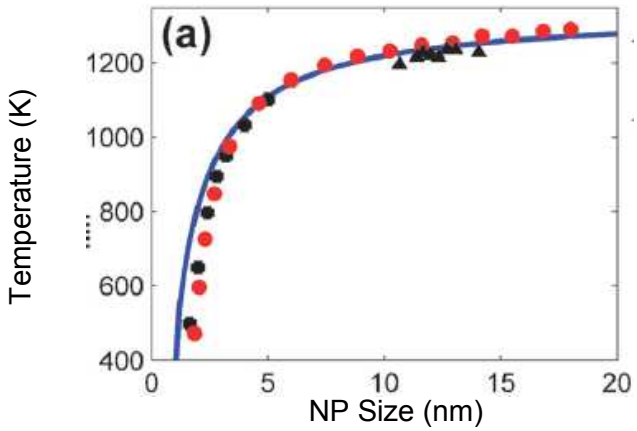

Figure 3. Melting temperature of free gold NPs. Solid circles[7] and solid triangles from J. R. Sambles, *Proc. R. Soc. London, Ser. A*, 1971, *324*, 339. Reproduced from [8] with permission of the PCCP Owner Society.

These nanostructures are usually comprised of two main components: a core and molecules that bind to the surface through physisorption[9] (intermolecular forces, i.e. van der waals) or chemisorption[10] (chemical bonds, i.e. covalent). The NP core can be made from many different materials such as metals[11], metal oxides[12], magnetic compounds[13], semiconductors[14], polymers[15], organic molecules[16], and elements from the p-block[17]. The core can be tuned into different morphologies such as colloidal, octahedral[18], or cubic (**Figure 4**).[19,20] Molecules that form an outer-layered shell play vital roles which will be discussed in the sections 1.1.2. The composition of these ligands or capping agents are made from organic and inorganic materials as discussed in a review by Ghosh Chaudhuri *et al.*[21] For instance, organic shells can be composed of silica oxide[12], small molecular weight ligands, or polymers[22]. Inorganic shells are made from metals (Ag[23], Co[24], Pd[25]), metal oxides (Fe_2O_3[26]) or semiconductors (CdS[27] and CdSe[28]).

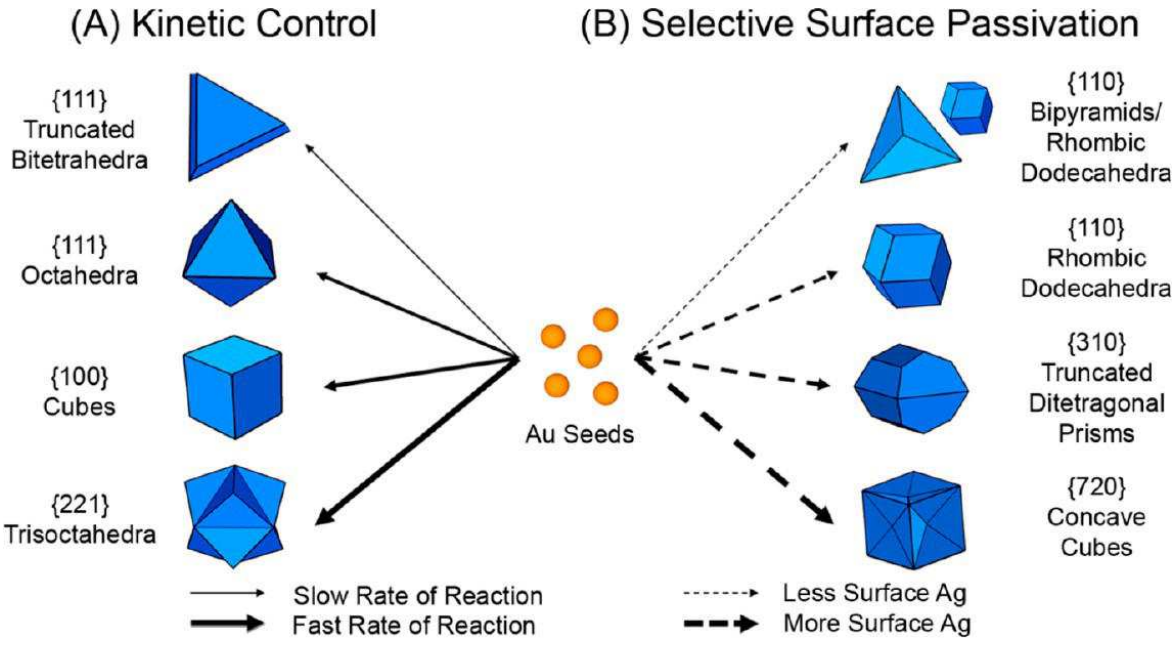

Figure 4. Gold NPs can be synthetically tuned into various shapes and sizes by silver ion absorbates.[29] Reprinted with permission from Langille, M. R., Personick, M. L., Zhang, J. *et al*. *J. Am. Chem. Soc.*, **2012**, *134* (35), 14542–14554. Copyright 2012 American Chemical Society.

1.1.1. Metal NPs

Metal nanoparticles (MNPs), such as gold[30], silver[31], palladium[32], platinum[33], hold many advantages over other core compositions due to their straightforward synthesis[34] and tunability in size and morphology.[19] Gold is one of the most commonly used metals for NPs because they can show good conductivity[35], show interesting optical properties for analytical methods[36], and their inertness to oxidation and non-toxicity makes them good candidates for emerging biological/medicinal materials.[2]

1.1.2. Self-Assembled Monolayers on Metal NPs

Organic ligands are usually comprised of three components (**Figure 5**): the head group, the spacer region, and the terminal moiety.[2] The head group is the primary contact between the metal surface of NPs and the ligand. The spacer region is the bridge between the head group and the terminal group. The terminal group comes in contact with the external environment (i.e. Solvents, adjacent nanoparticles).

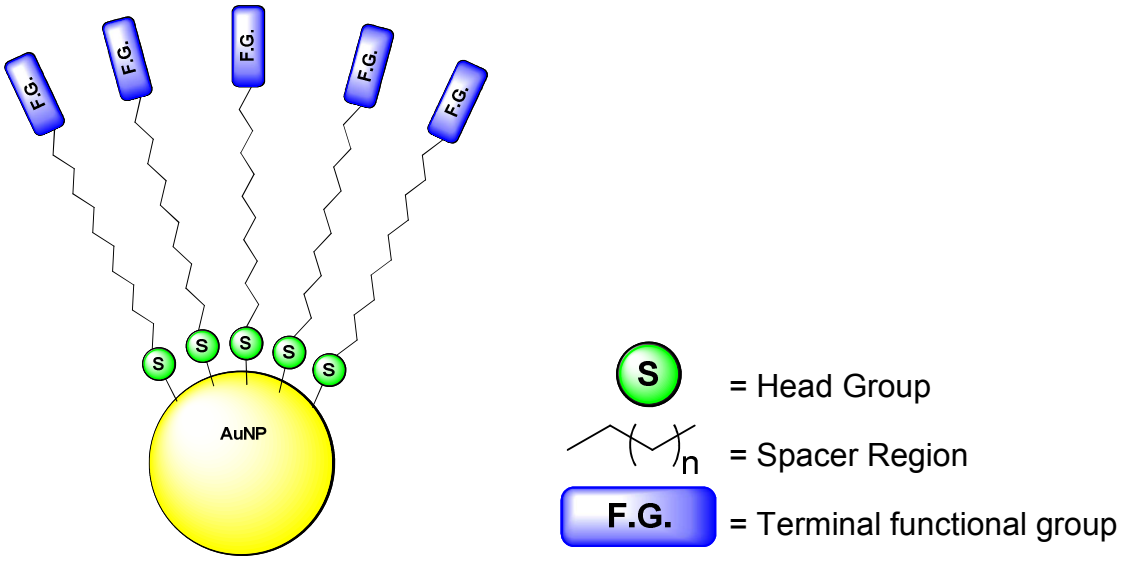

Figure 5. Nanoparticles consist of a core protected by organic ligands. Ligands are composed of the head group (green), spacer region, and terminal group (blue).[2]

Self-assembly is defined as the process of spontaneous rearrangement of molecules into an ordered periodic structure.[2] In the context of NPs, ligands form a thin film or monolayer on the surface of a metal core, known as self-assembled monolayers (SAMs). SAMs NPs are synthesized via bottom-up approach and involve two major events: nucleation and growth of the particles. The first step deals with the reduction of a metal precursor with a reducing agent. The latter step is the capping of the surface of NPs with ligands to control its growth. Readers interested on NPs assembly procedures can refer to Astruc's review.[34]

Organic protected ligands of NPs have imperative roles in controlling the morphology of the NPs during synthesis, providing functionality through its terminal group, and maintaining stability.[37]

Ligands have preferential binding to different faces of the metal core. This selective binding to certain facets causes growth retardation and elongation at unprotected sites resulting in an anisotropic nanoparticle. For instance, sodium dodecyl sulfate has shown to bind more readily to {110} and {100} facets which slows their growth and allowing for {111} facets to form pentatwinned ends ultimately forming pentagonal and hexagonal shaped gold NPs.[38]

Ligands also serve the role of bringing physical properties (solubility, wettability) to the entire NP through its terminal group. For example, hydrophilic terminal groups such as alcohols or carboxylic acids render the particles soluble in polar solvents. In the presence of hydrophobic environments, these NPs will precipitate from solution.

Lastly, ligands provide stability to the metal core. Its high surface area to volume ratio is accompanied with high surface free energy which is indicative of instability. The surface free energy is stabilized when molecules reduce the surface area. Uncontrolled

binding of molecules (i.e. contaminants, adjacent nanoparticles) absorbing to the metal core may result in larger particles with reduced overall surface area called aggregation.[39] These aggregates have crystal facets of the NPs in different directions resulting in grain boundaries[40]. They are also amorphous and the loss of surface area renders the surface of NPs dysfunctional for further surface functionalization. In addition, its growth into larger assemblies resembles bulk materials and relinquishes its properties at the nanoscale. Particle aggregation also results in polydispersity (distribution of varying particle sizes) and larger numbers of defects that complicate the study and interpretation of properties of NPs.[41,42] Thus, it is vital to provide NPs with stable ligands on its surface to circumvent aggregation and subsequently coalescence into larger particles.[40]

1.2. Applications of Metal NPs

Organic ligand can be synthetically engineered into specific structures and functionalized on metal NPs. Properties from both ligand and the metal core are utilized in a myriad of applications.

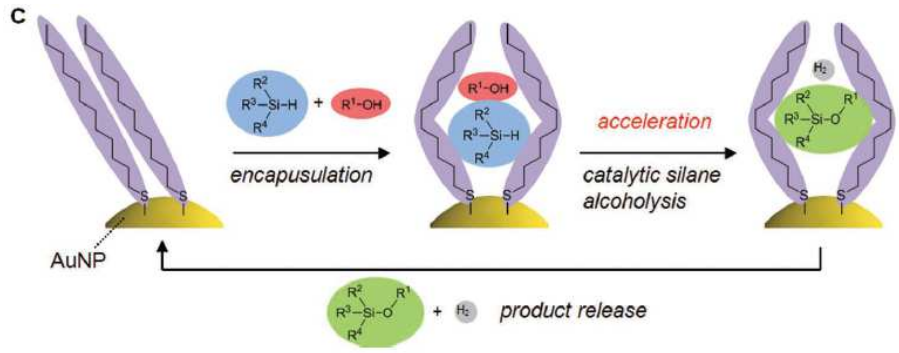

Figure 6. Alkanethiol gold NPs catalyzes the butanolysis of dimethylphenylsilane on the monolayer.[43] Enhanced Catalytic Activity of Self-Assembled-Monolayer-Capped Gold Nanoparticles, Taguchi T. *et al*., *Advanced Materials 24 (48).* Copyright (c) 2012 WILEY-VCH Verlag GmbH & Co. KGaA, Weinheim.

MNPs as nanocatalytic systems have been written in many reviews[44,45,46]. The monolayer of gold NPs can serve as a catalytic site. Taguchi *et al.* demonstrated that alkanethiol protected gold NPs catalyzed the n-butanolysis of dimethylphenylsilane (**Figure 6**). High turnover frequency (number of reagents reacting per substrate per time[47]) and turnover number of 55 000/h and 200 000 are observed respectively.[43] The hydrophobic monolayer promotes stronger binding of longer alkyl chain alcohols due to hydrophobic intermolecular forces.

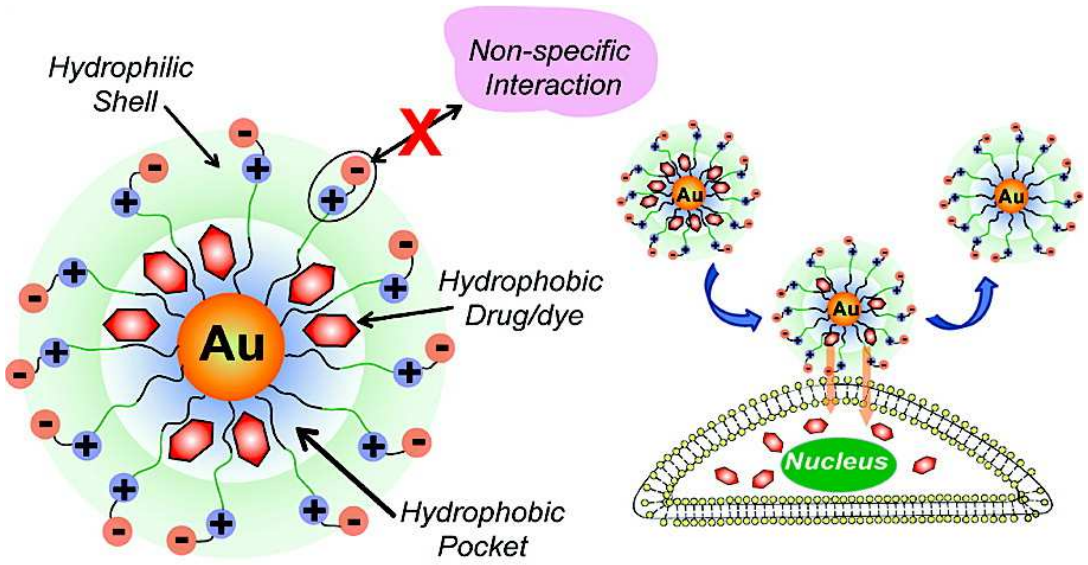

Figure 7. Gold NPs protected by ligands with hydrophobic and hydrophilic domains act as drug delivery transporters to breast cancer cells.[48] Reprinted with permission from Chae Kyu Kim, Partha Ghosh, Chiara Pagliuca, *et al. J. Am. Chem. Soc.*, 2009, *131* (4), 1360–1361. Copyright 2009 American Chemical Society.

Gold NPs are utilized as drug delivery systems.[21,49,50] Rotello's group functionalized gold NPs with a ligand containing an interior hydrophobic alkanethiol and an exterior hydrophilic tetra(ethylene glycol) with terminal zwitterionic groups (**Figure 7**).[48] The hydrophobic alkanethiol facilitates the incorporation of hydrophobic drugs such as tamoxifen (TAF) and β-lapachone (LAP). The charged terminal region permits the NPs to be compatible in aqueous conditions of the body. These gold NPs successfully delivers the drugs to breast cancer cells without being encapsulated into the cells.

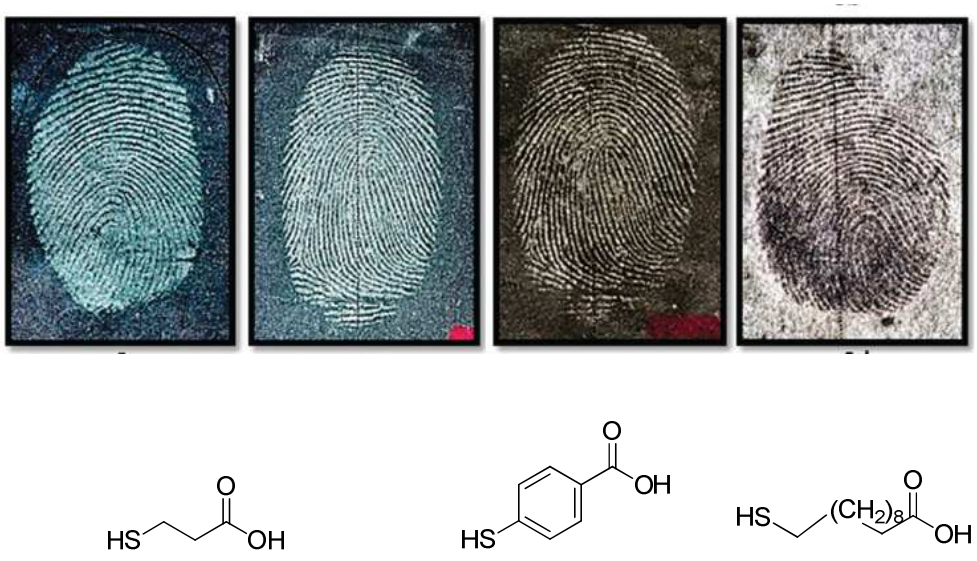

Figure 8. a) 3-mercaptopropionic acid b) 3-meracptopropionic acid (14 months), c) 4-mercaptobenzoic acid, d) 11-mercaptoundecanoic acid. Adapated from [51] with permission of The Royal Society of Chemistry.

MNPs have been extensively used in sensor chemistry. Recently, Shenawi *et al.*[51] showed that gold NPs protected by thiolate ligands with terminal carboxylic acids can be used in reverse fingerprint sensing (**Figure 8**). These NPs will bind to the hydrophilic cellulose of paper via hydrogen bonding and not to the oily sebum rich fingerprints. Upon precipitating in silver solution, the NPs stain the paper resulting in a negative reading of the fingerprints. Ligands with increasing alkyl chain lengths show slight affinity for the sebum fingerprints due to hydrophobic interactions and a positive reading is achieved (Figure 8d). The length of the alkyl spacer is tuned to render different fingerprint readings.

1.3. Stability of SAMs

The longevity of these functionable NPs ultimately relies on the stability of the monolayer shell. The durability of these SAMs depends on the bond strength of the ligand's head group with the surface, the intermolecular interactions between ligands within the monolayer, and the terminal group's interaction with the external environment. The ligands of the monolayer are mobile on the surface[52] and susceptible to desorption when different stresses are applied (i.e. heat, chemicals, in solution) or simply aging over time[53]. The extent of monolayer decomposition subsequently causes growth of the particle core, which can be characterized via microscopy (AFM, TEM, SAXS) and spectroscopically (UV-vis, XRD).[54] Readers should consult the review on the stability of NPs in *Colloids Surf., A*. **2011**, *390*, 1-19.

1.3.1. Head Group Effects on NPs Stability

The head group is the primary contact of ligands with the surface, thus should possess high affinity for the metal surface. The strength of this bond affects the dynamics of ligand mobility (ie. chemisorption, physisorption) and influences the overall monolayer stability. Many different head groups (amines, thiolates, N-heterocyclic carbenes (NHCs), phosphines, carboxylates) have shown to coat metal NPs, but possess varying degrees of stability. Phosphine (Schmid's ligand) and citrate ligands are usually labile and protect gold NPs weakly. They bind electrostatically and can be easily displaced upon introducing stronger binding ligands or altering the ionic strength of the solution. NHC ligands protected gold NPs were shown to be stable in the solid state at temperatures below ambient conditions. Despite having a high calculated bond energy of 150 kJ/mol, which is 25 kJ/mol more stable than thiol-gold bonds,[55] a complex is

formed and aggregation in solution occurs after 12 h. The instability may be caused by the steric hindrance from the tert-butyl substituents on the NHC preventing ligand packing on the core (**Figure 9**).[56]

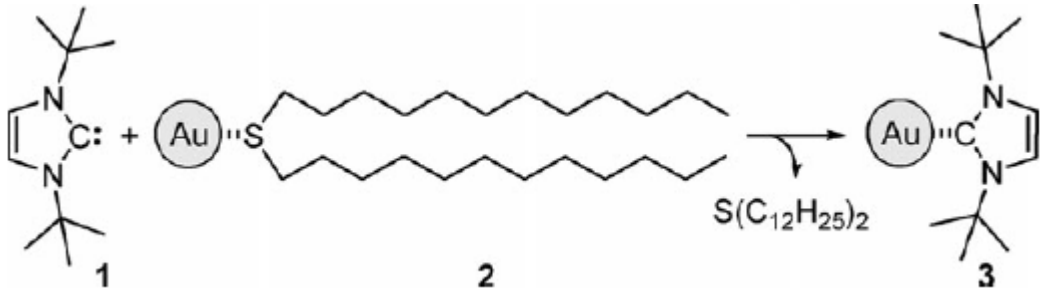

Figure 9. NHC ligand (1) undergoes ligand exchange with didodecylsulfide protected gold NPs (2) and forms a new monolayer (3). Reproduced from [56] with permission of The Royal Society of Chemistry (RSC) on behalf of the European Society for Photobiology, the European Photochemistry Association and the RSC.

Alkyl amine ligands protected gold NPs have been demonstrated by Heath and coworkers.[57] Dodecylamine-capped gold NPs in solution are relatively unstable as the NPs grow from 26 to 300 Å in 4 days compared to being in the solid state where they are stable for months. DSC (differential scanning calorimetry) shows an endothermic peak around 110 °C. TGA (thermogravimetric analysis) indicates a mass loss at 250 °C. Another similar study shows the thermal properties of alkyl amines (dodecyl- and octadecylamine) have two binding modes (electrostatically or covalently) with two distinct weight loss temperatures at approximately 250-260 and 500-520 °C. Amine capped gold NPs are unstable to ligand exchange to ethylenediamine (EDA) as much aggregation was observed.[58]

Chalcogen based ligands (S, Se[23], Te[59,60]) have been shown to protect gold NPs. Although Se-Au and Te-Au bonds may be stronger than S-Au (due to similar electronegativity with gold), these ligands are air-sensitive[60], have a weaker chalcogen-carbon bond[61] compared to gold-sulfur bond, and leads to decomposition. Sulfur binding groups are shown to form relatively strong bonds with gold (~125 kJ/mol[62]) compared to other binding groups. Dodecanethiol protected gold NPs begin to aggregate in air in the solid state after two weeks.[53] Multiple dispersions in solution and drying also promote aggregation. Its thermal stability is higher than amine ligands by 10 °C according to TGA and have a higher onset temperature by 40 °C on DSC.[57]

1.3.2. Multidentate

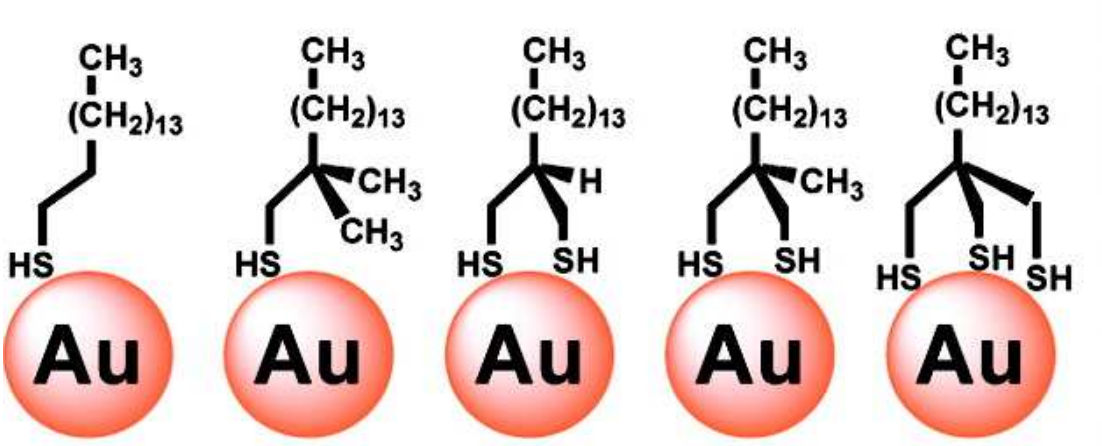

Figure 10. Multidentate binding of hexadecanethiolates enhances the thermal stability of gold NPs.[63] Adapted with permission from Shishan Zhang, Gyu Leem, La-ongnuan Srisombat, *et al. J. Am. Chem. Soc.*, 2008, *130* (1), 113–120. Copyright (2008) American Chemical Society.

The use of multidentate binding groups tethered to a single ligand has enhanced thermal and chemical stability of NPs in comparison to monodentate ligands as analyzed by Lee's group (**Figure 10**).[63,64] 2-tetradecylpropane-1,3,-dithiol (C16C2), 2-methyl-2-

tetradecylpropane-1,3-dithiol (C16C3), 1,1,1-tris(mercaptomethyl)-pentadecane (t-C16) improves NPs stability in solution (water/THF) for over one month at ambient conditions compared to hexadecanethiol which aggregated within 24h as the surface plasmon band (SPB) red-shifted. t-C16 ligand shows the highest stability in solution as desorption requires simultaneous breakage of all three gold-sulfur bonds.

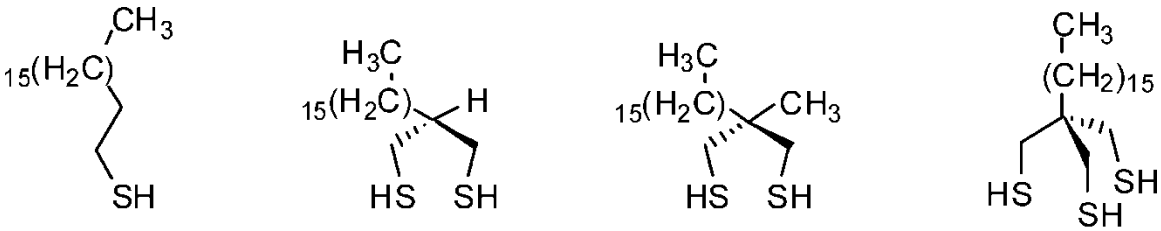

***n*-C18** **C18C2** **C18C3** ***t*-C18**

Figure 11. n-octadecanethiol (n-C18), 2-hexadecylpropane-1,3-dithiol (C18C2), 2-hexadecyl-2-methylpropane-1,3-dithiol (C18C3), and 1,1,1-tris(mercaptomethyl)heptadecane (t-C18).[65] Reprinted with permission from La-ongnuan Srisombat, Joon-Seo Park, Shishan Zhang*, et al.* *Langmuir*, 2008, *24* (15), 7750–7754. Copyright 2008 American Chemical Society.

In another similar study by Lee's group, n-C18 ligands display higher thermal stability in solution as its SPB does not change at 80 and 100 °C for two days and withstand ligand desorption at 120 °C (**Figure 11**).[66] Tridentate binding t-C18 ligands show greatest resistance to octadecanethiol displacement compared to the bidentate (C18C2 and C18C3) and monodentate ligands. Its thermal stability in the solid state also prevents gold NPs from coalescing. However, the chemical stability trend is different as t-C18 ligands have the least packing density on the surface, allowing cyanide to penetrate the monolayer and etch the surface. Of the two bidentate ligands (C18C2 and C18C3), the extra methyl group of C18C3 retards cyanide penetration, thus showing greater chemical resistance.[65,67]

1.3.3. Change in spacer length

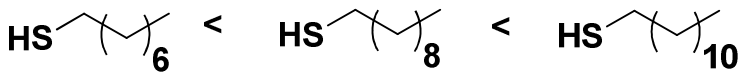

Figure 12. The increase of methylene groups on the spacer region stabilizes the monoalyer via van der waals interactions.[68]

Synthetic alterations in the spacer region of the ligand affect the stability of the monolayer by increasing the intermolecular interactions between ligands. In most cases, the hydrocarbon chains between ligands interact via London dispersion forces, adding approximately 4.1-8.4 kJ/mol for each methylene group.[32,62] An early study by Terrill *et al.* have shown that increasing the number of methylene groups within the alkane spacer of thiolate ligands protected gold NPs bolsters its thermal stability (**Figure 12**). For n-octane-, n-dodecane-, and n-hexadecanethiols gold NPs, the onset temperatures of mass loss increases from 230 ºC to 266 ºC and finally to 310 ºC which is indicative of the extra stabilization from additional methylene groups.[64,68] Murray and coworkers have also shown that chemical stability increases for longer alkanethiols (C4<C8).[69] They conclude that alkanethiols equal or greater than ten carbons yield relatively the same chemical stability. The same trend is also seen with n-decane-, n-tetradecane-, and n-octadecaneamines as longer alkyl chains are less prone to aggregation.[70]

1.3.4. Influence of additional functional groups in the ligand on NP stability

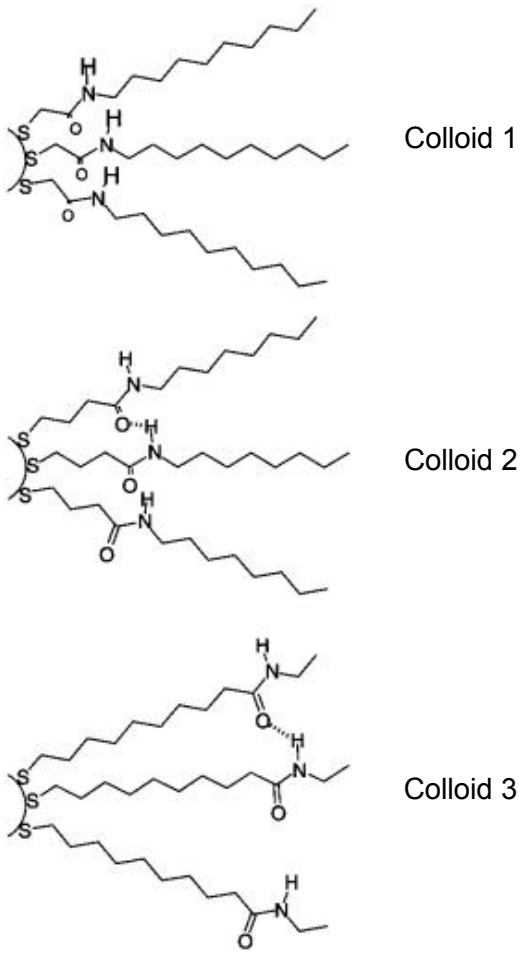

Figure 13. Hydrogen bond is not favoured in colloid 1 as ligands are twisted out of plane. Colloid 2 experiences good conformation between amide groups which maximizes hydrogen bonding. Ligands of colloid 3 have loose packing at the terminal ends disfavouring hydrogen bonding.[71] Reprinted with permission from Andrew K. Boal, Vincent M. Rotello. *Langmuir*, 2000, *16* (24), 9527–9532. Copyright 2000 American Chemical Society.

The stability of ligands with functional groups capable of hydrogen bonding within the spacer region was demonstrated by Rotello and coworkers.[71] Amide moieties were synthesized in different positions along the ligand (**Figure 13**). In the solid state, SAMs of **colloid 1** are disordered as amides close to the metal surface require moving out of

plane. As the ligand protrudes away from the surface, the loose packing of the terminal portion disallows the amides from forming effective hydrogen bonds in **colloid 3**. Interparticle hydrogen bonding was seen in TEM as aggregates formed. **Colloid 2** shows sufficient space for amide moieties to form intraparticle hydrogen bonds.

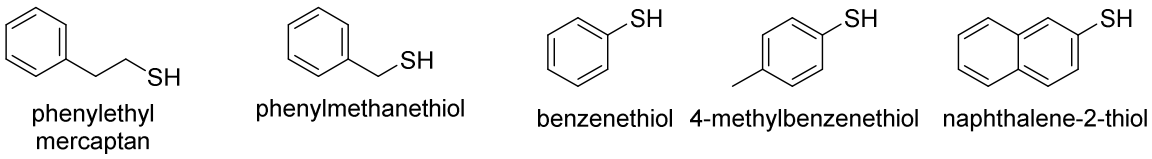

Figure 14. Various arene thiolates protected gold NPs.[72]

Murray and coworkers analyzed the effect of incorporating aromatics into the spacer region (**Figure 14**).[72] They found that arene thiolate (phenylethyl mercaptan, benzylthiol, thiophenol, 4-thiocresol, and 2-napthalenethiol) surprisingly had higher ligand packing compared to hexanethiols. But its thermal stability is less as it decomposes at temperatures below 260 °C. These SAMs also show less chemical stability compared to alkanethiols.

Other ligand designs include amino acids bearing charged moieties. Levy *et al.* found that the interior portion of the peptide ligand with hydrophobic (isoleucine and phenylalanine) or hydrophilic (asparagine and alanine) amino acids interact with intraparticle ligands via dispersion forces and hydrogen bonding respectively.[73] Charged amino acids (aspartic acid, lysine) induced electrostatic repulsion between ligands, leading to aggregated NPs in aqueous buffer solutions (>1 M NaCl).

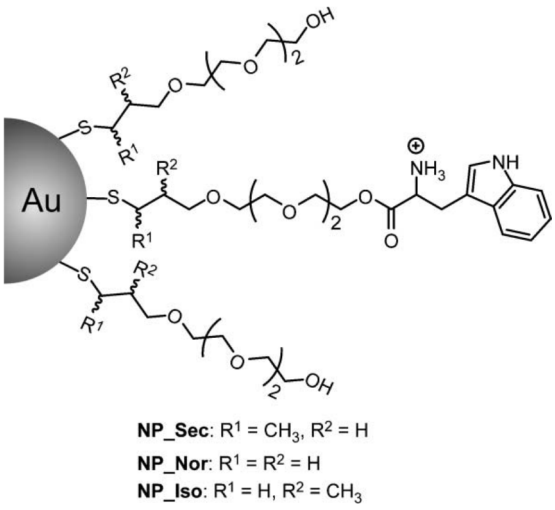

Figure 15. Water soluble ligand derivatives with methyl groups at the alpha and beta carbons from the sulfur yield different stabilities. Reproduced from [74] with permission of The Royal Society of Chemistry.

Rotello and coworkers incorporated methyl groups at the alpha (NP_Sec) and beta (NP_Iso) carbons from the thiolate of the ligands (**Figure 15**).[74] From TGA, the ligand bearing the methyl group at the beta carbon is more stable than its counterpart. Chemical etching with cyanide also shows the same trend. Due to the splay conformation of ligands, the beta methyl fills this space, and experiences van der waals interactions with adjacent ligands, thus slows down cyanide penetration. The same stability trend is observed when subjected to ligand exchange tests with dithiothreitol (DTT), dihydrolipoic acid (DHLA), and glutathione (GSH).

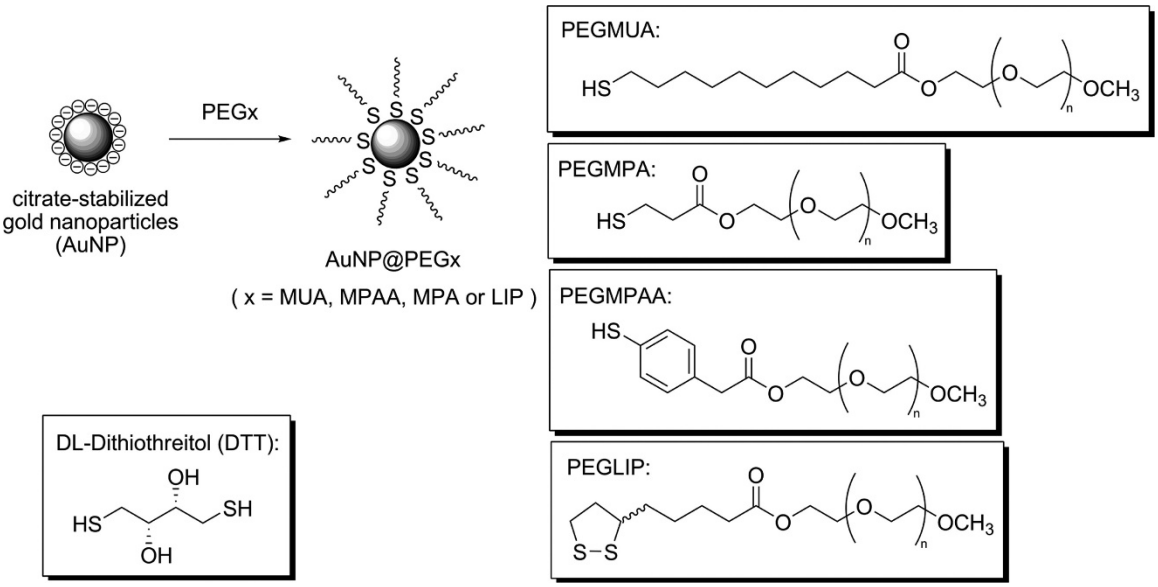

Figure 16. Ligands with different spacer moieties with terminal PEG groups undergo ligand exchange with citrate stabilized gold NPs.[75] Reprinted with permission from Florian Schulz, Tobias Vossmeyer, Neus G. Bastús, et al. *Langmuir*, 2013, *29* (31), 9897–9908. Copyright 2013 American Chemical Society.

A comparative study by Vossmeyer and coworkers showed the chemical stability of PEG ligands with varying spacer derivatives: PEGMUA with a spacer length of ten carbons, PEGMPA with a spacer length of two carbons, and PEGMPAA with a phenylene spacer (**Figure 16**). These ligands prevent aggregation in 400 mM NaCl solutions for 6h.[75] PEGMUA NPs exemplifies the highest chemical stability by withstanding 100 mM cyanide etching for 23 h while PEGMPA and PEGMPAA NPs last for only 4 min. The authors reason that the increased alkyl spacer and less steric hindrance compared to the phenylene spacer allow for better packing on the surface. At lower concentrations of cyanide, PEGMPAA are more stable than PEGMPA due to higher packing order on the surface. DTT ligand exchange is also tested and PEGMPA gold NPs and shows good stability but its bidentate derivative (PEGLIP) is much more stable due to its chelation effects.

1.3.5. Change in Terminal Group

The functionality of the terminal group affects the monolayer stability and interparticle interactions. An early study performed by Evan and coworkers on aromatic thiols bearing terminal hydroxyl, carboxylate, amine, and methyl groups.[76] It is observed that NPs bearing terminal amine and carboxylate experiences hydrogen bonding that lead to aggregation. They find that altering the pH for carboxylate phenyl thiols helps reduce the amount of aggregation but is not effective for amine phenyl thiols.

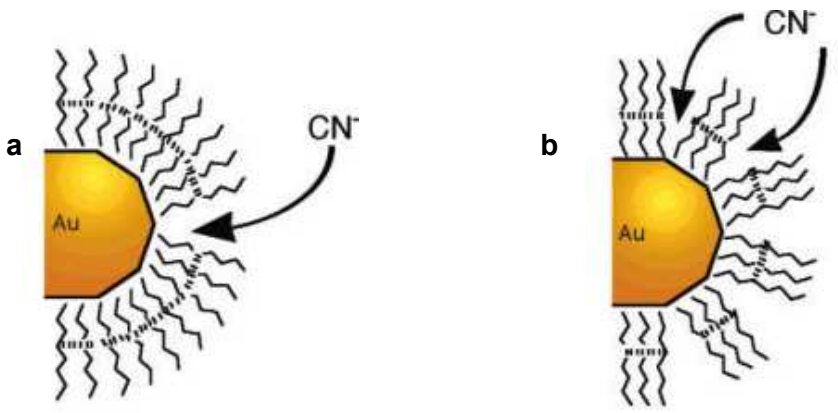

Figure 17. The modification of the terminal group affects the chain packing of the monolayer. a) Diphenylmethyl terminal groups shows higher chemical resistance; b) bulky tert-butyl terminal groups prevent ligands from close packing and allows for cyanide to etch the surface.[77] Reprinted with permission from Roy Shenhar, Vincent M. Rotello. *Acc. Chem. Res.*, 2003, *36* (7), 549–561. Copyright 2003 American Chemical Society.

Rotello and coworkers also examined the effect of hydrogen bonding from amides bearing terminal substituents with different sizes (diphenylmethyl, isobutyl, propyl, and tert-butyl).[77,78] When subjected to cyanide etching, diphenylmethyl had the

highest resistance followed by isobutyl, propyl, and tert-butyl. The packing formation of the terminal groups affect the stability as diphenylmethyl moieties experience pi-pi interactions, increasing the chemical stability against cyanide (**Figure 17a**). The large tert-butyl groups experience steric hindrance, repelling the alkyl chains and permitting cyanide to penetrate the monolayer at the vertices (**Figure 17b**). They also test the same terminal groups by modifying the amides with esters and observe weaker chemical stability due to the lack of hydrogen bonding.

1.3.6. Polymers

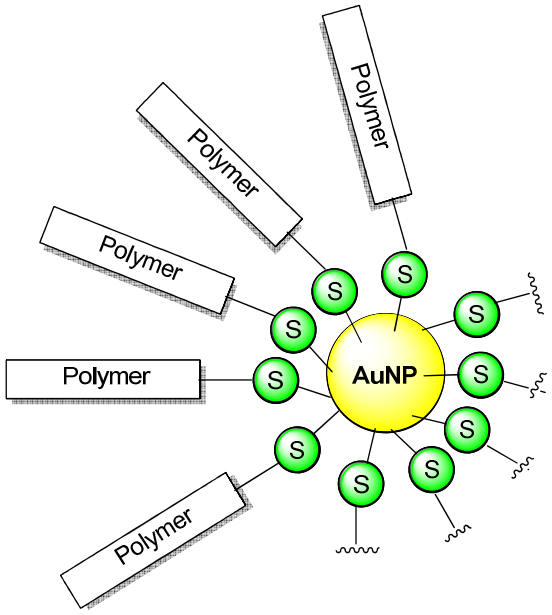

Figure 18. Polymeric ligand protected gold NP.

Small molecules have provided gold NPs with low to moderate stability but the durability of these NPs can be ameliorated with the use of polymeric ligands (**Figure 18**). The added bulkiness provides a robust physical barrier between particles. A recent

review by Jadhav and coworkers shed some light on the current polymers as NPs ligands.[22] Polymeric ligands, unlike small surfactants, have larger hydrodynamic radii, contain bifunctional groups for further grafting of monomers, and are capable of creating a stable cross-linked shell if polymerizable groups are present.

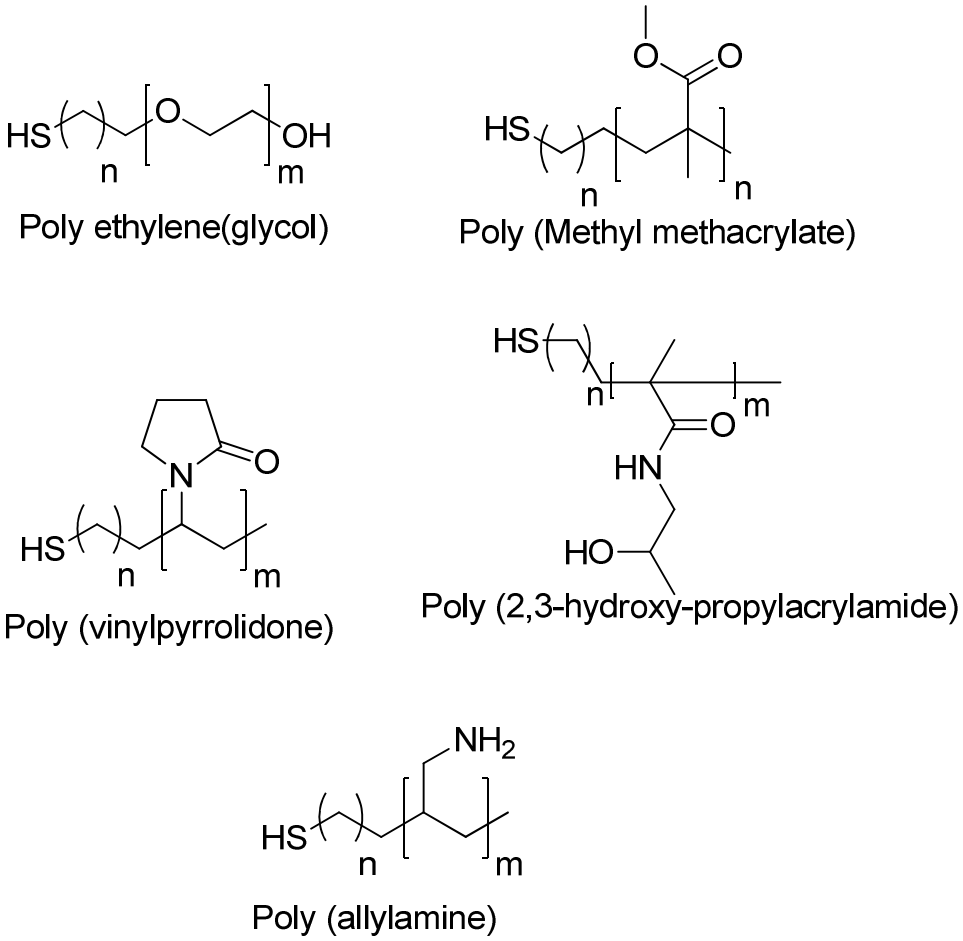

Figure 19. Commonly used polymers for protecting gold NPs include poly ethylene (glycol), poly (methyl methacrylate), poly (vinylpyrrolidone), poly (2,3-hydroxy-propylacrylamide), and poly (allylamine).[22]

Polymer protected NPs are synthesized via in-situ method and post-synthesis grafting. Commonly used polymers to protect metal NPs listed in Jadhav's review include poly(ethylene glycol) (PEG)[79], poly(methyl methacrylate) (PMMA)[80], poly (2,3-

hydroxypropylacrylamide)[79], plasma-polymerized allylamine[81], and poly (vinylpyrrolidone) (PVP)[82] (**Figure 19**).

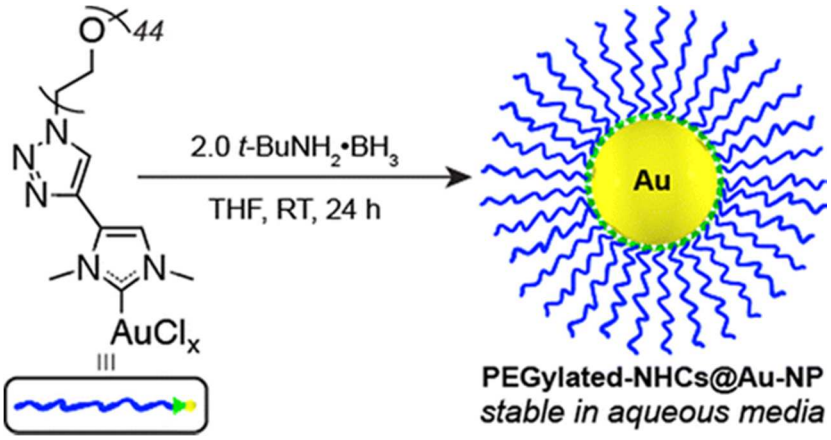

Figure 20. PEGylated-NHC Au-NPs (1-Au-NP) displays stability towards heat, chemical, and ligand exchange reactions.[83] Reprinted with permission from Michelle J. MacLeod, Jeremiah A. Johnson. *J. Am. Chem. Soc.*, 2015, *137* (25), 7974–7977. Copyright 2015 American Chemical Society.

The incorporation of polymers on small molecular weight ligands has drastically improved its stability. For instance, Johnson and coworkers[83] presented that previously studied unstable NHCs protected gold NPs (**Figure 20**) withstood aggregation for over 3 months in solution when grafted with PEG groups and were thermally stable from -78 to 95 °C for 5 h. These NPs also display great stability against pH changes for 8 weeks. Chemical stability is also durable against reducing agents 2-mercaptoethanol and H_2O_2 for 26 h and 24 h respectively. However, they are unstable to 250 mM NaCl solutions and ligand exchange reactions with thiolated PEG resulting in full aggregation after 6 h.

1.3.7. Polymerizable Groups on the Surface

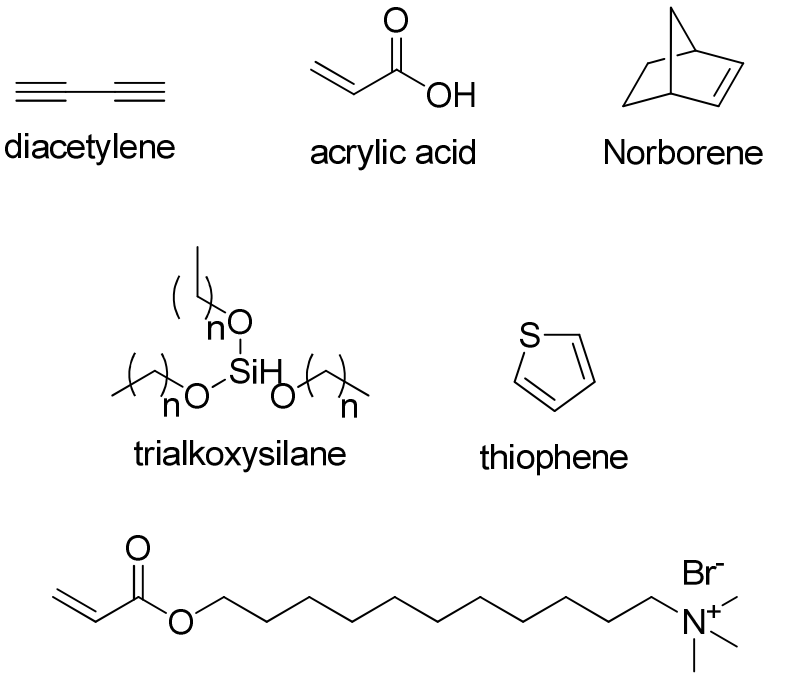

Figure 21. Polymerizable groups allows for lateral ligand cross-linking include diacetylene, acrylic acid, norborene, trialkoxysilane, thiophene, 11-(acryloyloxy) undecyltrimethyl ammoniumbromide.[22]

A strategy of minimizing the lability of the monolayer is to cross-link ligands within a monolayer or polymer bearing polymerizable groups on the surface (**Figure 21**). A few examples from Jadhav's review include diacetylene[84], poly(2-(dimethylamino)ethyl methacrylate) (PDMA)[85], 11-(acryloyloxy) undecyltrimethyl ammoniumbromide[86], norborane[87], trialkoxysilane, and thiophene[88].[22] These cross-linking reactions can be initiated thermally, photolytically, and electrochemically. Matyjaszeski and coworkers have shown that gold NPs with an inner cross-linked organic shell by dimethacrylate and

linear tethered polymer brushes enhances its thermal stability by enduring temperatures of 110 °C over 24 h without changes in its SPB.[89] The uncross-linked NPs aggregate within 1 h at 110°C.

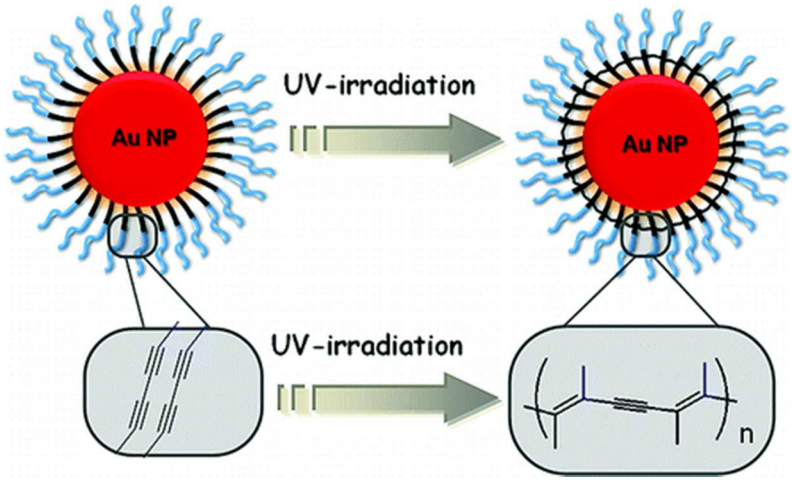

Figure 22. Water soluble DA-PEG with diacetylene moieties functionalized gold NPs. Cross-linked shell gold NPs after UV-irradiation, blue = PEG chain, black = diacetylene cross-linkage, red = gold NP.[90] Reprinted with permission from Dorota Bartczak, Antonios G. Kanaras. ***Langmuir*****, 2010, *26* (10), 7072–7077. Copyright 2010 American Chemical Society.**

Kanaras and coworkers[90] extended this idea of cross-linking individual water soluble ligands. Their water-soluble ligand, [46-mercapto-22,43-dioxo-3,6,9,12,15,18-hexaoxa-21,44-diazahexatetraconta-31,33-diyn-1-oic acid, (DA-PEG), cross-linked via diacetylene moieties (**Figure 22**). These gold NPs display great stability against aggregation in high ionic strength mediums, solvents (water and isopropanol), different pH solutions (1.2 to 14), heat (100 °C), and are undeterred from exchanging with incoming thiolate ligands (mercaptoethanol, dithiothreitol, cysteamine, cysteine, alpha-

lipoic acid, 11-amino-1-undecanothiol). These NPs also exhibit robustness under freezing and heat treatments to 100 °C.

Bumjoon and Bang and coworkers have also shown that thiolated block copolymers of PS and PS-N_3 can undergo Reversible Addition-Fragmentation chain Transfer (RAFT) via photoinitiation.[91] TEM images revealed very small changes in diameter (2.62 and 2.71 nm) after thermal treatment which is indicative of the cross-linking effect.

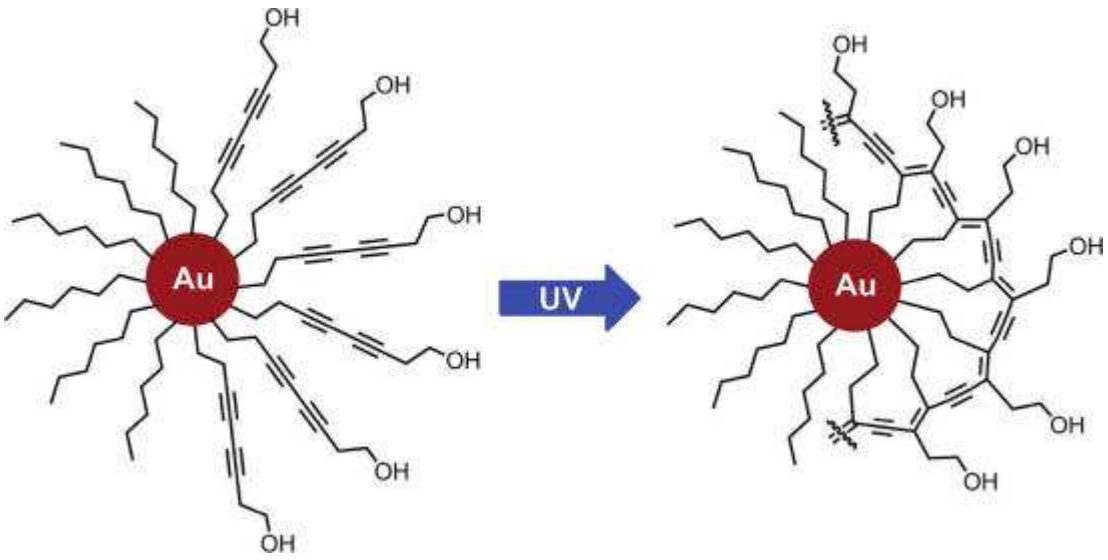

Figure 23. Cross-Linked hydrophilic portion of Janus NPs.[84] Reprinted with permission from Yang Song, Liana M. Klivansky, Yi Liu, et al. *Langmuir*, 2011, *27* (23), 14581–14588. Copyright 2011 American Chemical Society.

Chen and coworkers have applied the concept of photopolymerization to stabilize small molecular weight ligands of Janus gold NPs from ligand desorption and ligand mobility on the surface (**Figure 23**).[84] The cross-link of hydrophilic ligand, 3,5-octadiyne-

1-ol-8-thiol (DAT) via diacetylene groups enhances its stability for over 30 days in solution. Similarly, Jiang and coworkers have developed a cross-linkable ligand bearing a thiol head group, diacetylene moieties, and charged carboxybetaine.[92] Functionalized gold NPs that are cross-linked display great robustness in solutions with a wide range of pH values and heat treatment of 80 °C after 3h. In addition, these NPs withstand aggregation in serum and survives protein absorption.

1.3.8. Molecular Cross-Linkers Stabilizing the Surface

Cross-linked ligands within the monolayer can also be shown by introducing separate molecular cross-linkers that tether adjacent ligands to each other. Levy and coworkers have formed a monolayer of binary peptide ligands on gold NPs. This group introduces bis[sulfosuccinimdyl]suberate as molecular cross linkers to estimate the proximity between ligands on the surface.[93]

Basu and coworkers studies functionalized gold NPs with polynorbornene cross-linked with diamine derivatives.[94] Cross-linked NPs have shown higher resistance to cyanide etching compared to polymer protected NPs without cross-links. Different cross-linkers provide different chemical stability. More rigid linkers show higher resistance to cyanide etching (i.e. triethylenegylcol diamine > trans-1,5-diaminocyclohexane). The location of the cross-linkable moiety on the ligand also displays differences in stability as ligands with terminal activated esters provided higher robustness compared to that near the metal surface. The less stable NPs with cross-linkers closer to the gold may suggest a lesser degree of cross-linking due to slow diffusion of cross-linkers through the shell or slow reactivity.

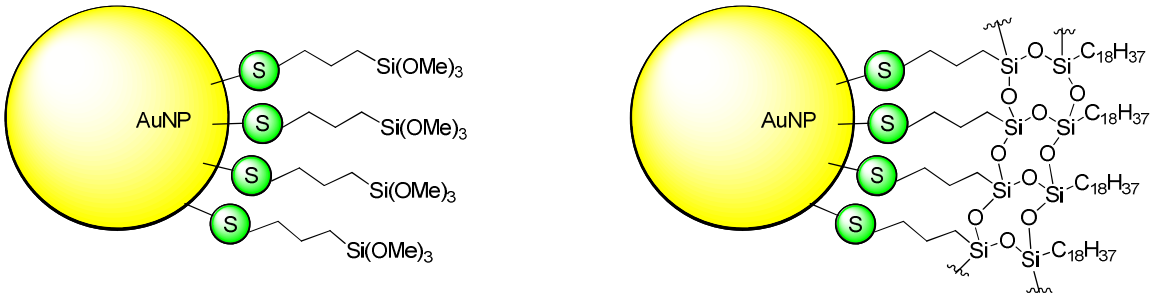

Figure 24. Siloxane cross-linked gold NPs withstood high heat treatments without aggregation.[95]

Hegmann's group have also demonstrated the enhanced robustness of the monolayer when cross-linking ligands via polysiloxane formation.[95] They protect gold NPs with 3-mercaptopropyltrimethyoxysilane follow by cross-linking with alkyltrimethoxysilane to generate a siloxane monolayer (**Figure 24**). This nanostructure endures sonication and thermal treatment without particle growth. This new ligand shell made these gold NPs suitable as dopants into liquid crystal hosts as they can withstand high temperatures.

1.4. Ligand Designs for Stability and Monolayer Functionality

Although polymerization on the monolayer shell drastically increases nanoparticle robustness against heat, chemical etching, salt and buffer solutions, and competing ligand exchange reactions, there are major deficiencies in many applications such as nanocatalysis. In a recent review by Li and coworkers,[45] they highlight the current advances in nanocatalysis and the role of capping agents. A disadvantage of these strongly stabilizing ligands is the prevention of reagents accessing the active metal substrate sites.[96,97] In addition, many polymeric ligands are insoluble, causing precipitation from solution and rendering NP catalysts inactive. These catalysts should be homogeneous to fully maximize their potential. However, incorporating ligands on NPs that are soluble in solution may swell and desorb from the surface, resulting in aggregation with hampered catalytic activity. Regeneration of these nanocatalysts may also cause the ligands to desorb and reducing the effectiveness in subsequent reactions.

A strategy employed is to have surface free catalysts by removing the capping agents via thermal heat treatment, electrochemical cleaning, washing with solvents, and ligand exchange with smaller molecules. Recently, Hutchinson and coworkers have shown the use of diluted ozone treatment to thiol protected AuNPs with minimal particle growth.[98] TEM images suggest that size changes after O_3 treatment are minimal. XPS data and calculations show that approximately 10 of the 35 bound thiol ligands are removed and catalytic activity of CO oxidation have increased. However, the longevity of these NPs are well diminished.

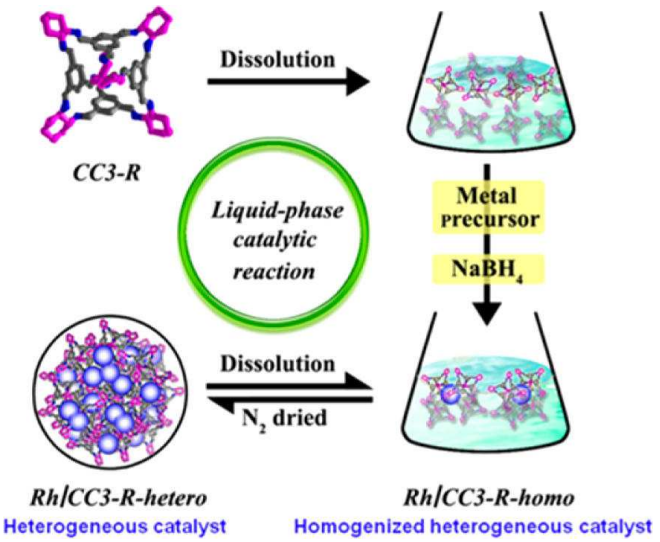

Figure 25. CC3-R organic cage stabilizes Rh NPs.[99] Reprinted with permission from Jian-Ke Sun, Wen-Wen Zhan, Tomoki Akita, et al. *J. Am. Chem. Soc.*, 2015, *137* (22), pp 7063–7066. Copyright 2015 American Chemical Society.

Another remedy is to use a more porous shell such as silica shell coating platinum NPs.[100] More recently, Xu and coworkers have attempted addressing this issue by functionalizing Rh NPs with a porous organic cage, CC3-R (**Figure 25**).[99] They synthesize a 1.1 nm diameter Rh NPs with high stability in solution as no colour change is observed. When comparing the catalytic activity of ammonia borane methanolysis, these Rh NPs in solution outperform solid Rh NPs, Rh NPs protected by PVP, and surfactant free Rh NPs.

Decreasing the thickness of protective polymeric layers for metal NPs regains more functional monolayers as low molecular weight ligands can be exchanged, the NPs are rendered soluble, and higher utilization of the monolayer and metal surface is feasible. Nevertheless, the stability is compromised as shown in previous examples. Designing these ligands should achieve both goals of providing functionality and good stability for the NPs.

1.5. Objective of this Thesis

The scope of this thesis is to synthesize a novel ligand that will share the durability of polymeric ligands and the monolayer functionality of small molecular ligands. The proposed ligand is comprised of its bulky 3,4,5-tris(octadecyloxy)benzene terminal group, tetra-alcohol spacer, and flexible anchoring monothiol head group (**Figure 26**).

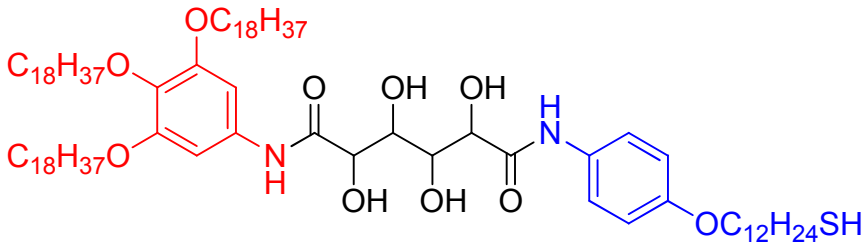

Figure 26. Proposed Cross-Linkable Ligand bearing a terminal bulky 3,4,5-tris(octadecyloxy)benzene (red), cross-linkable tetra-alcohols spacer (black), and flexible anchoring group (blue).

Upon surface functionalization, the bulky 3,4,5-tris(octadecyloxy) chains of the terminal group will hinder closed packing on the metal surface and promote dispersed packing of ligands on the surface (**Figure 27**). The augmented intraparticle distance between ligands should allow for small molecules to access the surface. In comparison to shorter alkoxy chains (i.e. methoxy or ethoxy), octadecyloxy chains will help induce higher solubility in organic mediums for these particles. The longer alkoxy chains will also prevent potential interparticle cross-linking when introducing commercially available disiloxane cross-linkers. The monothiol anchoring group is chosen over multidentate groups to maximize the amount of free metal surface area. Although the monolayer seems labile with monodentate binding to the surface and loose packing, monolayer stabilization can be achieved with molecular cross-linkers connecting adjacent linkers via

tetra-alcohols. Ligand lability will be diminished due to the cross-linked network of ligands. The proposed monolayer will mimic properties of both the durability of polymeric cross-linked shells and surface functionality of small monolayers. This novel ligand is useful for applications such as nanocatalysis and drug delivery systems.

Chapter 2 will describe the synthetic procedure and challenges for this novel ligand. Chapter 3 will reflect upon the outcomes, short comings, and future works of this project.

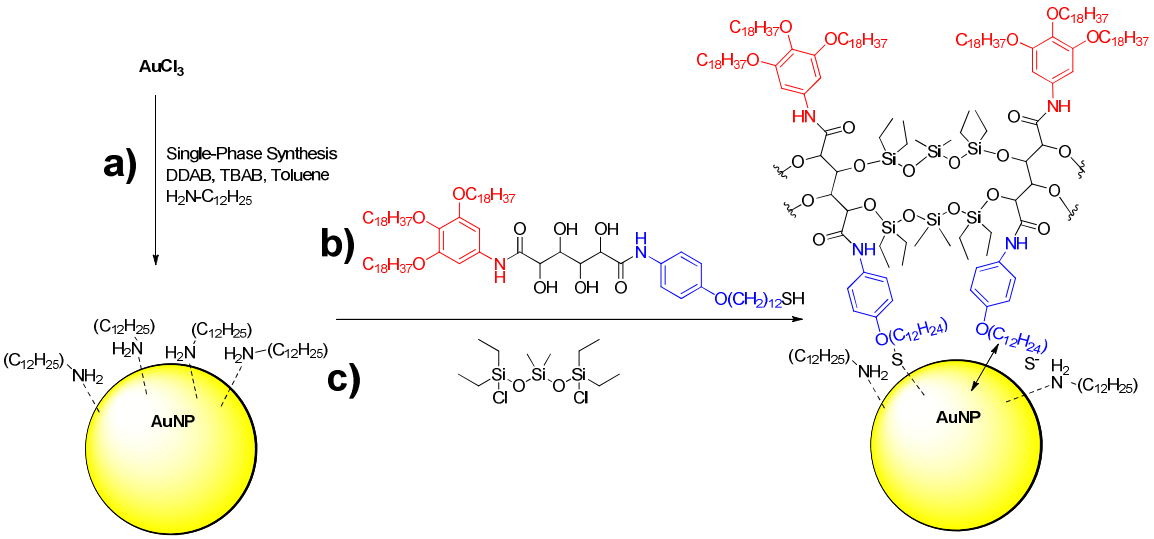

Figure 27. Proposed steps of the project involves a) Synthesis of 1-2 nm gold NPs via single phase method[101] with dodecylamine ligands; b) ligand exchange reaction with novel cross-linkable ligand; c) addition of commercially available disiloxane cross-linkers.

CHAPTER 2: DISCUSSION AND RESULTS

2.1. Introduction

The general overview of the proposed synthesis of this novel ligand involves the preparation of two different aniline derivatives (**3** and **5**) which are coupled to the carboxylic acid groups of a protected tetra-alcohol version of mucic acid **6** to form a non-symmetric diamide intermediate **8** as drawn in **Scheme 1**. This intermediate **8** will then undergo thiolation at the carbon bearing bromine. Deprotection of the esters on **Compound 14** will finally yield the desired thiol ligand. The overall experimental outline is shown in **Scheme 2**.

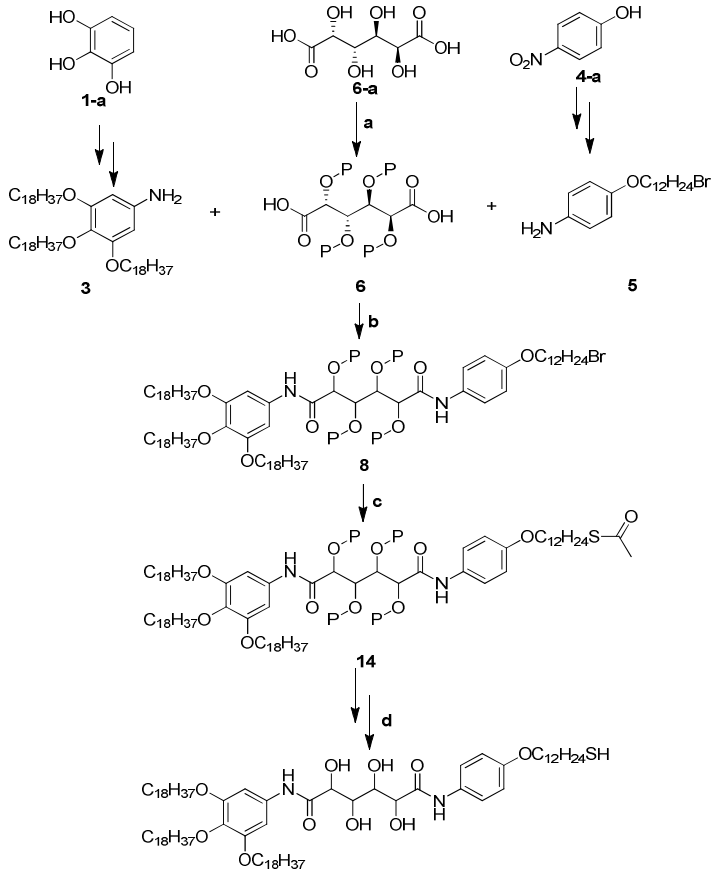

Scheme 1. Proposed synthesis of the ligand. a) Protection of mucic acid b) Non-symmetric diamide formation c) Thiolation d) Deprotection of hydroxy and thiol groups. Note: Stereochemistry of mucic acid is racemic.

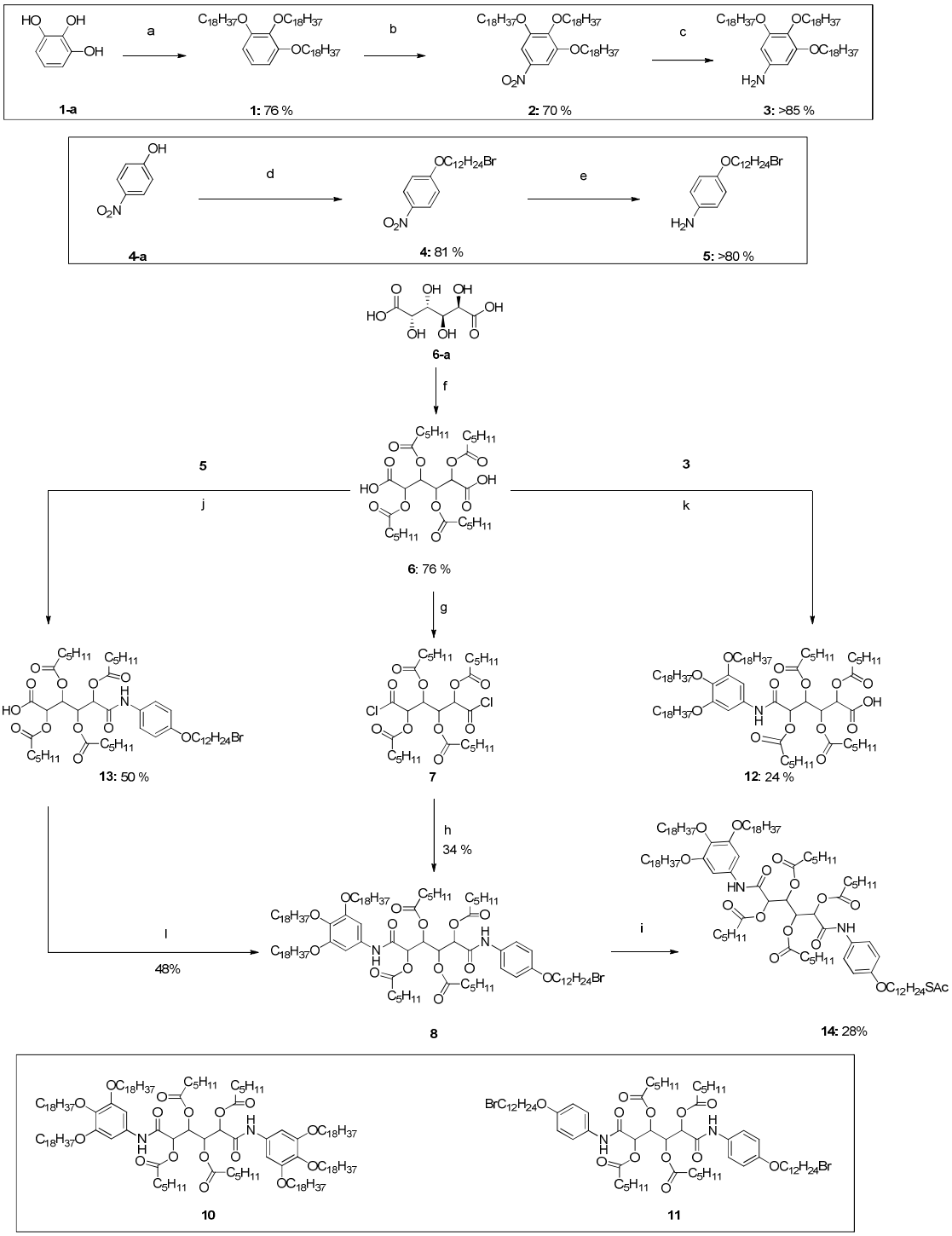

Scheme 2. Experimental scheme. Reaction conditions: (a) 3.4 eq. $BrC_{18}H_{37}$, 4.5 eq. K_2CO_3, DMF, N_2, 60 °C, 42 h; (b) 7.6 eq. HNO_3. SiO_2, CH_2Cl_2, N_2, 0 °C to r.t., 3.5h; (c) 5.0 eq. $NH_2NH_2.H_2O$, 49 eq. graphite, EtOH, N_2, r.t. to 85 °C, 48 h; (d) 2.0 eq. $BrC_{12}H_{24}Br$, 1.05 eq. K_2CO_3, N_2, r.t., 24 h; (e) 3.4 eq. $SnBr_2$, 37% HCl, EtOH, N_2, r.t. to 70 °C, 24 h; (f) 9 eq. $CH_3(CH_2)_4COCl$, 10 mol % $ZnCl_2$, N_2, 90 °C, 24 h; (g) 5.6 eq. $SOCl_2$, DMF $_{(cat)}$, CH_2Cl_2, N_2, 0 °C, 15 min, r.t.,>12h; (h) 1.06 eq. Cpd **3**, 1.12 eq. Cpd **5**,10.4 eq. TEA, CH_2Cl_2, r.t. 18h; (i) 5.4 eq. CH_3COSH, 4 eq. Cs_2CO_3, DMF, N_2, 3 days; (j) 4.75 eq. Cpd **6**, 1.0 eq. Cpd **5**, 4.34 eq. DMAP, 4.14 eq. DCC, DMF, CH_2Cl_2, 0 °C, 1 h, r.t., 24 h; (k) 1.0 eq. Cpd **6**, 1.0 eq. Cpd **3**, 0.33 eq. DMAP, 1.0 eq. DCC, DMF, CH_2Cl_2, r.t., 24 h; (l) Similar to g, h.

2.2. Protection of Tetra-alcohols of Mucic Acid

Mucic acid (**6-a**) requires protection of the alcohol sites in order to induce reactive selectivity at the carboxylic acid groups in the subsequent amidation. In addition, these protecting groups render the products soluble in organic solvents, which ease the synthesis and purification. **6-a** poses some synthetic issues such as its insolubility in most organic solvents and incompatibility on silica-based thin-layer chromatography (TLC). Uhrich's group have shown the protection of the alcohol sites with esters with alkyl lengths greater than five.[102] They monitored the esterification via ^{1}H NMR where the doublet and triplet signals of the methines would shift downfield from 5 ppm and 4 ppm to about 5.7 and 5.2 ppm as the alcohols were esterified.

Table 1. Synthetic attempts of protecting alcohols on mucic acid

Entry	Mucic Acid (eq)	Protecting Reagent (eq)	$ZnCl_2$ (mol%)	Base (eq)	Temp (°C)	Solvent	Time (h)	Outcome
1	1	AcCl (12)	10.0	-	45	AcCl	18h	Some product formed
2	1	AcCl (35)	12.6	-	90	AcCl	22	23% crude
3	1	AcCl (59)	15.4	-	90	AcCl	96	Some product formed
4	1	AcCl (6)	-	Pyridine (26)	Rt	Pyridine	-	Decomposition
5	1	AcCl (12)	-	TEA (12)	Rt	NEt_3	-	Decomposition
6	1	Ac_2O (55)	21.2	-	90	Ac_2O	24	9%
7	1	Ac_2O (11)	-	TEA (9.9)	Rt	DMF	16	Product formed
8	1	$PhCH_2Cl$ (10)	-	Cs_2CO_3 (6.8)	Rt	DMF	24	No product
9	1	$PhCH_2Cl$ (14)	-	Cs_2CO_3 (14)	60	DMF	24	No product
10	1	Hexanoyl Chloride (9)	10.0	-	90	Hexanoyl Chloride	24	77%
11	1	Hexanoyl Chloride (7.8)	10.0	-	90	Hexanoyl chloride	24	7.8%

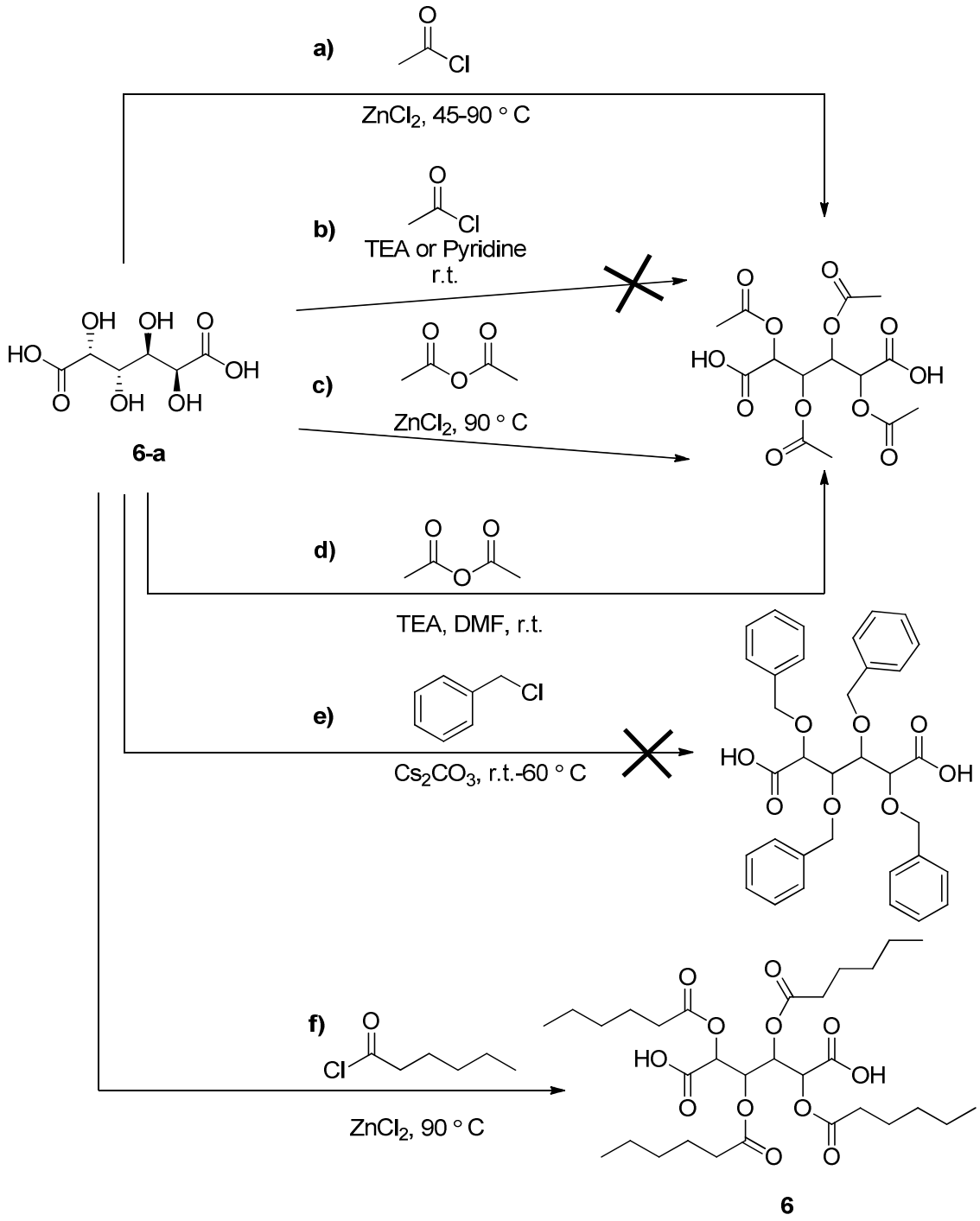

Scheme 3. Protection of tetra-alcohols of mucic acid. a) Entries 1,2,3; b) Entries 4, 5; c) Entry 6; d) Entry 7 e) Entries 8, 9; f) Entries 10, 11.

Table 1 lists the attempts on protecting mucic acid at its alcohol sites. Firstly,

Entry	Mucic Acid (eq)	Protecting Reagent (eq)	ZnCl2 (mol%)	Base (eq)	Temp (◦ C)	Solvent	Time (h)	Outcome
1	1	AcCl (12)	10.0	-	45	AcCl	18h	Some product formed
2	1	AcCl (35)	12.6	-	90	AcCl	22	23% crude
3	1	AcCl (59)	15.4	-	90	AcCl	96	Some product formed
4	1	AcCl (6)	-	Pyridine (26)	Rt	Pyridine	-	Decomposition
5	1	AcCl (12)	-	TEA (12)	Rt	NEt3	-	Decomposition
6	1	Ac2O (55)	21.2	-	90	Ac2O	24	9%
7	1	Ac2O (11)	-	TEA (9.9)	Rt	DMF	16	Product formed
8	1	PhCH2Cl (10)	-	Cs2CO3 (6.8)	Rt	DMF	24	No product
9	1	PhCH2Cl (14)	-	Cs2CO3 (14)	60	DMF	24	No product
10	1	Hexanoyl Chloride (9)	10.0	-	90	Hexanoyl Chloride	24	77%
11	1	Hexanoyl Chloride (7.8)	10.0	-	90	Hexanoyl chloride	24	7.8%

Uhrich's procedure was modified by acetylation of mucic acid with acetyl chloride catalyzed by 10 mol% $ZnCl_2$ at room temperature (**Scheme 3a**). However, the methine peaks did not shift entirely into the expected region. The temperature was then increased to 45 °C and some peaks were observed in the desired region indicating only partial protection (Entry 1). When increasing the temperature above acetyl chloride's boiling point, some product formation was observed in ^{1}H NMR and a crude yield of 23% was obtained. Potential problems with this harsh reaction condition included the need for constant replenishment of acetic chloride and possible decomposition or polymerization of **6-a**. This reaction may have a high kinetic barrier which explains the partial protection even though $ZnCl_2$ is used and acyl chlorides are very good electrophile.

Weak bases, such as pyridine (Entry 4) and trimethylamine (TEA) (Entry 5), were

used in place of a Lewis acid (**Scheme 3b**), but they immediately generated a black solid after addition. Either these reaction conditions decomposed the product or the product is formed but has low solubility in organic solvents. Similar problems were experienced by Ulrich's group, which was why they did not report esters with carboxylic acid groups of less than 6 carbon atoms.

To ameliorate this issue of partial protection, acetic anhydride was used because its high boiling point (140 °C) permitted more flexibility in raising the temperature.[103] In **Scheme 3c**, 9% of the product was obtained with the structure confirmed by mass spectrometry. The low yield may be accounted from the challenging purification procedure. The crude mixture did not run on silica gel possibly because of strong hydrogen bonding between the carboxylic acids and silica, thus ruling out chromatography as a purification technique. Recrystallization with non-polar solvents was attempted with hexanes and petroleum ether, but showed poor miscibility resulting in an oil rather than a solid.

Another protecting group such as benzyl chloride was chosen to create a benzyl ether in the presence of cesium carbonate with 4 Å molecular sieves (**Scheme 3e**). Based on simulated ^{1}H NMR predictions and similar literature results[104], the expected methine proton environments should shift downfield to the 4.0 to 3.5 ppm region with doublet and triplet signals. However, signals within this region were not observed but contained mainly unreacted benzoyl chloride. The temperature was increased to 60 ºC in the next trial (entry 9). Since there are four tetra-alcohols on mucic acid, monitoring the degree of protection via TLC is difficult. In entry 9, reaction was monitored by TLC where benzyl chloride was added in small portions. The benzyl chloride spot would diminish as the product would appear. After purification, the product was not observed which suggested decomposition.

Uhrich's procedure was then followed using hexanoyl chloride catalyzed by $ZnCl_2$ under reflux at 90 °C (**Scheme 3f**).[102] The boiling point of hexanoyl chloride (150-153 °C) allowed for higher temperatures without the need of solvent replenishment and similar reported yields of 70-80% were obtained.[102] The presence of moisture in the reaction flask was detrimental to the overall yield as it decomposed the Lewis acid (entry 12). After 24 h, the crude ^{1}H NMR showed many impurities within the 6-5 ppm range. The catalytic loading was doubled and the reaction was allowed to react for an addition 24 h. However, ^{1}H NMR of the crude material did not change resulting in a low yield of 7.8 %. This problem was ameliorated by drying mucic acid under vacuum for 5 h at 150 ºC to achieve reported yields of 70-80%.

2.3. Synthesis of Bulky Terminal Group[105]

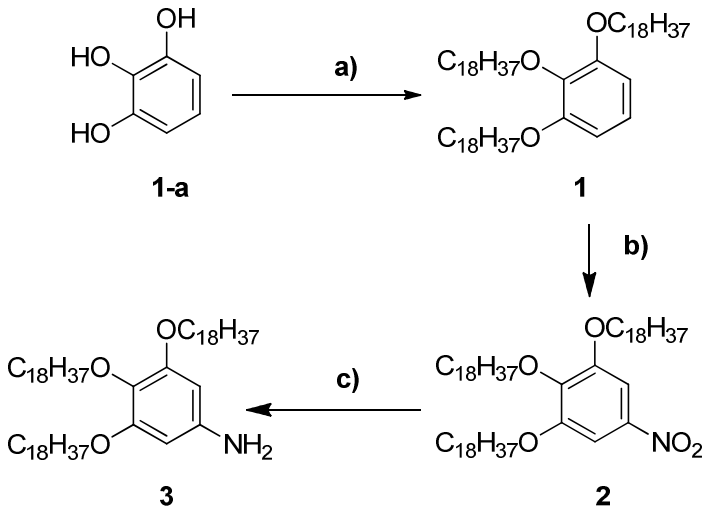

Scheme 4. Synthesis of 3,4,5,-tris(octadecyloxy)aniline (3)[106]. a) Alkylation of pyrogallol; b) Aryl nitration of (2); c) Nitro reduction supported on graphite.

2.3.1. 1,2,3-tris(octadecyloxy)benzene (1)

The overall synthesis of **3,4,5-tris(octadecyloxy)aniline (5)** was first published by Percec's group.[106] The synthesis of **1,2,3-tris(octadecyloxy)benzene (3)** involves an S_N2 process of alkylating pyrogallol (**Scheme 4a**). Pyrogallol was subjected to deprotonation by a weak base, such as potassium carbonate, in order to undergo alkylation for 48 h. Potassium carbonate was prepared by mechanical grinding and drying under high-vacuum to increase surface area and remove any moisture respectively in order to achieve good yields. Employing a stronger base, such as cesium carbonate, improved the reaction timeframe and yields (24 h, >90%). It was vital that compound **(1)** was purified from the bi- and mono-alkoxyl benzene by-products since any free alcoholic group can partake in subsequent reactions. Reported synthetic purification procedures suggested that one precipitation step was sufficient.[106] However,

mono- and bi-alkoxyl benzene by-products on TLC were observed (TLC has limits of detection of 1/100 of a microgram[107]). An attempt on isolating the product by sublimation was performed but this technique was not effective as no compound sublimed. Isolation of the product by flash column chromatography on silica gel (7:3 hexanes/CH_2Cl_2) was successful but compromised the yield to ~10%. Instead, the product can be separated well on activated basic Al_2O_3 with dichloromethane as the eluant and precipitated in acetone to remove any excess of 1-bromododecane.[108]

2.3.2. 5-nitro-1,2,3-tris(octadecyloxy)benzene (2)

The synthesis of **5-nitro-1,2,3-tris(octadecyloxybenzene) (2)** involves electrophilic aromatic substitution at the 5 position on the benzene of **(1)** supported on silica gel charged with 30 % nitric acid (**Scheme 4b**).[106] Many published reports showed deviating reaction times ranging from 10 min to 5 h.[109,110] Initially, a low yield of 20% was obtained when the reaction time was 5 h. The initial assumption was that the acidic conditions may be too harsh, leading to ether cleavage. The reaction was monitored for 1 h and a better yield of 48% was obtained. After 3 h, full conversion occurred as the aromatic proton of the product appeared at 7.47 ppm while the proton environments of the starting material diminished. However, much of the product was loss due to the workup procedure as the product was trapped on the silica gel. Warm CH_2Cl_2 was used to sufficiently rinse off any remaining product on silica gel. Acetone was used to remove the yellow impurities resulting in a white solid.

2.3.3. 3,4,5-tris(octadecyloxy)aniline (3)

3,4,5-tris(octadecyloxy)aniline (3) was synthesized by a graphite supported reduction of **(2)** (**Scheme 4c**). The mechanism of this reduction involves three 2e-donations from hydrazine to the nitroaryl starting material.[111] The purity of the graphite dictated the completion of the reaction. Insufficient rinsing of graphite prior disallowed the reaction to proceed despite refluxing at high temperatures for over two days. Yields of this reaction were generally good (>85%). In terms of chemical stability, this electron-rich aniline was susceptible to oxidation under ambient conditions, which may form other unwanted products such as polyaniline derivatives[112]. **(3)** was usually kept under inert gas (nitrogen) and in cold temperatures to retard its decomposition.

2.4. Synthesis of Flexible Anchoring Group[105]

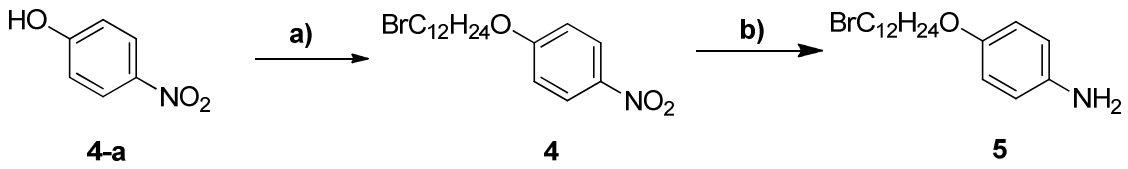

4-a **4** **5**

Scheme 5. Synthesis of Flexible Anchoring Group;[105] a) Alkylation of 4-nitrophenol; b) Nitro-reduction with $SnBr_2$

2.4.1. 1-((12-bromododecyl)oxy)-4-nitrobenzene (4)

4-nitrophenol (4-a) was substituted with 1,12-dibromododecane at the phenolic site to produce **(4)** (**Scheme 5a**). Better yields of 81% compared to 70% were obtained on the multi-gram scale. The remaining ~20% belonged to the disubstituted by-product, **1,12-bis(4-nitrophenoxy)dodecane**.

2.4.2. 4-((12-bromododecyl)oxy)aniline (5)

The synthesis of **(5)** involves the reduction of **(4)** with $SnCl_2$ as the reducing agent under acidic conditions at 70 °C (**Scheme 5b**). **(5)** was generated in a yield of 70-80%. From ^1H NMR, impurities with a triplet signal between 3.55-3.40 ppm was observed. The mixture was subjected to flash column chromatography to separate **(5)** from its impurities. TLC showed one spot which indicated a clean fraction. But ^1H NMR revealed the impurity was still present. Since the impurity may be soluble in organic solvents, protonation of the amine **(5)** with dilute HCl into an ammonium salt should precipitate from solution and filtered off. However, this technique did not separate the impurity from the desired product. ^{13}C NMR suggested an alkylchloro peak (δ ~ 45.5

ppm). Mass spectrometry of the subsequent amide product showed the presence of chlorine. Halide exchange occurred between the bromine with chloride source from $SnCl_2$. Alternatively, $SnCl_2$ was replaced with $SnBr_2$ and the triplet impurity was not seen which concluded that halide exchange occurred when reducing in the presence of a chloride source. **(5)** was unstable in the presence of air in solution and in the solid state which required storage under inert gas.

2.5. Non-symmetric Diamide Synthesis (8)

2.5.1 Acyl Chloride Route

Table 2. Synthetic attempts on non-symmetric diamide.

Entry	6 (eq)	3 (eq)	5 (eq)	TEA (eq)	Method	Time (h)	Outcome
1	1	1.06	1.13	10	**7** added to **3, 5**	24	**10:** (4.5%) **8**: 34% (65%) **11:** (10.7%)
2	1	0.93	1.12	8.9	**7** added to **3**, then **5** added to pot	48	TLC-**10** formed; **5** added-little change **By-product 5**
3	1	1	1	-	**3** to **7** dropwise and heated; then **5** to pot		SM **(6)**, **3** coupled to form by-product **5**; no diamide products
4	1	1.04	1.27	1.3; 1.3	**3**+**NEt_3** dp 2h @ 5 ml/h added to **7**; then **5** to solution, 30-50°C	48	TLC-**3** consumed; no product
5	1	1.1	1.01	1.2	**5** added to **7** dropwise 1 h, stirred 24h; **3** added to pot, 24h	48	No product
6	1	1	1	1.57, 2.02	**5** + NEt_3 to **7** dropwise 33 h, **3** + TEA to pot	48 h, 5 days	Isolated yields: **10:** (2.1%), **8:** (3.3%)

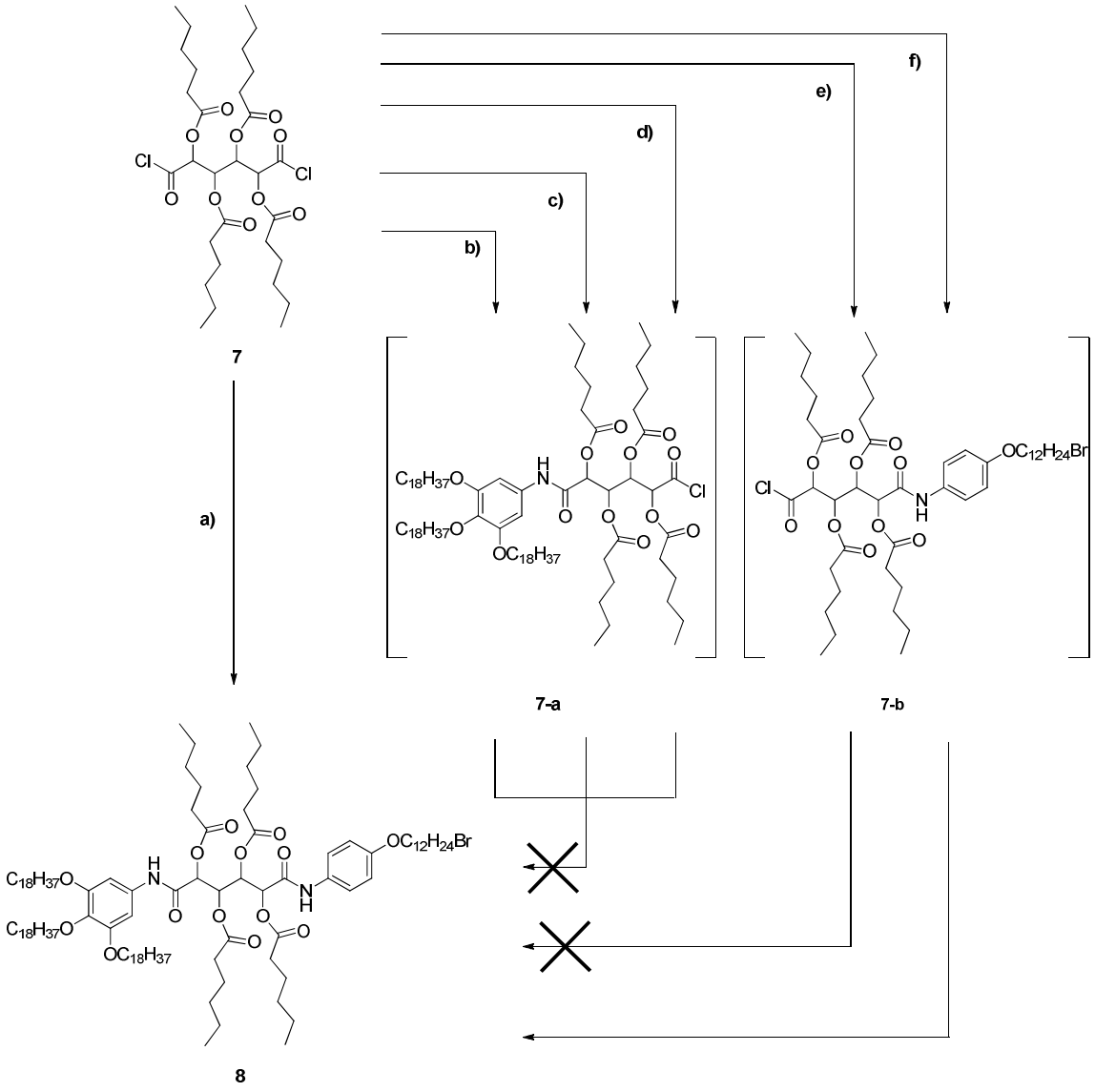

Scheme 6. Synthetic attempts on non-symmetric diamide 8 via stepwise addition. a) Entry 1: one pot addition of diacid solution to 3 and 5; b) Entry 2: diacid addition to dilute solution of 3 then addition of 5; c) Entry 3: addition of 3 to diacid solution 7, then addition of 5; d) Entry 4: addition of 3 to diacid solution 7, then addition of 5 with heating; e) Entry 5: addition of 5 to diacid solution 7, then addition of 3; f) Entry 6: addition of 5 to diacid solution 7, then addition of 3.

2.5.1.1. One Pot Addition

Prior to forming the non-symmetric diamide compound, stability of **(6)** with thionyl chloride was analyzed. After 24 h, ^{1}H NMR showed that the ester protecting groups survived thionyl chloride addition. Initially, **(6)** was activated with $SOCl_2$ and added to a single pot with compounds **(3)**, **(5),** and TEA (**Scheme 6a**). After one column chromatography purification, 65% of the crude desired product was formed along with traces of the by-products but multiple column chromatography steps generated a low yield of 34%. Symmetrical diamide products were also isolated **(10)** (4.5%) and **(11)** (10.7%).

2.5.1.2. Stepwise Addition

Despite feasible isolation of the three diamide products, low yields recovered for the three products were unsatisfactory. This reaction was not high yielding and inefficient as preparation of the starting materials span over six steps. A statistical approach was used where small amounts of one aniline derivative were added to diacid chloride solution **7** followed by the second aniline addition. Since the concentration of **(7)** is much greater than the aniline in solution, monoamide is expected to be produced in greater yields, allowing for the second aniline to react with the remaining site. In **Scheme 6b**, diacid chloride solution **(7)** was added to a diluted solution of **(3)** and stirred for 24 h. TLC indicated that **(10)** was formed but great intensity was found at the baseline, possibly indicating that **(7)** or the monoacid chloride (or monoamide) were the major reaction species. After the addition of aniline **(5)**, symmetric diamide **(10)** was isolated but the target intermediate **(8)** and other symmetric diamide **(11)** were not found. ^{1}H

NMR showed a by-product without the methine environments in the 6-5 ppm region and with aromatic proton environments of aniline **(5)**. The potential by-product may be N-(4-((12-bromododecyl)oxy)phenyl)hexanamide, which arose when residual hexanoic acid in the previous reaction was activated into hexanoyl chloride and coupled with **(5)** (**Scheme 7**).

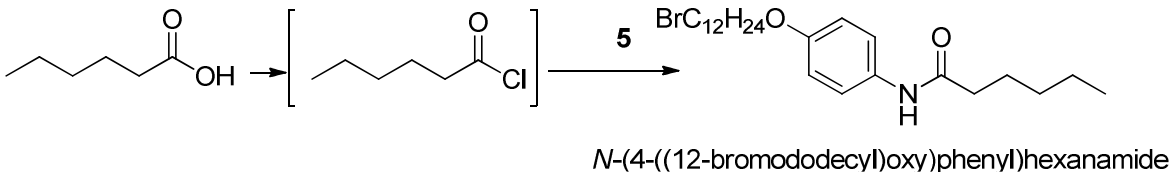

N-(4-((12-bromododecyl)oxy)phenyl)hexanamide

Scheme 7. By-Product Formation of N-(4-((12-bromododecyl)oxy)phenyl)hexanamide.

The aniline addition order was analyzed to observe any changes in the amide formation and yields. Aniline **(3)** was added to solution **(7)** dropwise prior to the addition of **(5)** **(Scheme 6c)**. ^{1}H NMR showed that upon the first addition of **(3)**, the aromatic proton shifted to 6.69 ppm which was indicative of amide coupling. However, no desirable diamide products were present as the signature peaks of the methine environments (5.8 and 5.4 ppm) were absent. In addition, unconverted starting materials of **(6)** and **(3)** prompted to heating the reaction. However, prolonged heating did not lead to total consumption of **(3)**. After the addition of **(5)** and purification, **(5)** did not form an amide as indicated on ^{1}H NMR. There were no diamide products as the expected peak at 5.40 ppm was absent. The reaction with similar conditions in which **(3)** and TEA were added together dropwise to the solution of **(7)** over 2 h (**Scheme 6d**) and the reaction

was heated to 50 °C for both aniline additions. However, the crude ^{1}H NMR revealed no coupling of aniline **(5)** to **(7)** which may have decomposed upon heating.

The order of aniline addition was altered by adding **(5)** dropwise over 1 h to a solution of diacid chloride **(7)** followed by the addition of **(3)** (**Scheme 6e**). Upon the first aniline addition, TLC suggested aniline **(5)** reacted completely which proceeded with the addition of aniline **(3)**. Surprisingly, the methine of mucic acid proton environments were not present. After purification with flash column chromatography, no diamide products were found. One fraction of **(3)** formed an amide due to shifts in its aromatic hydrogen (6.68 ppm) and amide hydrogen (7.17 ppm) but did not possess the methine environments, possibly coupling to other susceptible electrophilic species such as hexanoyl chloride as shown in **Scheme 7**. However, reasons for the poor coupling may be attributed to the insufficient amount of TEA present. Any untrapped HCl would protonate the incoming aniline derivatives, creating a non-nucleophilic ammonium salt which would be a very poor nucleophile. This could be seen as excess of **(3)** was observed. It is unclear why **(3)** does not form any product since it was added first along with TEA. In **Scheme 6f**, the reaction conditions were altered by increasing the amount of TEA and diamide formation was observed from ^{1}H NMR. However, the yields were very poor for **(10)** (46 mg, 2.1%) and **(8)** (55 mg, 3.3%).

2.5.1.3. Synthesis of Symmetric Diamide

Table 3. Symmetric Diamide Synthesis.

Entry	6 (eq.)	3 (eq)	5 (eq)	TEA (eq)	Method	Conditions	Results
1	1	-	-	3.	2.9 eq 3,5-dimethylaniline added to **7**	48 h, 30°C 2h	> 90% Yield
2	1	2.3	-	43	**3** + TEA to **7** dropwise	24h rt, 24h 30°C, 24h 40°C, 24h 50°C	Yield: 49 mg, 8.7%

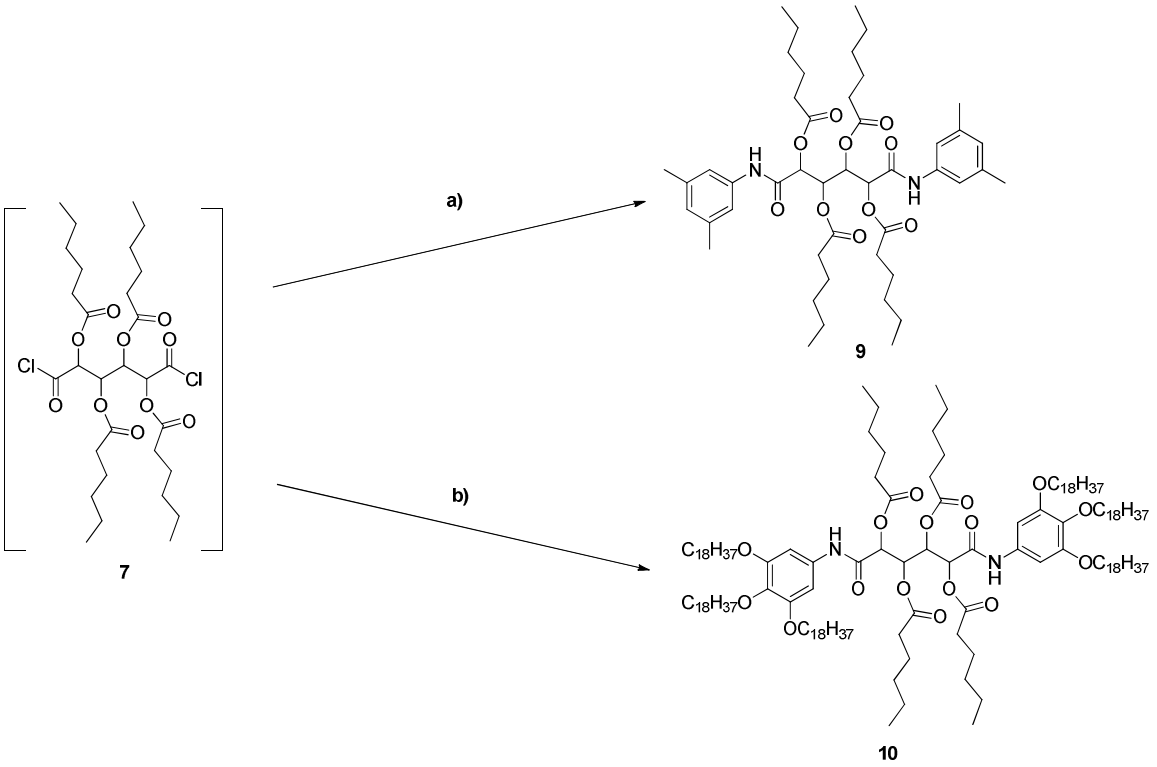

Scheme 8. a) Entry 1: 3,5-dimethylaniline addition to diacid chloride 7; b) Entry 2: Aniline 3 addition to diacid chloride 7

From the above results, the sequence of reagent additions between aromatic amines and carboxylic acids was investigated. In **Scheme 8a**, an excess of 3,5-dimethylaniline was added to solution **(7)** dropwise over 10 min and generated over 90%

yield. This result shows that smaller aromatic amine addition to diacid chloride **(7)** is feasible and should be applicable to the two synthesized anilines (**3** and **5**). Subsequently, stepwise addition of aniline and 3,5-dimethyaniline were added along with TEA obtained a yield of 52-56 % (70 mg). The IR spectra also suggested successful amidation with -C=O and -N-H stretches at 1674.86 cm^{-1} and 3341.69 cm^{-1} respectively. Determining the relative yields of the three expected mixtures was difficult as they shared similar retention factors on TLC. In **Scheme 8b**, the addition of an excess of aniline **(3)** to **(7)** was tested and monitored by TLC. Based on ^{1}H NMR, the aromatic protons of symmetric diamide **(10)** and **(3)** were compared and only 51.8% reacted completely despite using 2.2 eq. after 2 days at 40 °C. Raising the temperature to 50 °C slightly improved the NMR yield to 58.9%. The diamide product was isolated and generated a low yield (49 mg, 8.7%) despite adding excessive amounts of TEA.

The poor yields may be attributed from both the reaction conditions and challenging purification process. Firstly, the simultaneous addition of similar equivalents of aniline derivatives with TEA may not be sufficient in quenching residual acid in solution. The acid may not only protonates anilines **(3)** and **(5)**, but also cleaves the alkoxy chains, leading to decomposition. The dark spot located at the baseline on TLC may reflect the decomposition of anilines **(3)** and **(5)** rather than the assumed monoacid or diacid species. Good yields were generated from the test reaction involving the addition of two or more equivalents of 3,5-dimethylaniline to the diacid chloride solution. In contrast, anilines **(3)** and **(5)** may be unstable or more susceptible to oxidation. The monoamide intermediate may be too unstable, leading to decomposition prior to reacting with additional anilines to form diamide products (**8, 10, 11**). On TLC, all diamide compounds streaked on the silica plates, adding difficulty in visualizing the exact location of the products. These compounds tended to show strong adhesion to the silica which

drastically reduced the yield during chromatography. Fractional recrystallization was attempted using dichloromethane and methanol system, however, this technique was not effective in separating the products.

2.5.2. Monoamide Synthesis

2.5.2.1. Acyl Chloride Route

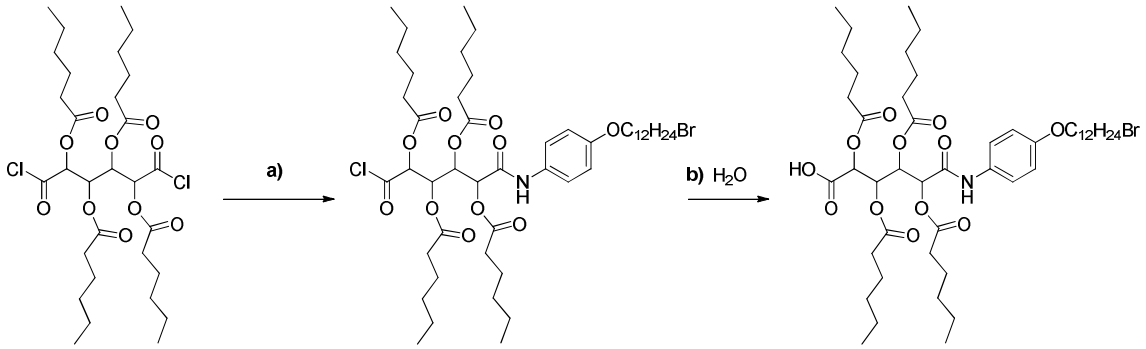

7

Scheme 9. Proposed reaction pathway for monoamide synthesis via acyl chloride. a) Addition of aniline (5) dropwise; b) quenching reaction mixture with acidic water.

To ease the purification of three diamide products, the synthesis and isolation of the monoamide may be more efficient. This method would separate unwanted by-products yielded in subsequent reactions generating mainly disubstituted, monosubstituted, and starting material **(6)**. The acyl chloride method was chosen where one equivalent of aniline was added slowly to an excess of diacid chloride solution **(7)** followed by quenching with water (**Scheme 9**). Aniline **(5)** was mainly used because its synthetic preparation was more convenient and required one fewer step than aniline **(3)**.

Table 4 summarizes the synthetic attempts on producing the monoamide via the acyl chloride route.

Table 4. Synthetic attempts on monoamide product via acyl chloride method.

Entry	6 (eq)	5 (eq)	TEA (eq)	Method	Time (h)	Results
1	1	0.8	26	**5** with TEA to flask dp for 3.5h	>12	NR
2	1	1	20.7	TEA to flask **5** dp for 3.5 h	>12	NR
3	1	1	Excess	TEA to pot, then **5** to pot	>12	NR
4	1	1	1.44	**7** to **5**	>12	15.18% **11** Potential Monoamide
5	1	1	20.6	**7** to **5**	>12	TLC-**11**, no monoamide

The addition of aniline **(5)** to diacid chloride solution **(7)** was tested. As insufficient base may be an issue, two experiments were conducted to analyze if the addition order of TEA had any influence on the yield. Aniline **(5)** was added to a solution of **(7)** dropwise in which excess TEA was added simultaneously and before the addition of the **(5)** (entries 1 and 2). Both reactions were completed over 12 h. The crude ^{1}H NMR did not show the expected methine peaks at 5.8 and 5.4 ppm. However, the aromatic proton environments of aniline **(5)** revealed that it formed an amide. The isolated fraction with the downfield aromatic protons of **(5)** indicated its coupling with hexanoic acid. The remaining residue on the column showed faint ^{1}H NMR signals of symmetric diamide product **(11)**. Thus, the addition of **(5)** to **(7)** was not promising. A published procedure by Uhrich's group was followed where **(6)** was activated by thionyl chloride under reflux for 4 h, dried to remove excess thionyl chloride, added excess base to the solution, and

then the addition of aniline **(5)** to **(7)** solution (entry 3). However, no product or aniline starting material was observed on ^{1}H NMR. These conditions suggested decomposition of **(5)**.

Observing from the non-symmetric diamide attempts, the addition of diacid chloride **(7)** to an aniline solution was feasible. The addition order was reversed by adding a solution of **(7)** to 1 eq. of aniline **(5)** and observed a 15% yield of symmetric diamide **(11)** (entry 4). The ^{1}H NMR did not show the expected four distinct methine environments which have splitting patterns of two doublets and two triplets. Recovered material from column chromatography showed mainly some diamide **(11)** and starting material **(6)**. A greater excess of TEA was then added and **(7)** to promote monoamide formation (entry 5). However, TLC and ^{1}H NMR of the crude mixture only showed formation of diamide **(11)** and monoamide **(13)** was absent.

The same procedure was also attempted utilizing aniline **(3)**. ^{1}H NMR showed coupling of aniline **(3)** to **(7)** as the symmetric diamide product **(10)** was formed. Two doublets were observed within the 6-5 ppm region on ^{1}H NMR but they did not correspond to the monoamide **(12)**. Further purification steps were abandoned due to the great amount of impurities.

In conclusion, synthesizing the monoamide via acyl chloride route was deemed difficult with no desired products observed. Aniline addition to an excess of diacid chloride solution did not generate the expected monoamide which was consistent with the previous experiments utilizing the step-wise addition. The reverse addition produced some symmetric diamide products but surprisingly did not yield the monoamide.

2.5.2.2. Cyclic anhydride synthesis

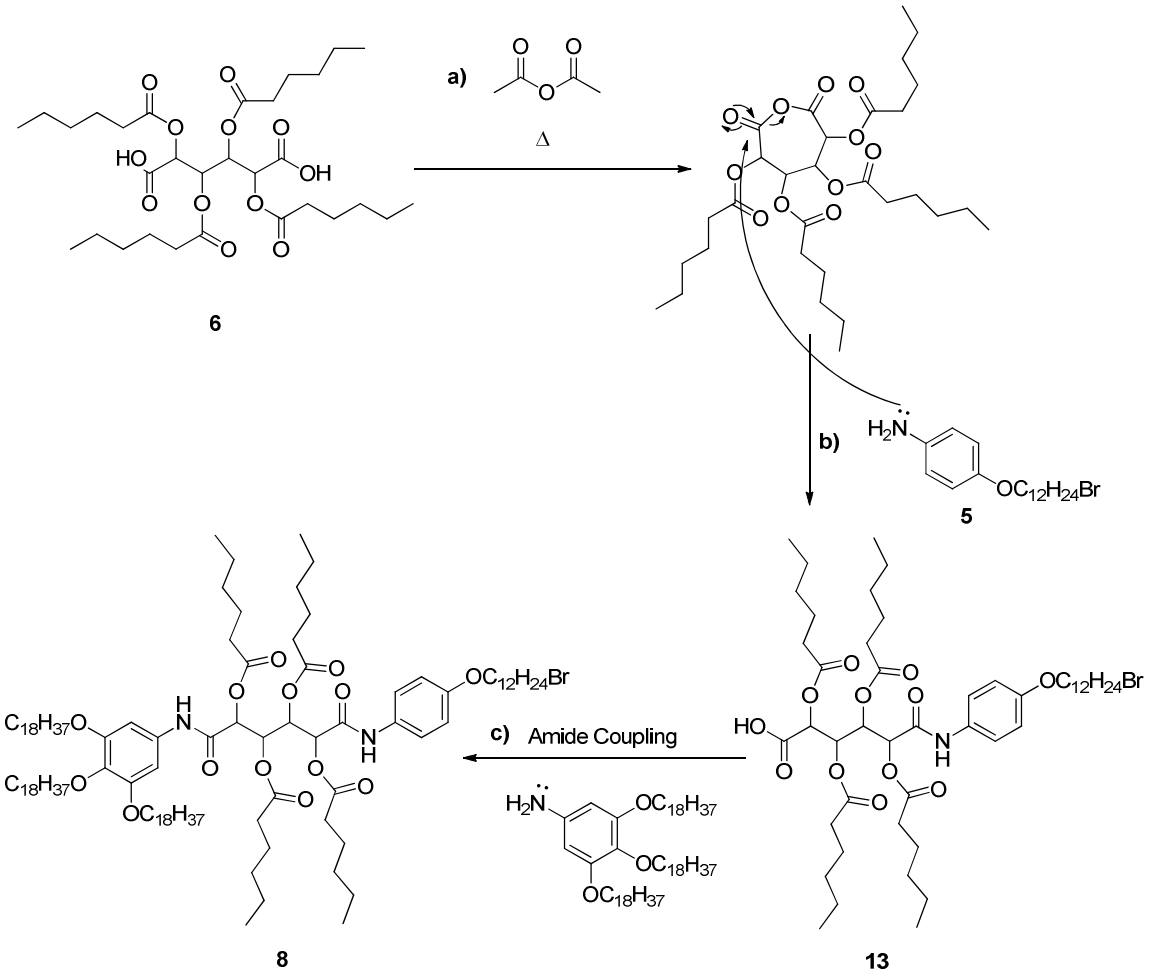

Scheme 10. Proposed synthetic route via cyclic anhydride. a) Activation of 6 with acetic anhydride to form a seven-membered cyclic anhydride intermediate; b) Aniline 5 would ring-open the cyclic anhydride intermediate to form the monoamide; c) Aniline 3 reacts with the free carboxylic acid site to generate 8

Limitations of the non-symmetric diamide formation with symmetrical carboxylic acids via the acyl chloride path included the rigid addition order of the reagents, purification difficulty, and the use of excess aniline derivatives with uncontrolled yields. A common strategy of inducing selectivity between dicarboxylic acids is the creation of a cyclic anhydride (**Scheme 10**). The creation of a cyclic anhydride from **(6)** to form a seven-membered heterocycle was proposed (**Scheme 10a**).[113] Upon activation of the

carboxylic acid group, it is attacked by a more nucleophilic species such as the intramolecular carboxylic acid. The formation of this structure is monitored via FT-IR when it exhibits its anhydride symmetric and non-symmetric stretches at 1870-1845 cm^{-1} and 1800-1775 cm^{-1} respectively while the carboxylic acid stretches simultaneously disappear.[114] A nucleophile (i.e. aromatic amine) would attack one of the carbonyl of the anhydride, causing the ring to open and forming a monoamide and carboxylate (**Scheme 10b**). The amount of aniline used is controlled as only one equivalent is needed.

Table 5. Summary of attempted synthesis of monoamide via cyclic anhydride.

Entry	Starting Material	Method	IR Result (cm^{-1})	Aromatic Amine	Outcome
1	6*	Ac_2O, 110 °C	1824.62, 1747.52	3,5-dimethylaniline	3,5-dimethylame coupled to acetic acid
2	6	Ac_2O, 120 °C, 4 Å Molecular Sieves	1820.37, 1729.07	-	Decomposed
3	6	Ac_2O, 120°C,	1823.82, 1748.73	3,5-dimethylaniline	3,5-dimethylaniline coupled to acetic acid
4	6	Ac_2O, 120°C	1824.14, 1745.91	**5**,TEA	**5** coupled to acetic acid
5	6	DCC, EtAc, DMF, THF, 0 °C-rt	1749.53, 1731.16	-	No anhydride stretches
6	6	$SOCl_2$ (1eq)	1848.91, 1755.48	3,5-dimethylaniline	No formation from ^1H NMR
7	6	$MgCl_2$, Boc_2O, THF, rt	1808.99, 1750.01, 1730.6	-	No change
8	6	$MgCl_2$, Boc_2O, THF, 60°C	1750.41, 173312	-	No anhydride and Boc_2O stretches, water present

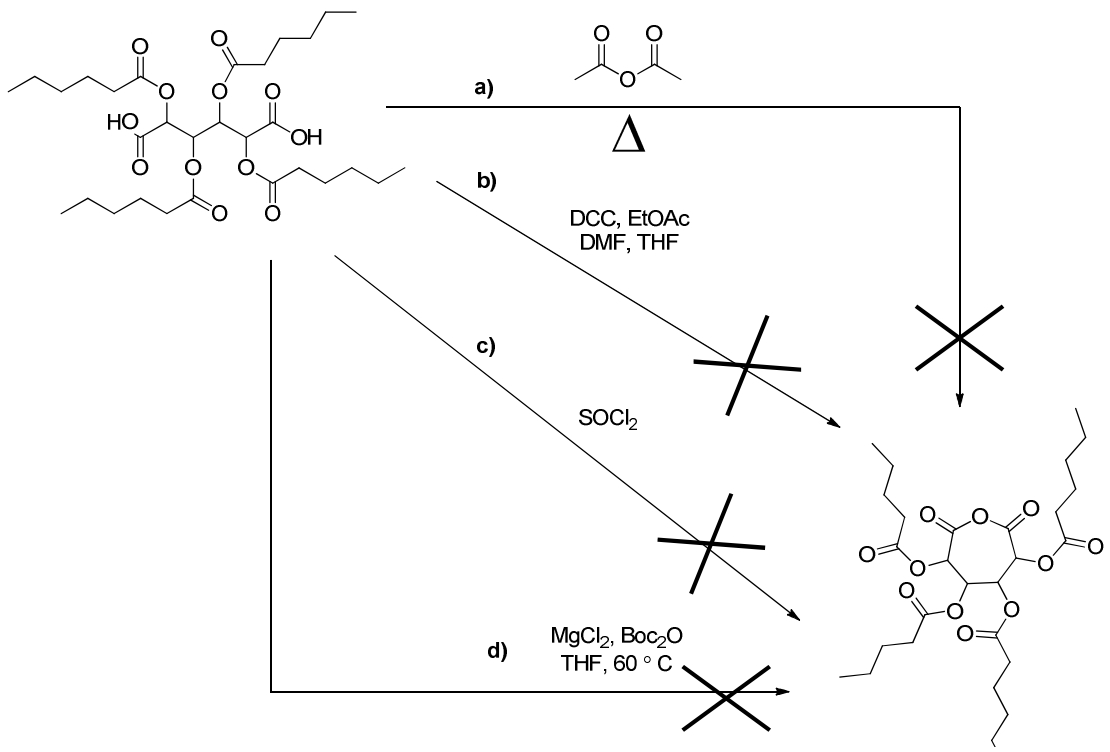

Scheme 11. Attempted synthesis of cyclic anhydride with 6. a) Acetic anhydride activation; Entries 1-4; b) DCC method; Entry 5; c) $SOCl_2$; Entry 6; d) Lewis acid with di-tert-butyl dicarbonate activation; Entries 7,8.

Synthetic trials of forming the cyclic anhydride are summarized in **Table 5**. The synthesis of the seven-membered cyclic anhydride with **(6)** by activating it with acetic anhydride above 100°C for >12 h was attempted (**Scheme 11a**). Any residual acetic anhydride was removed by heating under high-vacuum. The broad carboxylic acid and carbonyl stretches at 3497.08 cm^{-1} and 1721.28 cm^{-1} respectively both disappeared which indicated anhydride formation. However, the two anhydride stretches at 1824.62 and 1747.52 cm^{-1} did not correspond to the stretches of the seven membered ring. The strong stretch at 1747.52 cm^{-1} was assigned to the ester carbonyl stretches of **(6)** and may had overlapped the non-symmetric stretch. Nevertheless, 3,5-dimethylamine was added but did not yield the expected product (**Scheme 12**). The crude ^1H NMR spectrum

suggested that much of starting material **(6)** was present and did not form an amide. By-product N-(3,5-dimethylphenyl)acetamide was isolated which indicated that 3,5-dimethylaniline reacted with residual acetic anhydride in solution. Similar results were observed when drying for longer periods of time to remove acetic anhydride from the mixture. Monitoring the amount of acetic anhydride present was difficult to as it shared the same IR stretching frequencies.

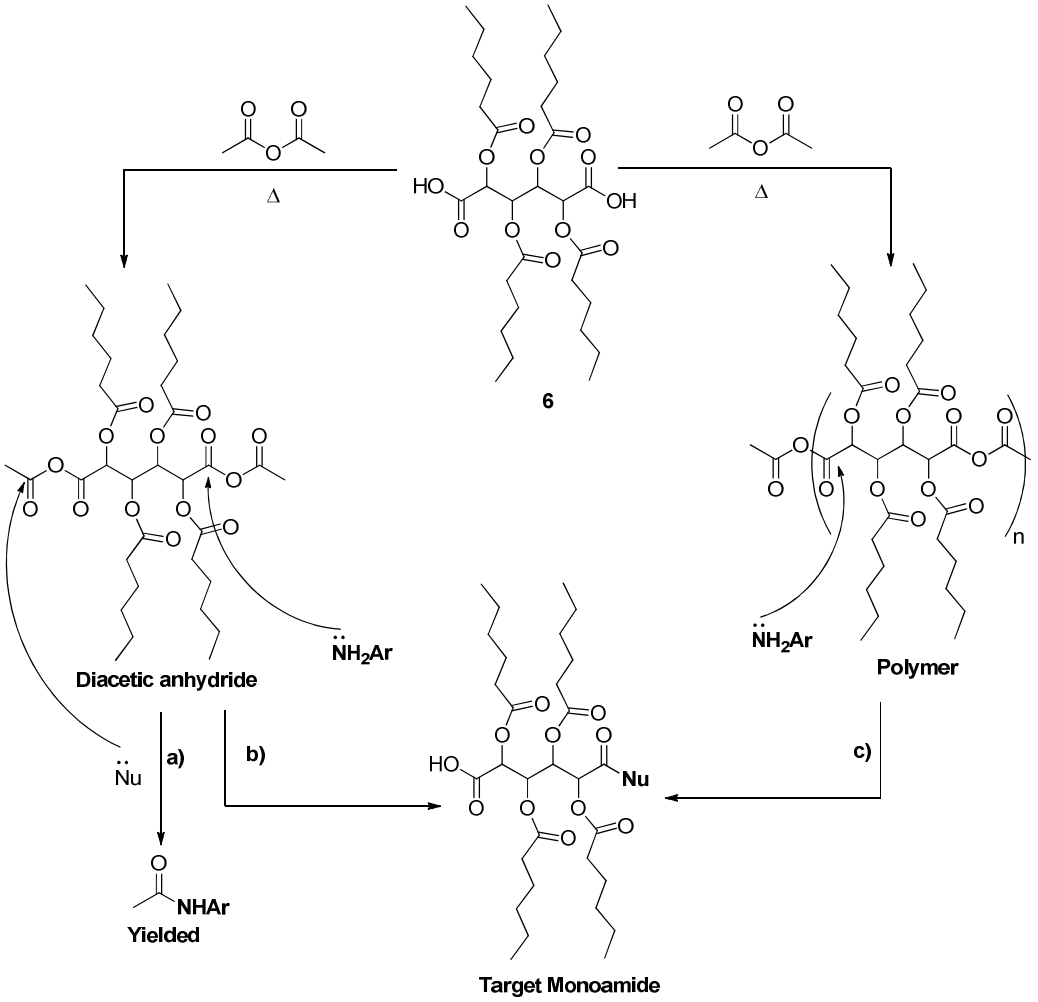

Scheme 12. Suggested reactivity through path **a)** yielding acetamide derivatives. **b)** aromatic amines can attack the carbonyl carbon closest to ester protecting groups on the diacetic anhydride to generate the target monoamide. c) aromatic amine can attack either carbonyl carbon of the polymer to generate the target monoamide. Note: stereochemistry on mucic acid is racemic.

Another possibility is the formation of polymers or linear diacetic anhydrides (**Scheme 12**). In the case of forming polymers (**Scheme 12c**), the internal non-cyclic anhydrides would allow for the incoming aromatic amine to react with either side, forming an amide and releasing the carboxylate of the polymer. However, the absence of the expected product suggested linear diacetic anhydride formation on both carboxylic acid positions of **(6).** In the case of the aniline attacking the linear anhydride of **(6)**, it is much faster to attack the carbonyl carbon furthest away from the molecule, resulting in starting material **(6)** and acetamide by-product (**Scheme 12a**). The intermediate structure was tested with aniline **(5)** in the presence of base and found similar results.

Alternatively, using different coupling agents to activate the carboxylic acid into a good leaving group was considered. N,N'-dicyclohexylcarboiimide (DCC) was employed Napoli *et al.* in creating seven membered cyclic anhydrides (**Scheme 11b**).[115] However, the reaction did not proceed as the carboxylic acid stretches remained the same and no anhydride stretches were observed.

The synthesis of the cyclic anhydride via acid chloride with 1 equivalent of thionyl chloride was conducted (**Scheme 11c**). A new stretch at a higher wavenumber of 1848.91 cm^{-1}, which fell within the predicted value, was observed. The non-symmetric stretch may have overlapped with the ester band. ^{13}C NMR revealed two new peaks at 161.01 and 160.86 ppm which suggested the formation of the cyclic anhydride. However, no amide was formed with 3,5-dimethylaniline.

A synthetic route by Thomas and coworkers on activating dicarboxylic acids with a Lewis acid ($MgCl_2$) and Boc_2O was utilized.[116] They have shown to synthesize cyclic anhydrides with varying ring sizes. Initially, this method did not result in any changes as the presence of water reduced the Lewis acid's activity (**Scheme 11d**). At 60 °C, no

product was observed as the carboxylic acid stretches were present and Boc_2O decomposed at this temperature.

In conclusion, the formation of a seven-membered heterocyclic was unsuccessful with various activating reagents on the carboxylic acid. Thionyl chloride showed the most promising result with IR stretches within reported cyclic anhydride values. In many cases the literature has shown the formation of cyclic anhydride between symmetric dicarboxylic acids on molecules with close proximity. The steric hindrance from the four ester groups on **(6)** may have prevented intramolecular interactions between the carboxylates.

2.5.2.3. DCC Method

Fortunately, amide synthesis via condensation of carboxylic acids and amines is well-studied, especially in peptide synthesis. One of the most employed amide coupling reagents is DCC which activates the carboxylic acid, rendering the -OH into a good leaving group as the incoming nucleophile (in this case, an amine) attacks the carbonyl, resulting an amide bond. Uhrich's group have synthesized amphiphilic macromolecules utilizing DCC and catalytic amounts of 3-(dimethylamino) pyridinium 4-toluenesulfonate to form mono-ester and mono-amide from PEG and aromatic amines respectively on dicarboxylic acid molecules (mucic acid and tartaric acid) in good yields (60-95%).[117–119] This amide coupling procedure was modified with aniline **(3)** and **(6)**, DCC catalyzed by 30 mol % DMAP (4-dimethylaminopyridine) and obtained a yield of 24 %. ^{1}H NMR showed four distinct environments between 5 – 6 ppm. This synthesis showed some advantages over the acyl chloride route as the monoamide compound was successfully separated from symmetric diamide and starting material and slightly showed improved yields. This coupling was also attempted with aniline **(5)** and **(6)** under similar conditions

but generated only 30 %. The yields were much lower than ones reported by Uhrich's group. Possible reasons include the formation of diamide product and the potential rearrangement into side product with N-acylurea. The yield was increased to approximately 50% when the reaction temperature was at 0 °C and an excess of DMAP was included.

In conclusion, monoamides **(12)** and **(13)** were successfully synthesized with DCC catalyzed by DMAP. This method supplanted the acyl chloride method as the reaction time was reduced and synthetic feasibility of the target monoamide was achieved. However, further optimization tests are needed to improve the reaction yields.

2.6. Thiolation of (8)

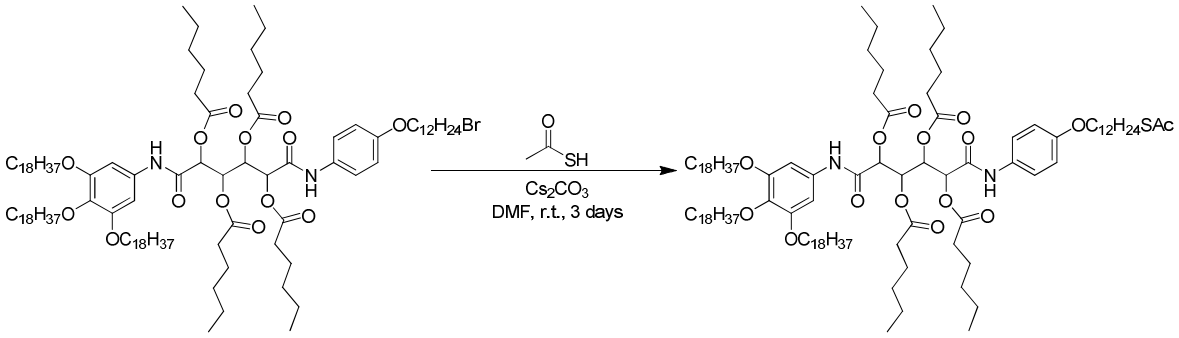

8 **14:** 28%

Scheme 13. Thiolation of Compound 8

The substitution on the carbon bearing the bromine on **(8)** with thioacetic acid in the presence of cesium carbonate in DMF was performed (**Scheme 13**). This S_N2 reaction generated **(14)** with a low yield of 28%. This is mainly due to the small scale of the reaction and the loss of product on purifying with preparative TLC. The ^1H NMR spectra showed successful substitution with a new triplet at 2.86 ppm.

2.7. Polarized Optical Microscopy Investigations

Diamide products **(8), (10), (11)** and monoamide products **(12)** and **(13)** have different segments. For instance, intermediate **(10)** possesses six hydrophobic octadecyloxy chains on the terminus while bearing four esters in the centre. The incompatible components within the same molecule will affect the packing order so that intermolecular interactions are maximized. For example, the molecule aligns in a parallel fashion so that the hydrophobic octadecyloxy chains will experience van der waal interactions while the esters interact via dipole-dipole. They may organize into different phases upon heating and display potential liquid crystal properties. The intermediate products **(10)**, **(11)**, and **(13)** were analyzed by polarized optical microscopy (POM) but no observable LC phases were present. Please refer to the Appendix B for POM images.

2.8. Synthesis of Novel Hydrophobic Ligand

Previously, our group has developed a novel hydrophobic ligand for metal NPs that may possess liquid crystalline properties and is interesting for the preparation of amphiphilic and Janus AuNPs.[120] Liquid crystallinity is a state of matter between that of the isotropic liquid and the anisotropic solid.[121] They display some positional order and fluidity simultaneously. Interested readers should address Nealon's review for further information. Compound **(19)** in **Scheme 14** features two rigid cores connected by an amide bond. The benzene core with three flexible octadecyloxy chains is incorporated to induce fluidity for the molecule. The incompatible components between the aromatic cores and octadecyloxy chains will cause the molecules to have preferential arrangements where components of similarity will interact. The ligand also features bidentate binding with two thiol groups to increase the number of gold-sulfur interactions with gold NPs.

The reaction conditions were optimized and the synthesis was demonstrated on the gram scale. In **Scheme 14a**, previous yields of **(15)** were low at 50% which was attributed to both the reaction conditions and purification steps. As discussed above, bases required sufficient drying in order to become effective for nucleophilic substitution. Precipitation with antisolvents was not a good method of purification since good yields were not generated. The purification was optimized with flash column chromatography and generated over 90% yield. In **Scheme 14d**, our group initially had difficulty in synthesizing **(17)** with yields below 80%. The yield was increased to 88% on the gram scale with thionyl chloride activating **(16)**. Furthermore, the addition sequence of aniline **(3)** and **(16)** had minimal effect on the yield. In the reduction of **(18)**, the reduction of thioester with lithium aluminum hydride for 24 h at room temperature was attempted but amide hydrolysis occurred as aniline **(3)** was regenerated. A more mild reaction

condition for successful thioester reduction was needed to reduce the side reaction. Another group member has shown successful reduction of the thioester without amide cleavage and has functionalized this novel ligand on gold NPs via the single-phase method. Overall, the reproducibility of this novel ligand was performed on the gram scale and certain moderate yielding reaction conditions were optimized.

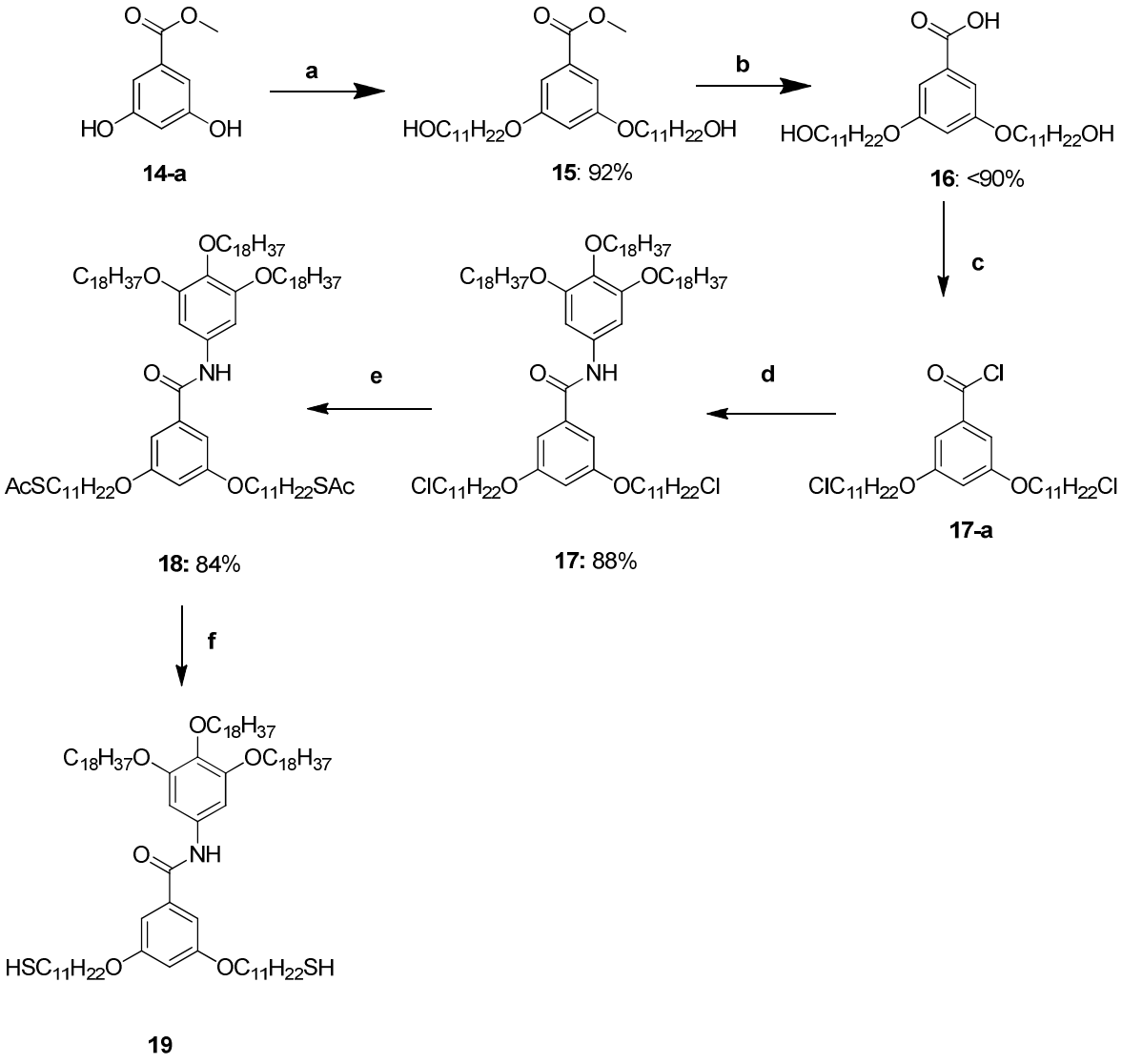

Scheme 14. Synthesis of Hydrophobic Ligand 18.[120] a) $BrC_{11}H_{22}OH$, K_2CO_3, DMF, 80 °C, 48h, $N_{2(g)}$ b) i) KOH, 100 °C, 4h, ii) HCl; c) i) $SOCl_2$, DMF, CH_2Cl_2, 0°C, 15 min, r.t. 24 h; d) (3), CH_2Cl_2, 24 h; e) Thioacetic acid, K_2CO_3, KI, DMF, 60 °C. f) $LiAlH_4$, THF, Decomposed

3. Conclusion and Future Works

In summary, the synthesis of the novel cross-linkable ligand in its protected form **(14)** in was demonstrated over 7 steps. Initial synthetic challenges to the protection of the alcohol groups on mucic acid, aniline derivatives **(3)** and **(5)** were overcame. The synthesis of **(8)** in high yields was very challenging due to the symmetrical dicarboxylic acid groups that inevitably generated symmetric diamide by-products. The acyl chloride method via dropwise addition of anilines **(3)** and **(5)** did not yield any product or minimal amounts of product. A main reason for this may be the instability of anilines **(3)** and **(5)** towards oxidation. The assumed monoamide/monochloride intermediates generated during the reaction may have decomposed prior to reacting with additional anilines in forming diamide products. Thus very little symmetric, non-symmetric diamide, and monoamide products were observed. The isolation of monoamide was attempted via different amide coupling syntheses (acyl chloride, cyclic anhydride, and DCC) to reduce the formation of symmetric diamide compounds **(10)** and **(11)**. The acyl chloride method did not generate any of the desired monoamide with the same issue of aniline stability. In the cyclic anhydride trials, the expected product was not synthesized possibly due to large steric hindrance from the ester protecting groups. DCC was also utilized and may be a more viable option with moderate yields of 50% in producing the monoamide which required optimization to match values from the literature. Lastly, the thiolation of **(8)** in generating the ligand in its protected form had a low yield of 28% due to the small reaction scale.

Future work will require optimization of the formation of the non-symmetric diamide **(8)**. The electron-rich aniline derivatives **(3)** and **(5)** may have been unstable for the formation of amides potentially due to oxidation, competitive side reactions (i.e. redox reactions), and decomposition of the monoamide intermediate in solution. A viable option to increase the stability of the aniline ligands is their transformation into isocyanates (**Scheme 15** and **Scheme 16**).[122,123] The advantage of isocyanates over anilines is their higher stability towards oxidation and they readily react with carboxylic acids, bypassing the use of thionyl chloride. The electron-deficient carbon of the isocyanate is attacked by the carboxylic acid oxygen, which subsequently forms the amide and releases carbon dioxide gas. Sasaki and Crich has demonstrated the formation of secondary amides with carboxylic acids containing free hydroxyls with isocyanates (**Scheme 17**).[124] This synthesis may help by-pass the protection of the tetra-alcohols and directly forming the secondary monoamide with a total of only four synthetic steps.

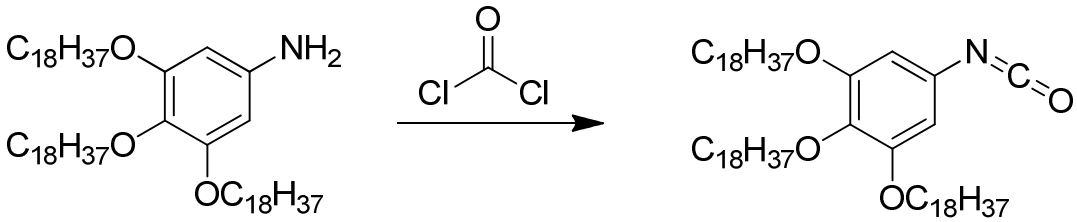

3

Scheme 15. Conversion of Aniline 3 to isocyanate.[123]

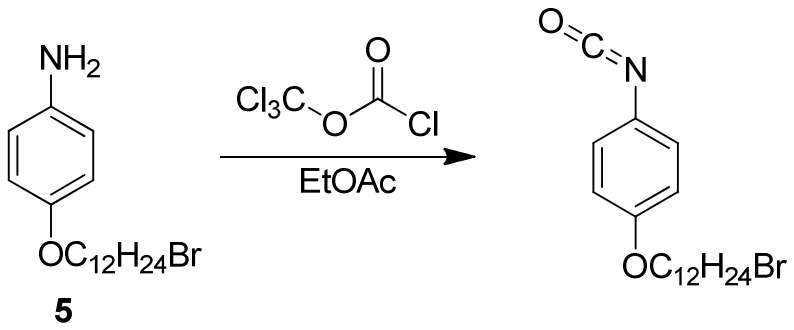

Scheme 16. Conversion of aniline 5 to isocyanate. [122]

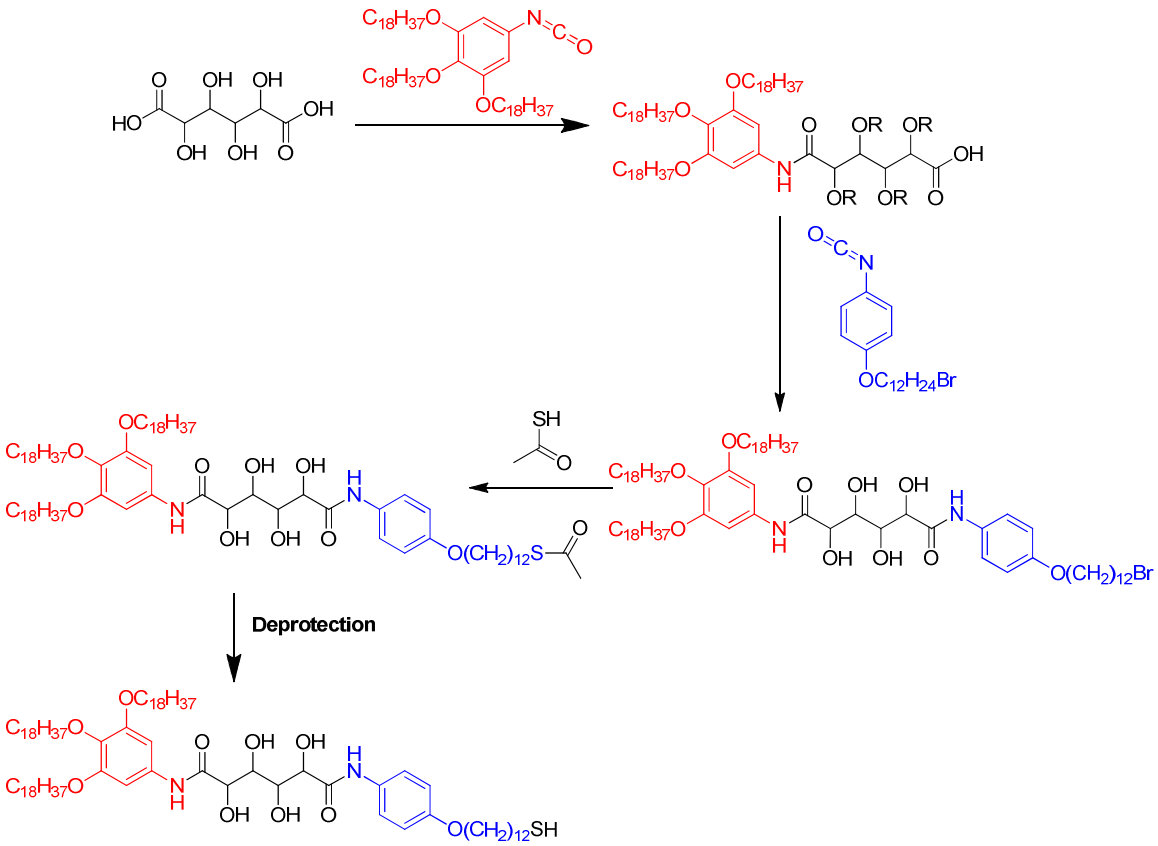

Scheme 17. Proposed synthetic scheme with isocyanate.[124]

Another consideration is to fully protect the carboxylic acids of mucic acid followed by monodeprotection (**Scheme 18**). The monocarboxylic acid will then react only at one site with either the anilines or isocyanate derivatives to generate the monoamide. The protected carboxylic acid will then undergo the second deprotection which subsequently reacts with the second aniline or isocyanate component. The advantage of this is process is the need for only one equivalent of aniline/isocyanate as formation of symmetric diamide products is eliminated. However, a drawback to this scheme is three additional synthetic steps (full protection followed by two stepwise deprotection) which is time-consuming.

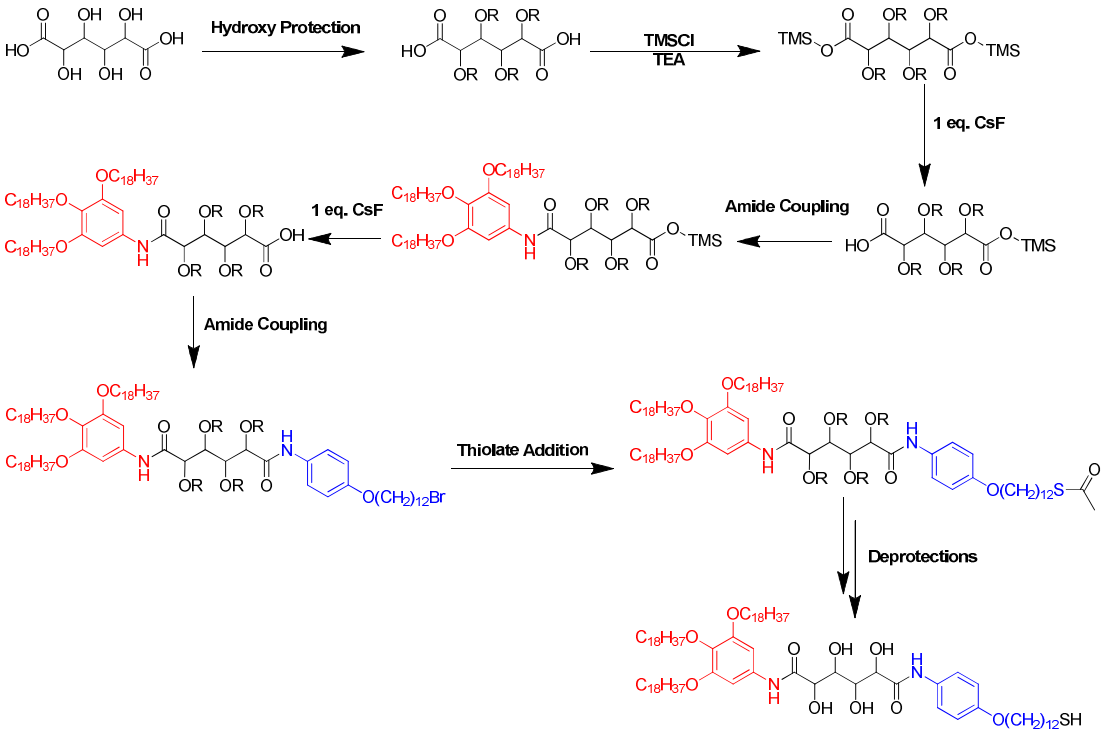

Scheme 18. Potential synthetic scheme involving full protection of the carboxylic acid sites followed by subsequent monodeprotection, monoamide formation, monodeprotection, non-symmetric diamide formation, thiolate addition, and deprotections.

Overall, both solutions of using isocyanates and stepwise deprotection could be utilized to obtain satisfactory yields to obtain at least one gram of the ligand in its deprotected form.

4. Experimental Data

Materials

All reagents and solvents obtained from Sigma-Aldrich, Fluka, Fischer Scientific, and Strem were used as received unless otherwise stated. Drying agents (3 Å and 4 Å molecular sieves) were purchased from VWR. Deuterated solvents were received from Sigma-Aldrich and Cambridge Isotope Laboratories and dried over 4 Å molecular sieves. Triethylamine, ethanol, DMF were filtered through activated basic Al_2O_3. Tetrahydrofuran, dichloromethane, toluene, and diethyl ether were obtained from the solvent purification system (Innovative Technology Inc. MA, USA, Pure-Solv 400). Flash column chromatography was performed using SiliaFlash F60 (230-400mesh, from Silicycle, Quebec Canada). Thin layer chromatography was conducted on SiliaPlate TLC Aluminum Backed TLC (200 μm thickness) and viewed under short wavelength UV light. Preparatory TLC was performed on SiliaPlate TLC Glass Backed TLC Extra Hard Layer, 60 Å (1000 μm thickness).

Methods and Instrumentation

^{1}H-NMR and ^{13}C-NMR spectra experiments were conducted on Bruker NMR spectrometers (DRX 500 MHz, DPX 300 US MHz, and DPX 300 MHz). The residual proton signal of deuterated solvents acted as the reference signal: $CDCl_3$ (δ 7.27 ppm) and CD_3OD (δ 3.31 ppm). Similarly, carbon signal of deuterated solvents acted as the reference signal: $CDCl_3$ (δ 77.16 ppm) and CD_3OD (49.99 ppm). Splitting patterns of assigned in the following: s = singlet, d = doublet, t = triplet, m = multiplet and dd = doublet of doublet. Data were reported in the following manner (multiplicity, coupling constant, integrations, proton assignment). 1st-order coupling constants were calculated in Hz.

Fourier Transform InfraRed Spectra (FT-IR) were obtained from Bruker Alpha FT-IR spectrometer. Peak intensities were reported as vs = very strong, s = strong, m = medium, w = weak, br = broad. Mass spectrometry experiments were conducted by Dr. Janeen Auld at the University of Windsor. Polarizing optical microscopy experiments were performed on Olympus TPM51 polarized light microscope with Linkam variable temperature stage HCS410. The images were obtained using digital photographic imaging system DITO1.

4.1. Synthesis of 1,2,3-tris(octadecyloxy)benzene (1)

Pyrogallol (1.514 g, 12.0 mmol, dried in vacuum at r.t. ºC 3 hours), 1-bromooctadecane (13.772 g, 41.3 mmol) and potassium carbonate (7.543g, 54.5 mmol, finely powdered and dried in vaccum at 115 ºC for 5 hours) were added to a solution of DMF (100 mL, filtered through activated basic Al_2O_3) in a 250 mL round bottom (rb) flask and the mixture was heated at 60 °C for 42 hours under $N_{2\,(g)}$. Ice-cold distilled water was added to the light-brown mixture and stirred for 1 hour. The resulting precipitate was filtered off, collected, dissolved in CH_2Cl_2 and extracted with water (100 mL X 3), dried over Na_2SO_4 and concentrated by rotary evaporation. Hot acetone was added to the flask to precipitate the product. The resulting white solid was then dissolved in CH_2Cl_2 and filtered through activated basic aluminum oxide. The solvent was removed to yield a white solid. Yield: 8.008g, 75.5%.

^{1}H NMR (300 MHz, $CDCl_3$): δ = 6.91 (t, *J* = 8.1 Hz, 1H), 6.54 (d, *J* = 8.1 Hz, 2H), 3.97 (t, *J* = 6.3 Hz, 4H), 3.95 (t, *J* = 6.2 Hz, 2H), 1.78 (m, *J* = 6.9 Hz, 6H), 1.47 (m, J, 6H), 1.26 (m, 84H), 0.89 (t, *J* = 6.3 Hz, 9H).

^{13}C NMR (300 MHz, $CDCl_3$): δ = 153.56, 138.56, 123.25, 106.91, 73.52, 69.23, 32.09, 30.50, 29.88, 29.59, 26.27, 22.85, 14.27.

Consistent with reported values[106]

4.2. Synthesis of 5-nitro-1,2,3-tris(octadecyloxy)benzene (2)

Silica gel (10g, 166.4 mmol) was stirred in 70% nitric acid solution (25 mL) for 2 h. The silica gel was filtered and dried under the high vacuum. The silica gel was titrated with 0.108 M NaOH and found to be 30% charged with HNO_3. Silica gel (3.841 g, 56.5 mmol) charged with 30% HNO_3 was suspended in dried CH_2Cl_2 (50 mL) in a 250 mL rb flask. Compound **1** (6.500g, 7.36 mmol) was dissolved in CH_2Cl_2 (100 mL) and added dropwise to the suspension at 0 °C. The purple reaction mixture was warmed to room temperature after 30 minutes and stirred for 3.5 hours under $N_{2\,(g)}$. The resulting orange mixture was then filtered and washed with 35 °C CH_2Cl_2. The filtrate was collected and extracted with water, dried over Na_2SO_4 and concentrated by rotary evaporation.

Acetone was warmed to 50 °C and added to the flask to precipitate the product. The precipitate was filtered and rinsed with cold acetone, dried under the high vacuum to yield a white solid. Yield: 4.794 g, 70.2%.

^{1}H NMR (300 MHz, $CDCl_3$): δ = 7.47 (s, 2H), 4.03 (t, *J* = 6.6 Hz, 6H), 1.84 (m, *J* = 6.9 Hz, 6H), 1.26 (m, 90H), 0.88 (t, *J* = 6.6 Hz, 9H)

^{13}C NMR (300 MHz, $CDCl_3$): δ = 152.85, 143.99, 143.30, 102.31, 73.97, 69.61, 32.08, 29.87, 29.52, 29.26, 26.17, 22.84, 14.26.

Consistent with reported values.[106]

4.3. Synthesis of 3,4,5-tris(octadecyloxy)aniline (3)

Compound **2** (3.637 g, 3.9 mmol) and graphite (2.328 g, 193.8 mmol) were added to a solution of ethanol (200 mL, filtered through basic activated Al_2O_3) in a 250 mL two-neck rb flask. Hydrazine monohydrate (1 mL, 19.9 mmol) was added to the reaction mixture dropwise at room temperature. The reaction mixture was heated at reflux for 2 days under $N_{2\,(g)}$. The resulting mixture was filtered and washed with CH_2Cl_2. The filtrate was concentrated by rotary evaporation and precipitated with hot ethanol. The obtained white solid was filtered and dried. Yield: 3.000g, 85%.

^{1}H NMR (300 MHz, $CDCl_3$): δ = 5.91 (s, 2H), 3.91 (t, *J* = 6.3 Hz, 2H), 3.84 (t, *J* = 6.3 Hz, 2H), 3.46 (br, 2H), 1.75 (m, *J* = 7.5 Hz, 6H), 1.55-1.22 (m, 96H), 0.88 (t, *J* = 6.6 Hz, 9H)

^{13}C NMR (300 MHz, $CDCl_3$): δ = 153.97, 142.51, 94.79, 69.24, 32.16, 29.95, 29.66, 29.60, 26.34, 22.92, 14.34.

Consistent with reported values.[106]

4.4. Synthesis of 1-((12-bromododecyl)oxy)-4-nitrobenzene (4)

4-nitrophenol (4.048 g, 29.0 mmol), 1,12-dibromododecane (18.935 g, 57.7 mmol), and K_2CO_3 (4.400 g, 30.8 mmol) were added to DMF (100 mL, filtered through activated basic Al_2O_3). The mixture was purged with $N_{2(g)}$ and was stirred at room temperature for 24 h. Ethyl acetate was added to the yellow solution was extracted brine (5 X 100 mL), dried over Na_2SO_4, and dried by rotary evaporation The resulting solid was subjected to flash column chromatography on silica gel (hexanes; 7:1 hexanes/diethyl ether) and dried by rotary evaporation to give a white solid. Yield: 8.549 g, 81.8%.

^{1}H NMR (300 MHz, $CDCl_3$): δ = 8.22 (d, *J* = 9.3 Hz, 2H), 6.94 (d, *J* = 9.3 Hz, 2H), 4.05 (t, *J* = 6.6 Hz, 2H), 3.41 (t, *J* = 6.6 Hz, 2H), 1.83 (m, *J* = 6.9 Hz, 4H), 1.29 (m, 16H)

Consistent with reported values.[105]

4.5. Synthesis of 4-((12-bromododecyl)oxy)aniline (5)

Compound **4** (3.500 g, 9.0 mmol), $SnBr_2$ (8.615g, 30.9 mmol), and 37% HCl (5 mL) were added to anhydrous EtOH (50 mL, filtered through activated basic Al_2O_3) in a 2-neck 100 mL rb flask. The mixture was stirred at reflux for 24 h under $N_{2(g)}$. The mixture was cooled to room temperature and KOH solution was added until a basic pH. The mixture was washed with CH_2Cl_2 (5 X 50 mL), the organic layer was collected and washed with neutral brine (2 X 50 mL), dried over Na_2SO_4 and dried to a pale burgundy solid. The solid was stored under inert gas. Yield: 2.402 g, 74.4%.

^{1}H NMR (300 MHz, $CDCl_3$): δ = 6.74 (d, *J* = 9 Hz, 2H), 6.64 (d, *J* = 8.7 Hz, 2H), 4.05 (t, *J* = 3.6 Hz, 2H), 3.41 (t, *J* = 6.6 Hz), 1.87 (m, *J* = 4.2 Hz, 2H), 1.75 (m, *J* = 3.3 Hz, 2H), 1.29 (m, 16H)

^{13}C NMR (300 MHz, $CDCl_3$): δ = 152.44, 139.93, 116.50, 115.77, 68.80, 45.29, 34.15, 29.66, 29.53.

Consistent with reported values.[105]

4.6. Synthesis of 2,3,4,5-tetrakis(hexanoyloxy)hexanedioic acid (6)

Mucic acid (0.500 g, 2.4 mmol), hexanoyl chloride (3.0 mL, 21.5 mmol), and $ZnCl_2$ (0.040g, 0.3 mmol) were added to a 2-neck 100 mL rb flask, stirred and heated to reflux for 24 h under $N_{(g)}$. The resulting black solution was dissolved in diethyl ether and cooled to room temperature. The mixture was added to a flask of ice cold water dropwise and stirred for 1 h. The organic layer was extracted with brine (3 X 50 mL), dried over Na_2SO_4, and concentrated by rotary evaporation. Warm hexanes was added to the flask, stored in the fridge, filtered, and collected as white solid. Yield: 1.104g, 77.0%.

^{1}H NMR (300 MHz, $CDCl_3$): δ = 5.71 (s, 2H), 5.18 (s, 2H), 2.45 (t, *J* = 6.3 Hz, 4H), 2.31 (t, *J* = 5.1 Hz, 4H), 1.65 (m, *J* = 7.5 Hz, 4H), 1.58 (m, *J* = 6.3 Hz, 4H), 1.35 (m, *J* = 6.3 Hz, 8H), 1.30 (m, *J* = 3.0 Hz, 8H), 0.92 (t, *J* = 3.9 Hz, 12H)

^{13}C NMR (300 MHz, $CDCl_3$): δ = 172.98, 172.27, 172.03, 68.98, 68.02, 33.90, 33.70, 31.32, 31.28, 24.52, 24.38, 22.49, 22.41, 14.06, 14.01

IR (ATR) cm^{-1}: 2958-2859 (m, C-H), 1748 (vs, C=O), 1727 (vs, C=O, COOH)

Consistent with reported values.[102]

4.7. Synthesis of 1,6-dichloro-1,6-dioxohexane-2,3,4,5-tetrayl tetrahexanoate (7)

Compound **6** (0.515 g, 0.854 mmol), DMF (1.0 mL, 12.9 mmol), filtered through activated basic Al_2O_3), 20 mL CH_2Cl_2 were added to a 100 mL rb flask. Under inert nitrogen gas, $SOCl_2$ (0.35 mL, 4.8 mmol) was added dropwise over 1 min at 0 °C and allowed to stir for 10 minutes. The mixture was stirred at room temperature for over 12 h. The resulting yellow solution was dried under high-vacuum, dispersed with anhydrous CH_2Cl_2, and dried under high vacuum three times. The product was not isolated and purified but used in-situ for subsequent reactions. ^{1}H-NMR of the crude product is provided below.

^{1}H NMR (500 MHz, $CDCl_3$): δ = 5.77 (s, 2H), 5.19 (s, 2H), 2.48-2.45 (m, *J* = 3.5 Hz, 4H), 2.33-2.30 (m, *J* = 2.5 Hz, 4H), 1.68-1.65 (m, 4H), 1.58-1.54 (m, *J* = 7.5 Hz, 4H), 1.35-1.30 (m, *J* = 4.0 Hz, 8H), 1.28-1.26 (m, 8H), 0.92-0.87 (t, 12H)

4.8. Synthesis of 1-((4-((12-bromododecyl)oxy)phenyl)amino)-1,6-dioxo-6-((3,4,5-tris(octadecyloxy)phenyl)amino)hexane-2,3,4,5-tetrayltetra hexanoate (8)

Compound **5** (0.300 g, 0.841 mmol) and **3** (0.712 g, 0.792 mmol) were added to a 2-neck 250 mL round bottom flask, and dried under high vacuum. 30 mL anhydrous $CH_2Cl_2$was added and stirred at room temperature under inert nitrogen gas. Dried trimethylamine (<1mL, filtered through activated basic Al_2O_3) was added. **1,6-dichloro-1,6-dioxohexane-2,3,4,5-tetrayl tetrahexanoate (7)** (0.450 g, 0.746 mmol) in 14 mL anhydrous $CH_2Cl_2$was added dropwise over 5-10 minutes. The reaction mixture was stirred at room temperature for 18 hours. The resulting brown mixture was washed with 0.1 M HCl water (25mL X 4) and brine (25 mL), dried over Na_2SO_4, filtered, and dried by rotary evaporation resulting in a brown solid (1.08 g). Flash chromatography on silica gel was applied (7:1 hexanes/ethyl acetate), concentrated by rotary evaporation and precipitated in CH_2Cl_2/MeOH, filtered, and resulting a white solid. Yield: 0.462 g, 34%.

^{1}H NMR (300 MHz, $CDCl_3$): δ = 7.49 (s, 1H, H_a), 7.45 (s, 1H, H_b), 7.33 (d, *J* = 9 Hz, 2H, H_c), 6.83 (d, *J* = 9 Hz, 2H, H_d), 6.68 (s, 2H, H_e), 5.80 (d, 2H, H_f), 5.41 (s, 1H, H_g), 5.39 (s, 1H, H_h), 3.94-3.86 (t, 8H, $H_{i,j,k}$), 3.41 (t, *J* = 6.9 Hz, 2H, H_l), 2.60-2.44 (m, *J* = 7.2 Hz, 4H, H_m), 2.31-2.16 (m, *J* = 7.2 Hz, 4H, H_n), 1.88-1.64 (m, 14H, $H_{o,p,q,r}$), 1.26 (m, 126H, $H_{s,t,u,v,w}$), 0.93-0.86 (t, 15H, $H_{x,z}$), 0.80-0.76 (t, 6H, H_y).

^{13}C NMR (300 MHz, $CDCl_3$): δ = 172.38, 172.84, 164.71, 156.80, 153.49, 135.83, 132.20, 129.53, 121.90, 115.08, 99.40, 73.71, 71.44, 69.45, 68.44, 68.36, 45.31, 36.86, 34.09, 33.94, 32.13, 29.92, 29.87, 29.64, 29.57, 26.31, 24.44, 22.89, 14.28

IR (ATR) cm^{-1}: 3307 (vw, N-H), 2917-2850 (s, C-H), 1750 (m, C=O), 1671 (m, C=O)

TLC (Silica, hexanes/ethyl acetate 6:1) Rf: 0.53

4.9. Synthesis of 1,6-bis((3,5-dimethylphenyl)amino)-1,6-dioxohexane-2,3,4,5-tetrayl tetrahexanoate (9)

Compound **9** was prepared similarly to the procedure of **8**. A solution of 3,5-dimethylaniline (0.11 mL, 0.8 mmol), triethylamine (0.12 mL, 0.8 mmol, filtered through activated basic Al_2O_3) in 3 mL CH_2Cl_2 were added to the diacid chloride **7** dropwise for 10 min and stirred for 24 h at r.t. The mixture was heated to 30 °C for 2 h. The mixture was extracted with 0.1 M HCl water (50 mL X 4) and 50 mL neutral brine, dried over Na_2SO_4, filtered, and dried by rotary evaporation, yielding an off-yellow solid. Yield: 0.260g, >90%.

^{1}H NMR (300 MHz, $CDCl_3$): δ = 7.48 (s, 2H, H_a), 7.08 (s, 4H, H_b), 6.77 (s, 2H, H_c), 5.81 (s, 2H, H_d), 5.40 (s, 2H, H_e), 2.61-2.45 (m, *J* = 7.2 Hz, 4H, H_f), 2.34-2.15 (m, *J* = 9.0 Hz, 16H, $H_{g,h}$), 1.75-1.65 (m, *J* = 7.2 Hz, 4H, H_i), 1.49-1.42 (m, *J* = 7.2 Hz, 4H, H_j), 1.40-1.32 (m, *J* = 3.6 Hz, 8H, H_k), 1.15-1.12 (m, 8H, H_l), 0.93 (t, *J* = 5.4 Hz, 6 H, H_m), 0.79 (t, *J* = 7.9 Hz, 6H, H_n)

^{13}C NMR (300 MHz, $CDCl_3$): δ = 172.30, 171.75, 164.76, 139.03, 136.47, 126.98, 117.74, 71.50, 68.31, 34.09, 33.90, 31.45, 31.25, 24.43, 24.38, 22.52, 22.33, 21.42, 14.02, 13.83

4.10. Synthesis of 1,6-dioxo-1,6-bis((3,4,5-tris (octadecyloxy) phenyl) amino) hexane-2,3,4-5-tetrayl tetrahexanoate (10)

Compound **10** was collected from reaction (g). It was dried by rotary evaporation. The solid was dissolved in small amounts of CH_2Cl_2 and precipitated with MeOH and stored in the fridge. The precipitate was filtered off and dried to yield a white solid. Yield: 80 mg, 4.5 %.

^{1}H NMR (300 MHz, $CDCl_3$): δ = 7.41 (s, 2H, H_a), 6.68 (s, 4H, H_b), 5.80 (s, 2H, H_c), 5.40 (s, 2H, H_d), 3.95-3.86 (t, *J* = 6.6 Hz, 12H, $H_{e,f}$), 2.64-2.45 (m, *J* = 7.5 Hz, 4H, H_g), 2.34-2.16 (m, *J* = 7.5 Hz, 4H, H_h), 1.81-1.67 (m, *J* = 6.9 Hz, 16H, $H_{i,j,k,l}$), 1.45-1.15 (m, 200 H, H_m), 0.93-0.86 (t, 24H, $H_{n.o}$), 0.80-0.76 (t, *J* = 6.6 Hz, 6H, H_p).

^{13}C NMR (300 MHz, $CDCl_3$): δ = 172.32, 171.79, 164.71, 153.52, 135.91, 132.13, 99.40, 73.70, 71.50, 69.47, 68.32, 34.11, 33.94, 32.13, 31.45, 31.31, 30.50, 29.92, 29.86, 29.57, 26.30, 24.45, 22.88, 22.56, 22.38, 14.28, 14.06, 13.93

TLC (Silica, hexanes/ethyl acetate 6:1) Rf: 0.7

IR (ATR) cm^{-1}: 3283 (vw, N-H), 2954-2850 (vs, C-H), 1755-1741 (s, C=O), 1671 (s, C=O).

4.11. Synthesis of 1,6-bis((4-((12-bromododecyl)oxy)phenyl)amino)-1,6-dioxohexane-2,3,4,5-tetrayl tetrahexanoate (11)

Compound 11 was collected from reaction (g). It was dried by rotary evaporation. The solid was dissolved in small amounts of CH_2Cl_2 and precipitated with MeOH and stored in the fridge. The precipitate was filtered off and dried to yield a white solid. Yield: 0.102 g, 10.7 %.

^{1}H NMR (300 MHz, $CDCl_3$): δ = 7.51 (s, 1H, H_a), 7.33 (d, *J* = 9.0 Hz, 4H, H_b), 6.82 (d, *J* = 8.7 Hz, 4H, H_c), 5.81 (s, 2H, H_d), 5.40 (s, 2H, H_e), 3.90 (t, *J* = 6.6 Hz, 4H, H_f), 3.40 (t, *J* = 6.9 Hz, 4H, H_g), 2.62-2.42 (m, *J* = 3.6 Hz, 4H, H_h), 2.32-2.13 (m, *J* = 5.4 Hz, 4H, H_i), 1.89-1.77 (m, 12H, $H_{j,k,l}$), 1.5-1.12 (m, 52H, $H_{m,n,o}$), 0.95-0.87 (t, 6H, H_p), 0.81-0.74 (t, *J* = 7.8 Hz, 6H, H_q)

^{13}C NMR (300 MHz, $CDCl_3$): δ = 172.26, 171.66, 164.59, 156, 129.38, 121.72, 114.79, 71.28, 68.24, 68.15, 45.14, 38.72, 34.00, 33.82, 33.64, 32.83, 31.22, 31.07, 29.70, 29.51, 29.42, 29.37, 29.23, 28.76, 28.17, 26.01, 24.19, 22.36, 22.21, 13.91, 13.77, 10.97.

IR (ATR) cm^{-1}: 3335 (w, N-H), 2954-2853 (s, C-H), 1747 (vs, C=O), 1671 (s, C=O).

MALDI-MS m/z for $C_{66}H_{106}Br_2N_2O_{12}$ calculated (MH^+) = 1278.6104. Found (MH^+)= 1278.6125.

TLC (Silica, hexanes/ethyl acetate 6:1) Rf: 0.3

4.12. Synthesis of 2,3,4,5-tetrakis(hexanoyloxy)-6-oxo-6-((3,4,5-tris(octadecyloxy)phenyl)amino)hexanoic acid (12)

Compound **6** (0.200 g, 0.3 mmol), **3** (0.298 g, 0.3 mmol), DMAP (0.074 mmol, 0.1 mmol), DMF (1-2 mL, filtered through activated basic Al_2O_3), and 25 mL anhydrous CH_2Cl_2 were added to a 100 mL rb flask. DCC (0.014 g, 0.3 mmol) in 5 mL CH_2Cl_2 were added dropwise into the reaction mixture and stirred at room temperature for 24 h under nitrogen gas. The reaction mixture was diluted with CH_2Cl_2, stored in the fridge, and filtered. The filtrate was washed with pH 1 water (25 mL X 5), dried over Na_2SO_4, filtered and concentrated via rotary evaporator. The mixture was purified via flash column chromatography on silica gel (2: 1 hexanes/ethyl acetate), dried, and collected an off-white solid. Yield: 118 mg, 23.98%.

^{1}H NMR (300 MHz, $CDCl_3$): δ = 7.43 (s, 1H, H_a), 6.68 (s, 2H, H_b), 5.85 (dd, *J* = 6.3 Hz, 1H, H_c), 5.68 (dd, *J* = 10.8 Hz, 1H, H_d), 5.43 (s, 1H, H_e), 5.11 (s, 1H, H_f), 3.94-3.86 (t, *J* = 6.3 Hz, 6H, $H_{g,h}$), 2.53-2.43 (m, 4H, H_i), 2.34-2.18 (m, 4H, H_j), 1.80-1.57 (m, 10H, $H_{k,l}$), 1.45-1.26 (m, 110H, $H_{m,n,o}$), 0.91-0.86 (t, 15H, $H_{p,q}$), 0.80-0.75 (t, 6H, H_r).

^{13}C NMR (300 MHz, $CDCl_3$): δ = 173.29, 172.33, 171.55, 164.73, 153.45, 135.62, 132.23, 99.23, 73.70, 71.51, 69.38, 68.49, 68.13, 66.08, 49.78,m 33.71, 32.14, 31.45, 30.49, 29.94, 29.89, 29.65, 29.54, 26.31, 25.68, 25.00, 24.51, 24.36, 22.91, 22.58, 22.54, 22.48, 22.40, 14.33, 14.22, 13.96

MALDI MS: Calculated for $C_{90}H_{163}NO_{14}$ (M^+) = 1483.21463 (100.0%). Founded (M^+) = 1482.2089.

4.13. Synthesis of 6-((4-((12-bromododecyl)oxy)phenyl)amino)-2,3,4,5-tetrakis(hexanoyloxy)-6-oxohexanoic acid (13)

Compound **6** (3.070 g, 5.9 mmol), **5** (0.443 g, 1.24 mmol), DMAP (0.600 g, 5.4 mmol), DMF (5 mL, filtered through activated basic Al_2O_3), were added to a 100 mL rb flask with anhydrous CH_2Cl_2 (50 mL). The mixture was purged with inert gas (nitrogen) and was stirred in an ice bath. DCC (1.060 g, 5.14 mmol) was dissolved in 10 mL CH_2Cl_2 and added dropwise over 5 min to the flask. The mixture was stirred at 0 °C for 1 h and then warmed to room temperature and stirred for 24 h. The mixture was then diluted with

CH_2Cl_2 and stored in the freezer to precipitate DCU for a few hours. The mixture was filtered and rinsed with minimal amounts of cold CH_2Cl_2 and the filtrate was collected, extracted with 0.1 M HCl water (50 mL X 3) and then neutral brine (50 mL), dried over Na_2SO_4, filtered, and dried by rotary evaporation. The mixture was subjected to flash column chromatography on silica gel (hexanes/ethyl acetate 4:1). White solid was dried by rotary evaporator and collected. Yield: 0.476g, 50.2%.

^{1}H NMR (300 MHz, $CDCl_3$): δ = 7.35 (s, 1H, H_a), 7.34 (d, *J* = 9.7 Hz, 2H, H_b), 6.83 (d, *J* = 8.7 Hz, 2H, H_c), 5.88 (dd, *J* = 9.9, 1.8 Hz, 1H, H_d), 5.67 (dd, *J* = 9.9, 1.8 Hz, 1H, H_e), 5.46 (d, *J* = 2.0 Hz, 1H, H_f), 5.13 (d, *J* = 1.8 Hz, 1H, H_g), 3.91 (t, *J* = 6.6 Hz, 2H, H_h), 3.41 (t, *J* = 6.9 Hz, 2H, H_i), 2.56-2.48 (m, 4H, H_j), 2.35-2.18 (m, 4H, H_k), 1.93-1.57 (m, 8H, H_l), 1.55-1.15 (m, 36H, H_m), 0.94-0.87 (t, 12H, H_n)

^{13}C NMR (300 MHz, $CDCl_3$): δ = 173.10, 172.22, 171.44, 164.59, 156.62, 129.47, 121.84, 114.95, 71.38, 68.40, 67.97, 45.28, 33.99.

IR (ATR) cm^{-1}: 3493 (vw, O-H), 3323 (w, N-H), 2954-2852 (s, C-H), 1749 (vs, C=O), 1722 (s, C=O), 1671 (s, C=O).

MALDI MS m/z for $C_{90}H_{163}NO_{14}$ Calculated (MNa^+) = 961.45268 (100%). Founded (MNa^+) = 962.4606.

4.14. Synthesis of 1-((4-((12-(acetylthio)dodecyl)o.xy)phenyl)amino)-1,6-dioxo-6-((3,4,5-tris(octadecyloxy)phenyl)amino)hexane-2,3,4,5-tetrayl tetrahexanoate (14)

Compound **8** (0.142 g, 0.077 mmol) and cesium carbonate (0.100 g, 0.30 mmol) were added to a 100 mL rb flask. DMF (10 mL, filtered through activated asic Al_2O_3) was added to the flask and stirred at r.t.. Thioacetic acid (0.05 mL, 0.7 mmol) was added dropwise to the flask and allowed to stir for 3 days under nitrogen gas. The opaque hazel coloured mixture was dissolved with CH_2Cl_2 and extracted with water (25 mL X 3) and brine (25 mL), dried over Na_2SO_4, filtered, and dried by rotary evaporation. The crude mixture was dissolved with small amounts of CH_2Cl_2 and precipitated with methanol and stored in the fridge overnight. The precipitate was collected and subjected

to preparative TLC on silica gel (hexanes/ethyl acetate 10:1), collected as a solid. Yield: 40 mg, 28%.

^{1}H NMR (300 MHz, $CDCl_3$): δ = 7.47 (s, 1H, H_a), 7.439 (s, 1H, H_b), 7.30 (d, *J* = 8.7 Hz, 2H, H_c), 6.83 (d, *J* = 9.0 Hz, 2H, H_d), 6.68 (s, 2H, H_e), 5.80 (s, 2H, $H_{f,f'}$), 5.41 (s, 1H, H_g), 5.39 (s, 1H, H_h), 3.94-3.86 (t, 8H, $H_{i,j,k}$), 2.89-2.84 (t, *J* = 7.2 Hz, 2H, H_l), 2.60-2.47 (m, 4H, H_m), 2.32 (s, 3H, H_n), 2.28-2.17 (m, 4H, H_o), 1.80 -1.67 (m, 12H, $H_{p,q,r}$), 1.59-1.26 (m, 128 H, $H_{s,t,u,v,w}$), (t, 15 H, H_{xz}), (t, 6H, H_y)

^{13}C NMR (300 MHz, $CDCl_3$): δ = 196.22, 172.30, 171.76, 164.67, 156.72, 153.43, 135.69, 132.09, 129.41, 12180, 115.00, 99.22, 73.64, 71.34, 69.35, 68.44, 68.31, 34.04

IR (ATR) cm^{-1}: 3517, 3401, 3312 (s, N-H), 2916-2850 (s, C-H), 1749.24 (m, C=O), 1671.49 (C=O), 1104 (S-C=O)

4.15. Synthesis of methyl 3,5-bis(11-hydroxyundecyl)oxy)benzoate (15)

3,5-dihydroxy methyl benzoate (2.000g, 11.8 mmol), 11-bromo-1-undecanol (7.469 g, 29.7 mmol), and dried potassium carbonate (6.575 g, 47.6 mmol) were added to a 250 mL rb flask in 100 mL DMF and stirred at 80 °C for 48h under nitrogen gas. The mixture was dissolved with ethyl acetate (200 mL) and extracted with water (50 mL X 6), dried over Na_2SO_4, filtered, and dried by rotary evaporation. The white mixture was subjected to flash gradient column chromatography on silica gel (1:1 hexanes/ethyl acetate, 2:1 hexanes/ethyl acetate, 1:1 hexanes/ethyl acetate), dried under high vacuum to yield a white solid. Yield: 5.601 g, 92.5%.

^{1}H NMR (300 MHz, $CDCl_3$): δ = 7.16 (s, 2H, H_a), 6.64 (s, 1H, H_b), 3.97 (t, *J* = 6.6 Hz, 4H, H_c), 3.90 (s, 3H, H_d), 3.66 (t, *J* = 5.7 Hz, 4H, H_e), 1.77 (m, *J* = 6.9 Hz, 4H, H_f), 1.30 (m, 32 H, H_g)

^{13}C NMR (300 MHz, $CDCl_3$): δ = 167.17, 160.28, 131.94, 107.76, 106.73, 68.44, 63.23, 52.34, 32.94, 29.62, 29.54, 29.46, 29.30, 26.13, 25.86

Consistent with reported values.[120]

4.16. Synthesis of 3,5-bis((11-hydroxyundecyl)oxy)benzoic acid (16)

Compound **15** (5.200g, 10.2 mmol) was added to 75 mL potassium hydroxide solution (4.8g, 74.8 mmol) in 50 mL EtOH in a 250 mL rb flask and refluxed at 100 °C for 4 h. The mixture was cooled to room temperature and then acidified dropwise with diluted HCl until reaching pH 1. The resulting white precipitate was filtered, washed with neutral water, and dried under the high-vacuum to yield a white solid. Yield: 5.562g (wet), >90%.

^{1}H NMR (300 MHz, $CDCl_3$): δ = 7.10 (s, 2H, H_a), 6.57 (s, 1H, H_b), 3.95 (t, 4H, H_c), 3.52 (t, 4H, H_d), 1.72 (m, 4H, H_e), 1.31 (m, 32H, H_f)

^{13}C NMR (300 MHz, $CDCl_3$): δ = 161.48, 108.71, 106.53, 69.22, 63.02, 33.67, 30.74, 30.67, 30.61, 30.49, 30.34, 27.14, 26.95

Consistent with reported values.[120]

4.17. Synthesis of 3,5-bis((11-chloroundecyl)oxy)-N-(3,4,5-tris(octadecyloxy)phenyl)benzamide (17)

Compound **16** (3.036 g, 6.1 mmol) was added to a 250 mL rb flask with 50 mL CH_2Cl_2 and DMF (1mL, filtered through activated basic Al_2O_3). Thionyl chloride (3.0 mL, 41.0 mmol) was added dropwise over 10 min to the mixture at 0 °C, stirred for 15 min and then warmed to room temperature and stirred for 24 h. The solution was dried by high-vacuum, dispersed in anhydrous CH_2Cl_2, and dried by high-vacuum three times. Compound **3** (2.722 g, 3.029 mmol) and triethylamine (6.0 mL, 43 mmol, filtered through activated basic Al_2O_3) were added to a 250 mL rb flask. The crude acid chloride was dissolved in 14 mL of CH_2Cl_2 and added dropwise to **3** over 5 min and stirred for 19.5 h at room temperature under nitrogen gas. The mixture was extracted with pH 1 brine (100 mL X 3) and neutral brine (100 mL), dried over Na_2SO_4, filtered, and dried by rotary evaporation. The mixture was purified via flash column chromatography on silica gel (hexanes/ethyl acetate 10:1), filtered through activated basic aluminum oxide with ethyl acetate, and dissolved in small amounts of CH_2Cl_2 and precipitated in warm methanol and stored in the fridge overnight. The off-white solid was filtered and dried under high-vacuum. Yield: 3.780g, 88.3%.

^{1}H NMR (300 MHz, $CDCl_3$): δ = 7.65 (s, 1H, H_a), 6.94 (s, 2H, H_b), 6.91 (s, 2H, H_c), 6.60 (s, 1H, H_d), 3.99 (t, *J* = 3.6 Hz, 8H, $H_{e,f}$), 3.93 (t, *J* = 6.6 Hz, 2H, H_g), 3.54 (t, *J* = 6.9 Hz, 4H, H_h), 1.76 (m, *J* = 6.9 Hz, 14H, $H_{i,j,k}$), 1.26 (m, 118 H, H_l), 0.88 (t, *J* = 6.6 Hz, 9H, H_m)

^{13}C NMR (300 MHz, $CDCl_3$): δ = 165.41, 160.59, 153.27, 137.07, 135.08, 133.62, 105.32, 104.70, 99.10, 73.55, 59.16, 68.40, 45.12, 32.71, 31.99, 30.39, 29.79, 29.73, 29.56, 29.50, 29.43, 29.25, 28.93, 26.93, 26.22, 26.17, 26.06, 22.74, 14.15

Consistent with reported values.[120]

4.18. Synthesis of S,S'-(((5-((3,4,5-tris)octadecyloxy)phenyl)carbamoyl)-1,3-(phenylene)bis(oxy))bis(undecane-11,1-diyl)) diethanethioate (18)

Compound **17** (0.714 g, 0.5 mmol), potassium carbonate (0.350 g, 2.5 mmol), catalytic amount of KI were added to a 250 mL rb flask in 50 mL anhydrous DMF. Thioacetate (0.15 mL, 2.12 mmol) was added dropwise into the reaction mixture at room temperature. The reaction mixture was then heated to 60 °C for 24 h under nitrogen gas. The mixture was washed with brine (3 X 100 mL), dried over Na_2SO_4, filtered, and dried under rotary evaporator. The mixture was dissolved in CH_2Cl_2 and filtered through activated basic aluminum oxide, precipitated in warm methanol, and stored in the fridge. White solid was filtered, collected, and dried under high-vacuum. Yield: 0.614 g, 81%.

^{1}H NMR (300 MHz, $CDCl_3$): δ = 7.65 (s, 1H, H_a), 6.95 (s, 2H, H_b), 6.91 (s, 2H, H_c), 6.60 (dd, *J* = 2.1 Hz, 1H, H_d), 3.99 (t, *J* = 6.3 Hz, 8H, H_e), 3.93 (t, *J* = 6.3 Hz, 2H, H_f), 3.54

^{13}C NMR (300 MHz, $CDCl_3$): δ = 196.24, 165.50, 160.69, 153.37, 137.17, 135.12, 133.67, 105.37, 104.69, 99.1, 73.67, 69.27, 68.51, 32.08, 33.77, 30.46, 29.87, 29.82, 29.63, 29.58, 29.52, 29.29, 29.23, 28.94, 26.25, 26.14, 22.84, 14.27

HR-MS (ESI): Calculated for $C_{93}H_{167}NO_8S_2$:1491.2167.

Consistent with reported values.[120]

REFERENCES/BIBLIOGRAPHY

(1) Eustis, S.; El-Sayed, M. A. *Chem. Soc. Rev.* **2006**, *35* (3), 209–217.
(2) Love, J. C.; Estroff, L. A.; Kriebel, J. K.; Nuzzo, R. G.; Whitesides, G. M. *Chem. Rev.* **2005**, *105* (4), 1103–1170.
(3) Rao, C. N. R.; Kulkarni, G. U.; Thomas, P. J.; Edwards, P. P. *Chem. Soc. Rev.* **2000**, *29* (1), 27–35.
(4) In *IUPAC Compendium of Chemical Terminology*; Nič, M., Jirát, J., Košata, B., Jenkins, A., McNaught, A., Eds.; IUPAC: Research Triagle Park, NC, 2009.
(5) Roduner, E. *Chem. Soc. Rev.* **2006**, *35* (7), 583–592.
(6) Edwards, P. P.; Johnston, R. L.; Rao, C. n. r. In *Metal Clusters in Chemistry*; Braunstein, P., Oro, L. A., Raithby, P. R., Eds.; Wiley-VCH Verlag GmbH, 1999; pp 1454–1481.
(7) Buffat, P.; Borel, J.-P. *Phys. Rev. A* **1976**, *13* (6), 2287–2298.
(8) Xiong, S.; Qi, W.; Cheng, Y.; Huang, B.; Wang, M.; Li, Y. *Phys. Chem. Chem. Phys.* **2011**, *13* (22), 10652–10660.
(9) In *IUPAC Compendium of Chemical Terminology*; Nič, M., Jirát, J., Košata, B., Jenkins, A., McNaught, A., Eds.; IUPAC: Research Triagle Park, NC, 2009.
(10) In *IUPAC Compendium of Chemical Terminology*; Nič, M., Jirát, J., Košata, B., Jenkins, A., McNaught, A., Eds.; IUPAC: Research Triagle Park, NC, 2009.
(11) Daniel, M.-C.; Astruc, D. *Chem. Rev.* **2004**, *104* (1), 293–346.
(12) Niederberger, M.; Garnweitner, G.; Buha, J.; Polleux, J.; Ba, J.; Pinna, N. *J. Sol-Gel Sci. Technol.* **2006**, *40* (2-3), 259–266.
(13) Huang, S.-H.; Juang, R.-S. *J. Nanoparticle Res.* **2011**, *13* (10), 4411–4430.
(14) Jung, D.-R.; Kim, J.; Nahm, C.; Choi, H.; Nam, S.; Park, B. *Electron. Mater. Lett.* **2011**, *7* (3), 185–194.
(15) Wang, W.; Lu, Y.; Yue, Z.; Liu, W.; Cao, Z. *Chem. Commun.* **2014**, *50* (95), 15030–15033.
(16) Horn, D.; Rieger, J. *Angew. Chem. Int. Ed.* **2001**, *40* (23), 4330–4361.
(17) Kango, S.; Kalia, S.; Celli, A.; Njuguna, J.; Habibi, Y.; Kumar, R. *Prog. Polym. Sci.* **2013**, *38* (8), 1232–1261.
(18) Seo, D.; Park, J. C.; Song, H. *J. Am. Chem. Soc.* **2006**, *128* (46), 14863–14870.
(19) Personick, M. L.; Mirkin, C. A. *J. Am. Chem. Soc.* **2013**, *135* (49), 18238–18247.
(20) Sau, T. K.; Rogach, A. L. *Adv. Mater.* **2010**, *22* (16), 1781–1804.
(21) Ghosh, P.; Han, G.; De, M.; Kim, C. K.; Rotello, V. M. *Adv. Drug Deliv. Rev.* **2008**, *60* (11), 1307–1315.
(22) Jadhav, S. A.; Brunella, V.; Scalarone, D. *Part. Part. Syst. Charact.* **2015**, *32* (4), 417–428.
(23) Güzel, R.; Üstündağ, Z.; Ekşi, H.; Keskin, S.; Taner, B.; Durgun, Z. G.; Turan, A. A. İ.; Solak, A. O. *J. Colloid Interface Sci.* **2010**, *351* (1), 35–42.

(24) Bao, F.; Li, J.-F.; Ren, B.; Gu, R.-A.; Tian, Z.-Q. *J. Phys. Chem. C* **2008**, *112* (2), 345–350.
(25) Xiong, D.; Li, Z.; An, Y.; Ma, R.; Shi, L. *J. Colloid Interface Sci.* **2010**, *350* (1), 260–267.
(26) Yin, H.; Ma, Z.; Chi, M.; Dai, S. *Catal. Today* **2011**, *160* (1), 87–95.
(27) Gu, C.; Xu, H.; Park, M.; Shannon, C. *Langmuir* **2009**, *25* (1), 410–414.
(28) Kim, H.; Achermann, M.; Balet, L. P.; Hollingsworth, J. A.; Klimov, V. I. *J. Am. Chem. Soc.* **2005**, *127* (2), 544–546.
(29) Langille, M. R.; Personick, M. L.; Zhang, J.; Mirkin, C. A. *J. Am. Chem. Soc.* **2012**, *134* (35), 14542–14554.
(30) Badia, A.; Singh, S.; Demers, L.; Cuccia, L.; Brown, G. R.; Lennox, R. B. *Chem. – Eur. J.* **1996**, *2* (3), 359–363.
(31) Bensebaa, F.; Ellis, T. H.; Kruus, E.; Voicu, R.; Zhou, Y. *Langmuir* **1998**, *14* (22), 6579–6587.
(32) Vericat, C.; Vela, M. E.; Benitez, G.; Carro, P.; Salvarezza, R. C. *Chem. Soc. Rev.* **2010**, *39* (5), 1805.
(33) Eklund, S. E.; Cliffel, D. E. *Langmuir* **2004**, *20* (14), 6012–6018.
(34) Zhao, P.; Li, N.; Astruc, D. *Coord. Chem. Rev.* **2013**, *257* (3-4), 638–665.
(35) Kim, Y.; Zhu, J.; Yeom, B.; Di Prima, M.; Su, X.; Kim, J.-G.; Yoo, S. J.; Uher, C.; Kotov, N. A. *Nature* **2013**, *500* (7460), 59–63.
(36) Gao, J.; Huang, X.; Liu, H.; Zan, F.; Ren, J. *Langmuir* **2012**, *28* (9), 4464–4471.
(37) Ortiz, N.; Skrabalak, S. E. *Langmuir* **2014**, *30* (23), 6649–6659.
(38) Kuo, C.-H.; Chiang, T.-F.; Chen, L.-J.; Huang, M. H. *Langmuir* **2004**, *20* (18), 7820–7824.
(39) Walter, D. *Comm. Investig. Health Hazards Chem. Compd. Work Area* 9.
(40) Ingham, B.; Lim, T. H.; Dotzler, C. J.; Henning, A.; Toney, M. F.; Tilley, R. D. *Chem. Mater.* **2011**, *23* (14), 3312–3317.
(41) Park, H. H.; Park, H.; Jamison, A. C.; Lee, T. R. *Colloid Polym. Sci.* **2014**, *292* (2), 411–421.
(42) Weisbecker, C. S.; Merritt, M. V.; Whitesides, G. M. *Langmuir* **1996**, *12* (16), 3763–3772.
(43) Taguchi, T.; Isozaki, K.; Miki, K. *Adv. Mater.* **2012**, *24* (48), 6462–6467.
(44) Lee, H. *RSC Adv.* **2014**, *4* (77), 41017–41027.
(45) Niu, Z.; Li, Y. *Chem. Mater.* **2014**, *26* (1), 72–83.
(46) Mikami, Y.; Dhakshinamoorthy, A.; Alvaro, M.; García, H. *Catal. Sci. Technol.* **2012**, *3* (1), 58–69.
(47) In *IUPAC Compendium of Chemical Terminology*; Nič, M., Jirát, J., Košata, B., Jenkins, A., McNaught, A., Eds.; IUPAC: Research Triagle Park, NC, 2009.
(48) Kim, C. K.; Ghosh, P.; Pagliuca, C.; Zhu, Z.-J.; Menichetti, S.; Rotello, V. M. *J. Am. Chem. Soc.* **2009**, *131* (4), 1360–1361.
(49) Duncan, B.; Kim, C.; Rotello, V. M. *J. Controlled Release* **2010**, *148* (1), 122–127.
(50) Rana, S.; Bajaj, A.; Mout, R.; Rotello, V. M. *Adv. Drug Deliv. Rev.* **2012**, *64* (2), 200–216.

(51) Shenawi, S.; Jaber, N.; Almog, J.; Mandler, D. *Chem. Commun.* **2013**, *49* (35), 3688.
(52) Nørgaard, K.; Weygand, M. J.; Kjaer, K.; Brust, M.; Bjørnholm, T. *Faraday Discuss.* **2004**, *125* (0), 221–233.
(53) Lacava, J.; Weber, A.; Kraus, T. *Part. Part. Syst. Charact.* **2015**, *32* (4), 458–466.
(54) Zhou, J.; Ralston, J.; Sedev, R.; Beattie, D. A. *J. Colloid Interface Sci.* **2009**, *331* (2), 251–262.
(55) Crudden, C. M.; Horton, J. H.; Ebralidze, I. I.; Zenkina, O. V.; McLean, A. B.; Drevniok, B.; She, Z.; Kraatz, H.-B.; Mosey, N. J.; Seki, T.; Keske, E. C.; Leake, J. D.; Rousina-Webb, A.; Wu, G. *Nat. Chem.* **2014**, *6* (5), 409–414.
(56) Hurst, E. C.; Wilson, K.; Fairlamb, I. J. S.; Chechik, V. *New J. Chem.* **2009**, *33* (9), 1837–1840.
(57) Leff, D. V.; Brandt, L.; Heath, J. R. *Langmuir* **1996**, *12* (20), 4723–4730.
(58) Kumar, A.; Mandal, S.; Pasricha, R.; Mandale, A. B.; Sastry, M. *Langmuir* **2003**, *19* (15), 6277–6282.
(59) Li, Y.; Silverton, L. C.; Haasch, R.; Tong, Y. Y. *Langmuir* **2008**, *24* (14), 7048–7053.
(60) Li, Y.; Love, O.; Tong, Y. J. *Nano Bull.* **2013**, *2* (2), 130221.
(61) Kurashige, W.; Yamaguchi, M.; Nobusada, K.; Negishi, Y. *J. Phys. Chem. Lett.* **2012**, *3* (18), 2649–2652.
(62) Ulman, A. *Chem. Rev.* **1996**, *96* (4), 1533–1554.
(63) Zhang, S.; Leem, G.; Srisombat, L.; Lee, T. R. *J. Am. Chem. Soc.* **2008**, *130* (1), 113–120.
(64) Srisombat, L.; Jamison, A. C.; Lee, T. R. *Colloids Surf. Physicochem. Eng. Asp.* **2011**, *390* (1–3), 1–19.
(65) Srisombat, L.; Park, J.-S.; Zhang, S.; Lee, T. R. *Langmuir* **2008**, *24* (15), 7750–7754.
(66) Srisombat, L.; Zhang, S.; Lee, T. R. *Langmuir* **2010**, *26* (1), 41–46.
(67) Chinwangso, P.; Jamison, A. C.; Lee, T. R. *Acc. Chem. Res.* **2011**, *44* (7), 511–519.
(68) Terrill, R. H.; Postlethwaite, T. A.; Chen, C.; Poon, C.-D.; Terzis, A.; Chen, A.; Hutchison, J. E.; Clark, M. R.; Wignall, G. *J. Am. Chem. Soc.* **1995**, *117* (50), 12537–12548.
(69) Templeton, A. C.; Hostetler, M. J.; Kraft, C. T.; Murray, R. W. *J. Am. Chem. Soc.* **1998**, *120* (8), 1906–1911.
(70) Shen, M.; Du, Y.; Hua, N.; Yang, P. *Powder Technol.* **2006**, *162* (1), 64–72.
(71) Boal, A. K.; Rotello, V. M. *Langmuir* **2000**, *16* (24), 9527–9532.
(72) Chen, S.; Murray, R. W. *Langmuir* **1999**, *15* (3), 682–689.
(73) Lévy, R.; Thanh, N. T. K.; Doty, R. C.; Hussain, I.; Nichols, R. J.; Schiffrin, D. J.; Brust, M.; Fernig, D. G. *J. Am. Chem. Soc.* **2004**, *126* (32), 10076–10084.
(74) Agasti, S. S.; You, C.-C.; Arumugam, P.; Rotello, V. M. *J Mater Chem* **2008**, *18* (1), 70–73.
(75) Schulz, F.; Vossmeyer, T.; Bastús, N. G.; Weller, H. *Langmuir* **2013**, *29* (31), 9897–9908.

(76) Johnson, S. R.; Evans, S. D.; Brydson, R. *Langmuir* **1998**, *14* (23), 6639–6647.
(77) Shenhar, R.; Rotello, V. M. *Acc. Chem. Res.* **2003**, *36* (7), 549–561.
(78) Paulini, R.; Frankamp, B. L.; Rotello, V. M. *Langmuir* **2002**, *18* (6), 2368–2373.
(79) Lin, I.-C.; Liang, M.; Liu, T.-Y.; Monteiro, M. J.; Toth, I. *Nanomedicine Nanotechnol. Biol. Med.* **2012**, *8* (1), 8–11.
(80) Shi, C.; Choi, H. S.; Armani, A. M. *Appl. Phys. Lett.* **2012**, *100* (1), 013305.
(81) Marega, R.; Karmani, L.; Flamant, L.; Nageswaran, P. G.; Valembois, V.; Masereel, B.; Feron, O.; Borght, T. V.; Lucas, S.; Michiels, C.; Gallez, B.; Bonifazi, D. *J. Mater. Chem.* **2012**, *22* (39), 21305–21312.
(82) Lin, S.; Cheng, Y.; Liu, J.; Wiesner, M. R. *Langmuir ACS J. Surf. Colloids* **2012**, *28* (9), 4178–4186.
(83) MacLeod, M. J.; Johnson, J. A. *J. Am. Chem. Soc.* **2015**, *137* (25), 7974–7977.
(84) Song, Y.; Klivansky, L. M.; Liu, Y.; Chen, S. *Langmuir* **2011**, *27* (23), 14581–14588.
(85) Luo, S.; Xu, J.; Zhang, Y.; Liu, S.; Wu, C. *J. Phys. Chem. B* **2005**, *109* (47), 22159–22166.
(86) Balan, L.; Melinte, V.; Buruiana, T.; Schneider, R.; Vidal, L. *Nanotechnology* **2012**, *23* (41), 415705.
(87) Koenig, S.; Chechik, V. *Langmuir* **2006**, *22* (11), 5168–5173.
(88) Koh, W. C. A.; Chandra, P.; Kim, D.-M.; Shim, Y.-B. *Anal. Chem.* **2011**, *83* (16), 6177–6183.
(89) Dong, H.; Zhu, M.; Yoon, J. A.; Gao, H.; Jin, R.; Matyjaszewski, K. *J. Am. Chem. Soc.* **2008**, *130* (39), 12852–12853.
(90) Bartczak, D.; Kanaras, A. G. *Langmuir* **2010**, *26* (10), 7072–7077.
(91) Yoo, M.; Kim, S.; Lim, J.; Kramer, E. J.; Hawker, C. J.; Kim, B. J.; Bang, J. *Macromolecules* **2010**, *43* (7), 3570–3575.
(92) Yang, W.; Ella-Menye, J.-R.; Liu, S.; Bai, T.; Wang, D.; Yu, Q.; Li, Y.; Jiang, S. *Langmuir* **2014**, *30* (9), 2522–2529.
(93) Duchesne, L.; Wells, G.; Fernig, D. G.; Harris, S. A.; Lévy, R. *ChemBioChem* **2008**, *9* (13), 2127–2134.
(94) Liu, X.; Basu, A. *Langmuir* **2008**, *24* (19), 11169–11174.
(95) Mirzaei, J.; Urbanski, M.; Kitzerow, H.-S.; Hegmann, T. *Philos. Trans. R. Soc. Math. Phys. Eng. Sci.* **2013**, *371* (1988), 20120256–20120256.
(96) Shao, M.; Odell, J. H.; Choi, S.-I.; Xia, Y. *Electrochem. Commun.* **2013**, *31*, 46–48.
(97) Li, D.; Wang, C.; Tripkovic, D.; Sun, S.; Markovic, N. M.; Stamenkovic, V. R. *ACS Catal.* **2012**, *2* (7), 1358–1362.
(98) Elliott, E. W.; Glover, R. D.; Hutchison, J. E. *ACS Nano* **2015**, *9* (3), 3050–3059.
(99) Sun, J.-K.; Zhan, W.-W.; Akita, T.; Xu, Q. *J. Am. Chem. Soc.* **2015**, *137* (22), 7063–7066.
(100) Wang, X.; He, B.; Hu, Z.; Zeng, Z.; Han, S. *Sci. Technol. Adv. Mater.* **2014**, *15* (4), 043502.

(101) Jana, N. R.; Peng, X. *J. Am. Chem. Soc.* **2003**, *125* (47), 14280–14281.
(102) Tian, L.; Yam, L.; Zhou, N.; Tat, H.; Uhrich, K. E. *Macromolecules* **2004**, *37* (2), 538–543.
(103) Dangschat, G.; Fischer, H. O. L.; MacDonald, D. L. *Carbohydr. Res.* **1987**, *164*, 343–355.
(104) Metzke, M.; Guan, Z. *Biomacromolecules* **2008**, *9* (1), 208–215.
(105) Yu, J. K. Towards Stable and Surface Active Metal Nanoparticles, University of Windsor: Windsor, Ontario, 2013.
(106) Percec, V.; Ahn, C.-H.; Bera, T. K.; Ungar, G.; Yeardley, D. J. P. *Chem. – Eur. J.* **1999**, *5* (3), 1070–1083.
(107) Cazes, J. *Encyclopedia of Chromatography*; CRC Press, 2005.
(108) Lincker, F.; Bourgun, P.; Masson, P.; Didier, P.; Guidoni, L.; Bigot, J.-Y.; Nicoud, J.-F.; Donnio, B.; Guillon, D. *Org. Lett.* **2005**, *7* (8), 1505–1508.
(109) Peterca, M.; Imam, M. R.; Ahn, C.-H.; Balagurusamy, V. S. K.; Wilson, D. A.; Rosen, B. M.; Percec, V. *J. Am. Chem. Soc.* **2011**, *133* (7), 2311–2328.
(110) Shu, J.; Dudenko, D.; Esmaeili, M.; Park, J. H.; Puniredd, S. R.; Chang, J. Y.; Breiby, D. W.; Pisula, W.; Hansen, M. R. *J. Am. Chem. Soc.* **2013**, *135* (30), 11075–11086.
(111) Larsen, J. W.; Freund, M.; Kim, K. Y.; Sidovar, M.; Stuart, J. L. *Carbon* **2000**, *38* (5), 655–661.
(112) Sapurina, I.; Stejskal, J. *Polym. Int.* **2008**, *57* (12), 1295–1325.
(113) Schultes, C. M.; Guyen, B.; Cuesta, J.; Neidle, S. *Bioorg. Med. Chem. Lett.* **2004**, *14* (16), 4347–4351.
(114) Smith, B. C. *Infrared Spectral Interpretation: A Systematic Approach*; CRC Press, 1998.
(115) Napoli, A.; Athanassopoulos, C. M.; Moschidis, P.; Aiello, D.; Di Donna, L.; Mazzotti, F.; Sindona, G. *Anal. Chem.* **2010**, *82* (13), 5552–5560.
(116) Carine Robert, F. de M. *ACS Catal.* **2014**, *2014* (4), 3586–3589.
(117) Faig, A.; Petersen, L. K.; Moghe, P. V.; Uhrich, K. E. *Biomacromolecules* **2014**, *15* (9), 3328–3337.
(118) Wang, J.; del Rosario, L. S.; Demirdirek, B.; Bae, A.; Uhrich, K. E. *Acta Biomater.* **2009**, *5* (3), 883–892.
(119) Wang, J.; Plourde, N. M.; Iverson, N.; Moghe, P. V.; Uhrich, K. E. *Int. J. Nanomedicine* **2007**, *2* (4), 697–705.
(120) Zghal, O. Design and Synthesis of Ligands for the Preparation of Amphiphilic Nanoparticles. Thesis, University of Windsor: Windsor, Ontario, 2013.
(121) Nealon, G. L.; Greget, R.; Dominguez, C.; Nagy, Z. T.; Guillon, D.; Gallani, J.-L.; Donnio, B. *Beilstein J. Org. Chem.* **2012**, *8*, 349–370.
(122) Wagner, S.; Law, M. P.; Riemann, B.; Pike, V. W.; Breyholz, H.-J.; Höltke, C.; Faust, A.; Renner, C.; Schober, O.; Schäfers, M.; Kopka, K. *J. Label. Compd. Radiopharm.* **2006**, *49* (2), 177–195.
(123) Zhan, W.; Li, Y.; Huang, W.; Zhao, Y.; Yao, Z.; Yu, S.; Yuan, S.; Jiang, F.; Yao, S.; Li, S. *Bioorg. Med. Chem.* **2012**, *20* (14), 4323–4329.
(124) Sasaki, K.; Crich, D. *Org. Lett.* **2011**, *13* (9), 2256–2259.

APPENDICES

APPENDIX A: ^{1}H and ^{13}C NMR Assignments and MALDI MS Spectra

APPENDIX B: Polarized Optical Microscopy Images

APPENDIX C: Copyright Permissions

APPENDIX A. ^{1}H and ^{13}C NMR Assignments and MALDI MS Spectra.

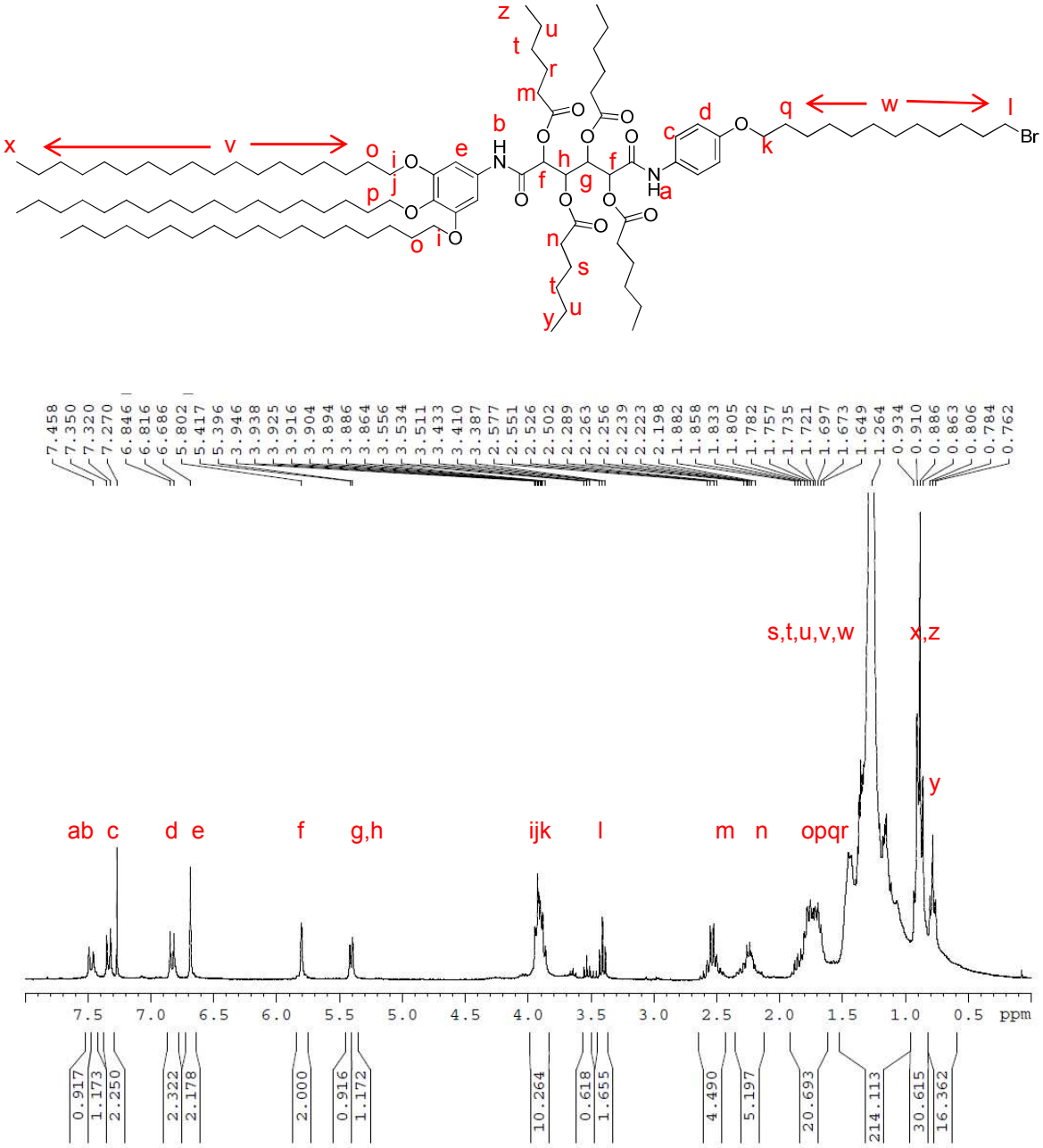

A1. ^{1}H NMR spectrum of (8) in $CDCl_3$ (300 MHz).

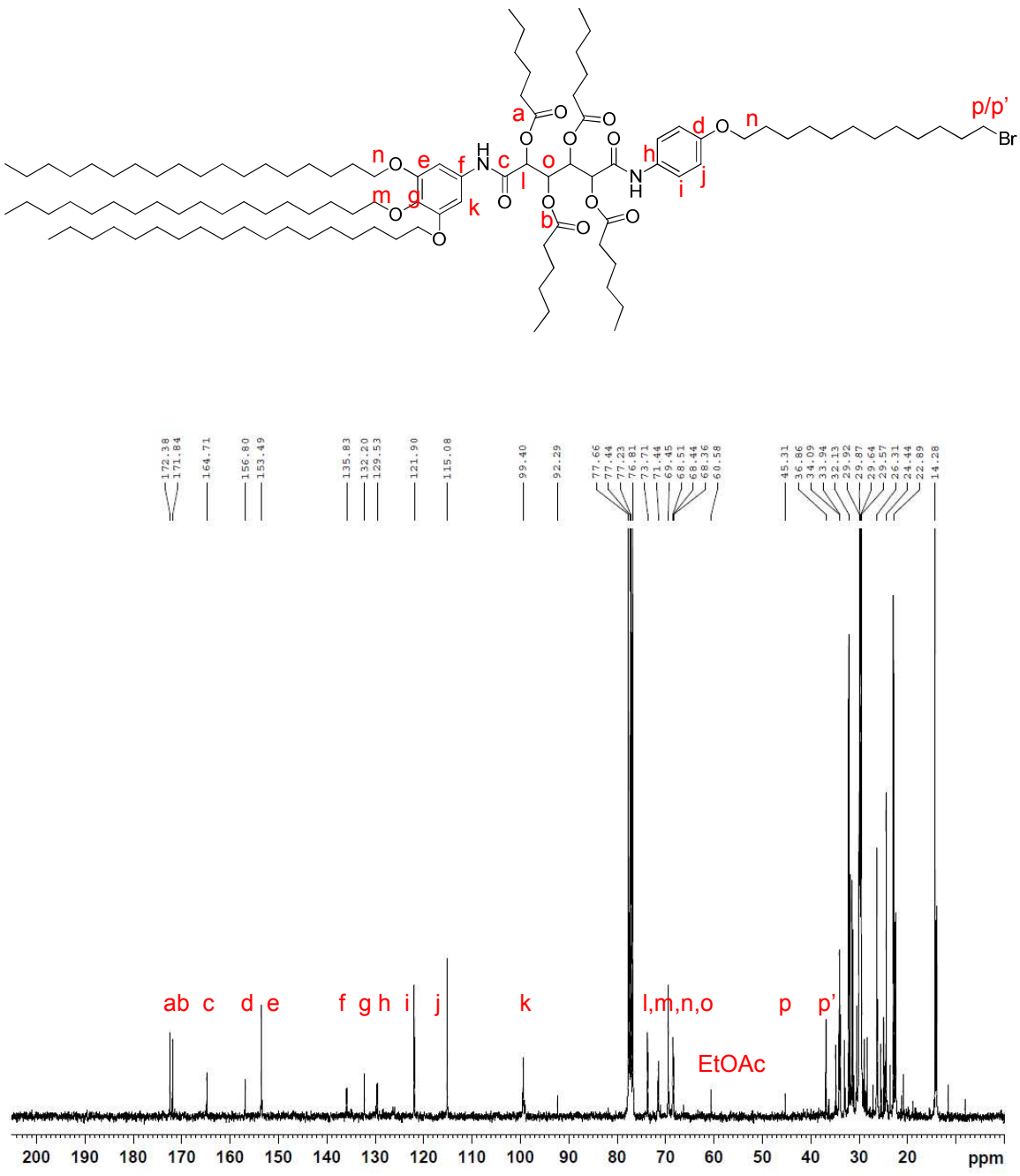

A 2. ^{3}C NMR spectrum of (8) in $CDCl_3$ (300 MHz).

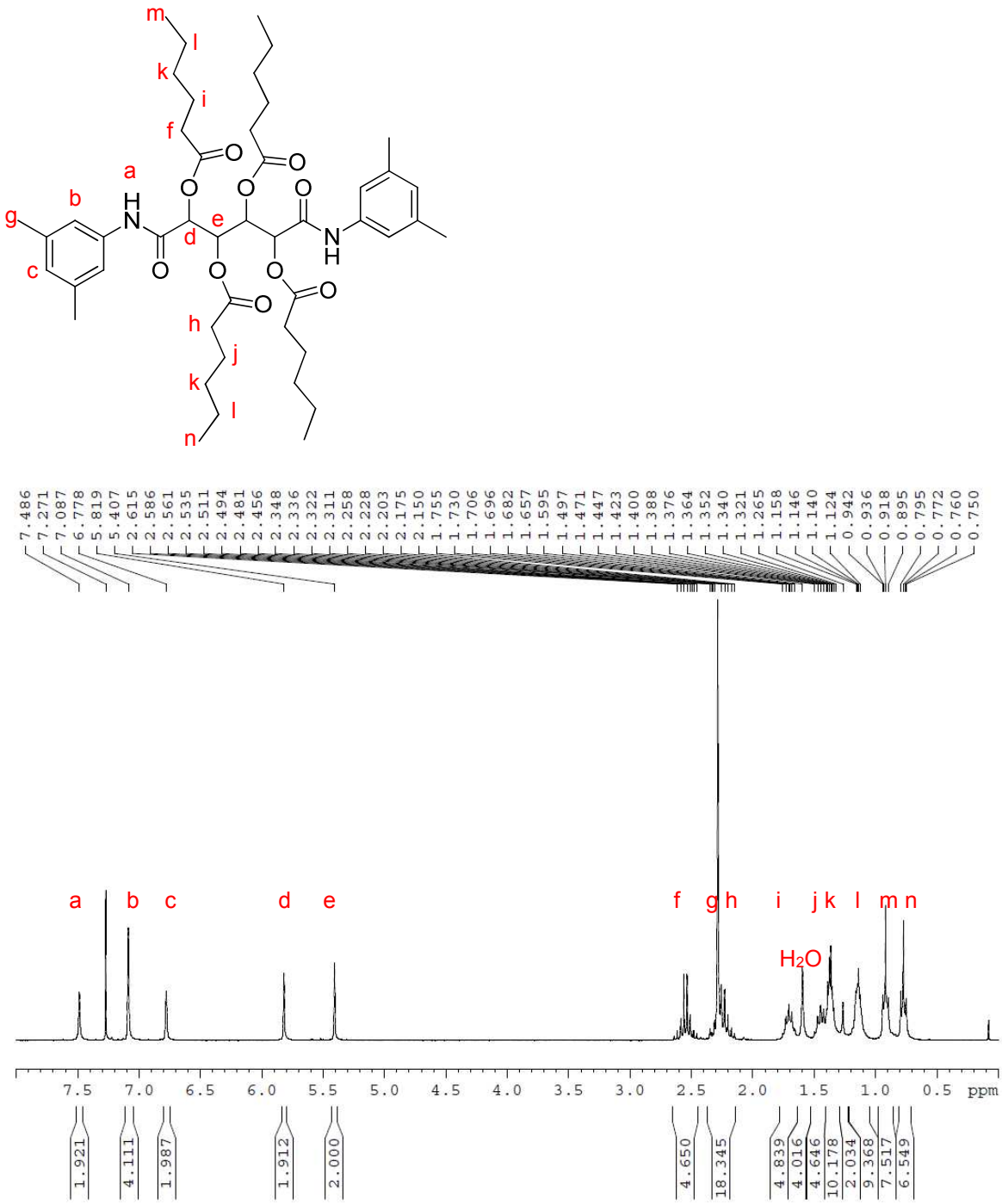

A 3. ^{1}H NMR spectrum of (9) in $CDCl_3$ (300 MHz).

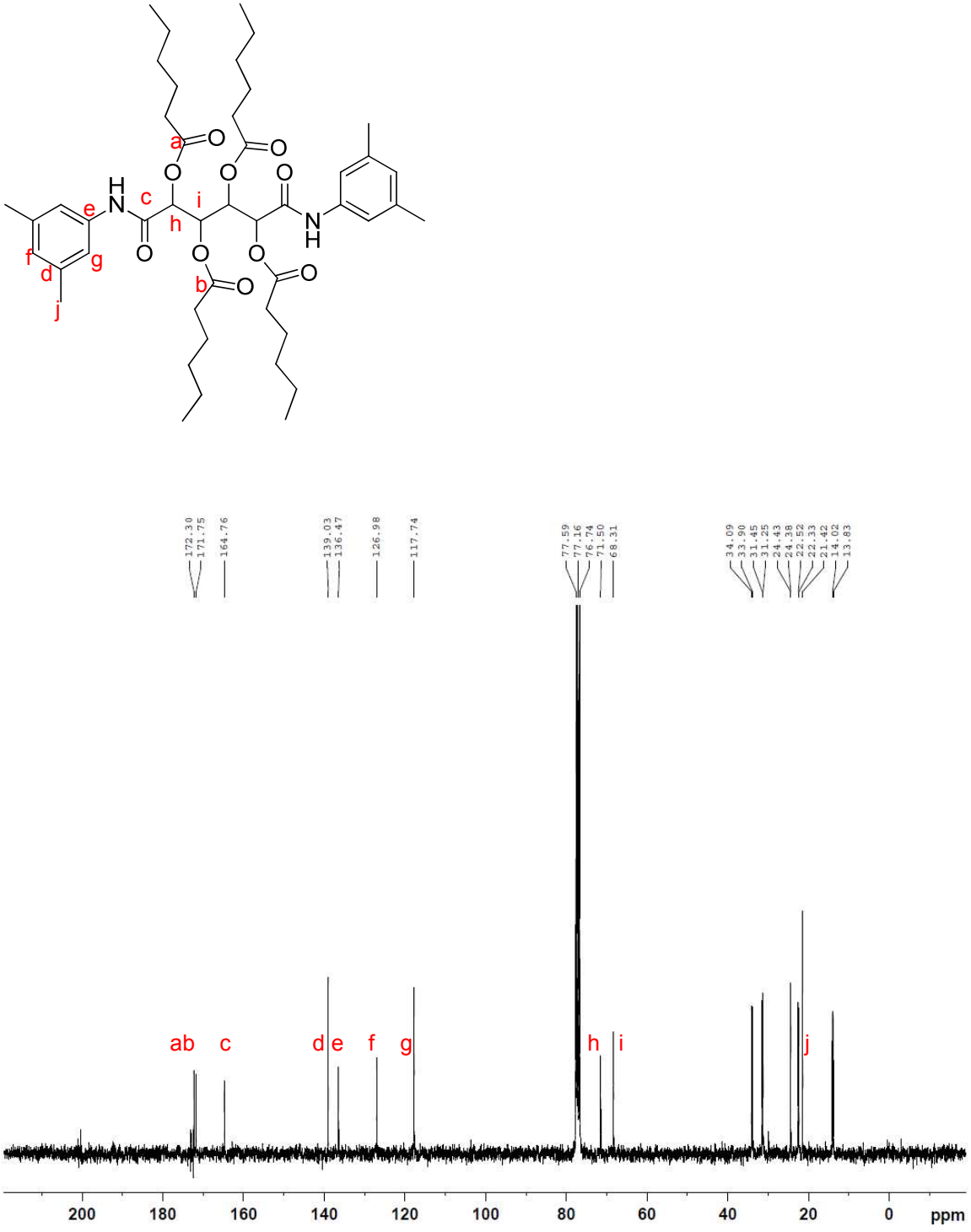

A 4. ^{13}C NMR spectrum of (9) in $CDCl_3$ (300 MHz).

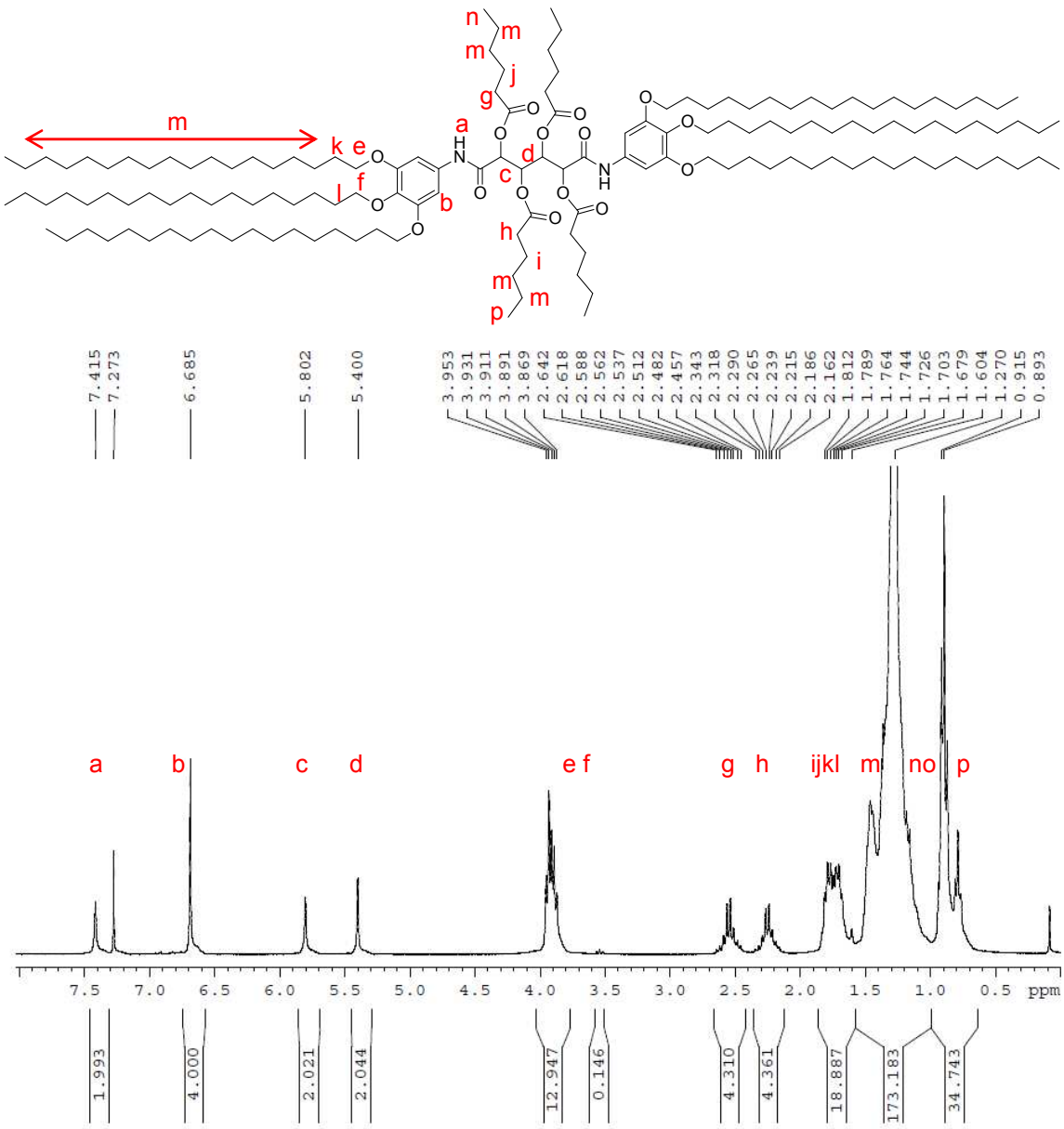

A 5. ^{1}H NMR spectrum of Compound (10) in $CDCl_3$ (300 MHz).

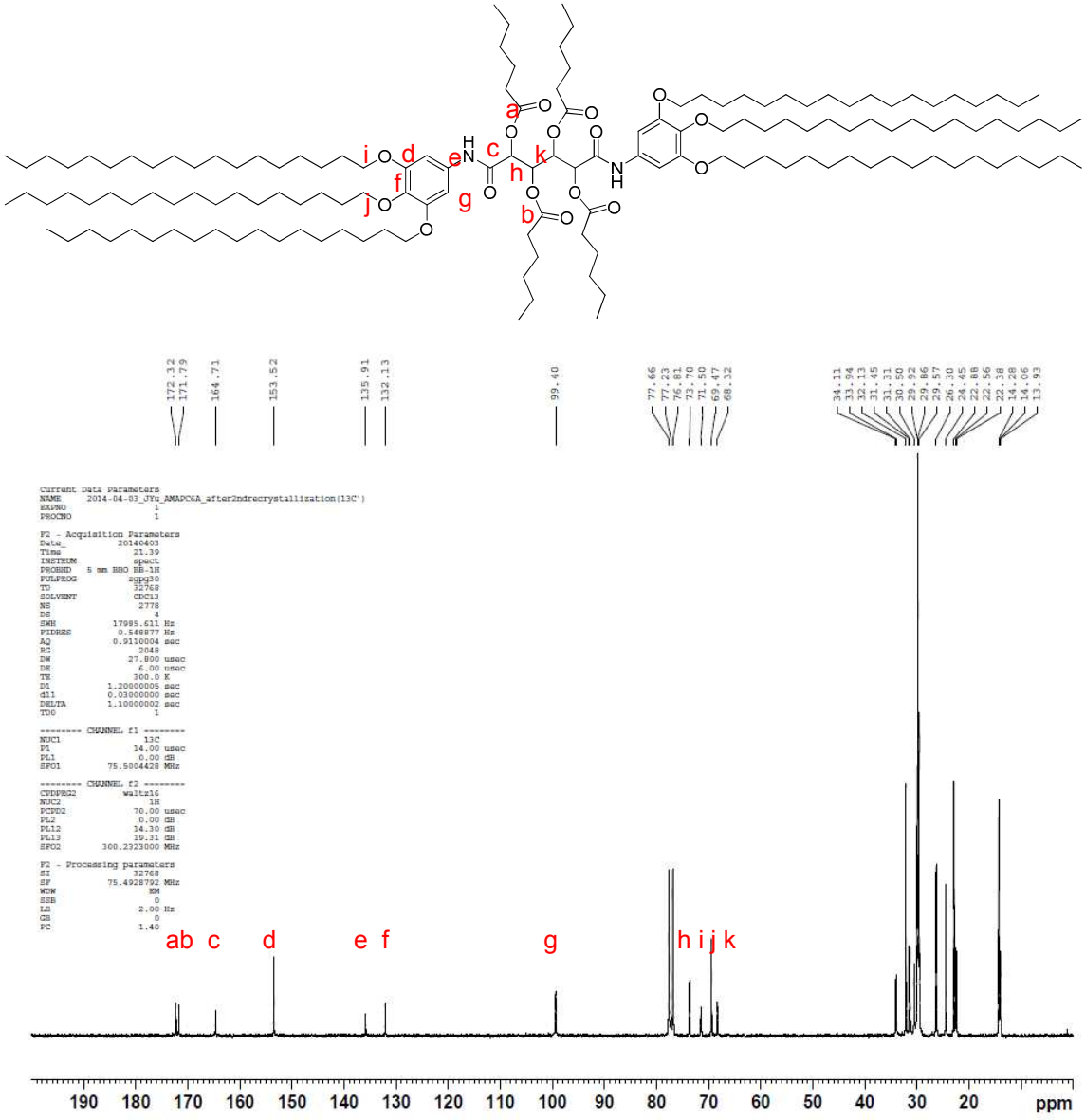

A 6. ^{13}C NMR Spectrum of (10) in $CDCl_3$ (300 MHz).

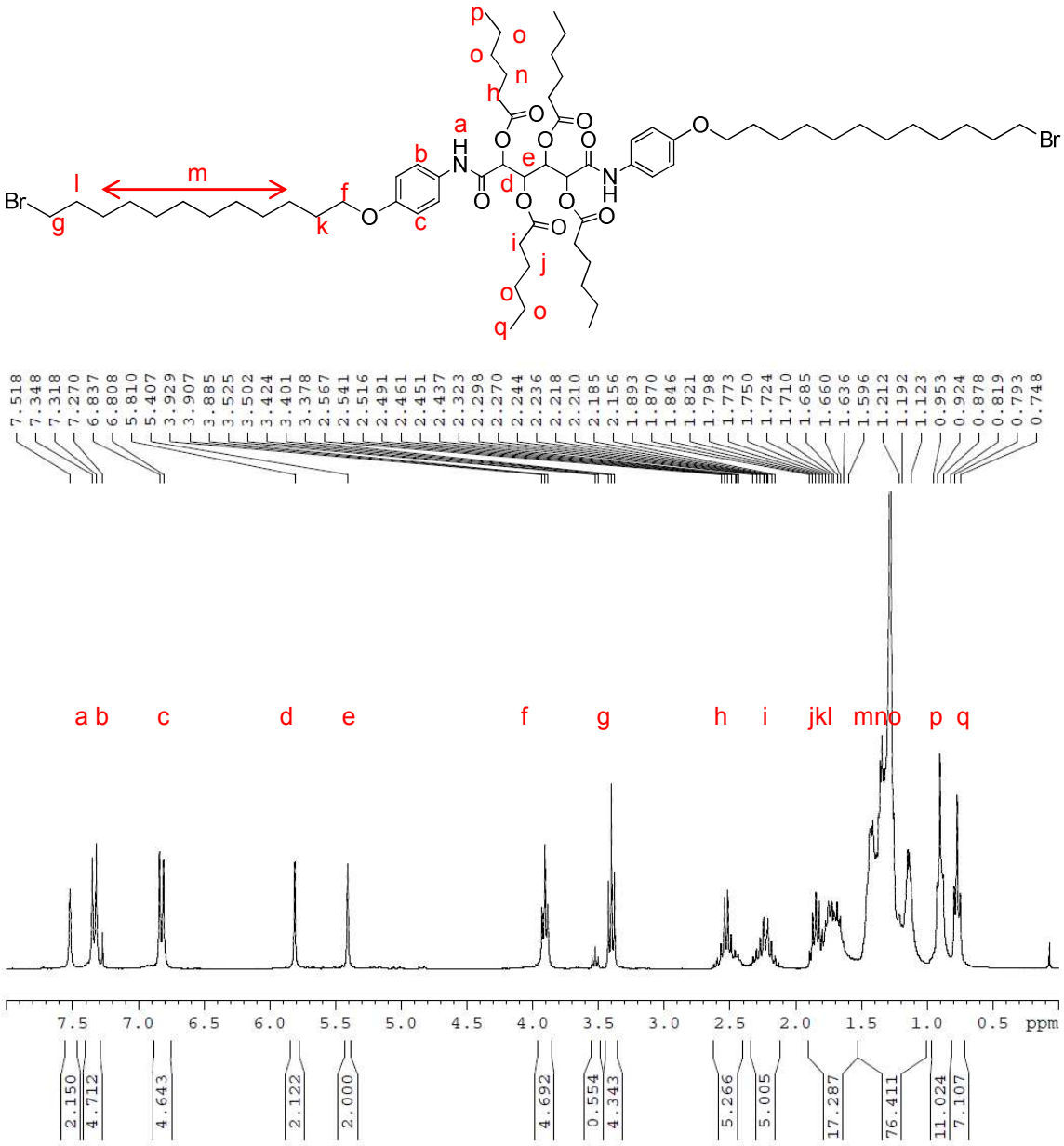

A 7. ^{1}H NMR spectrum of Compound (11) in $CDCl_3$ (300MHz).

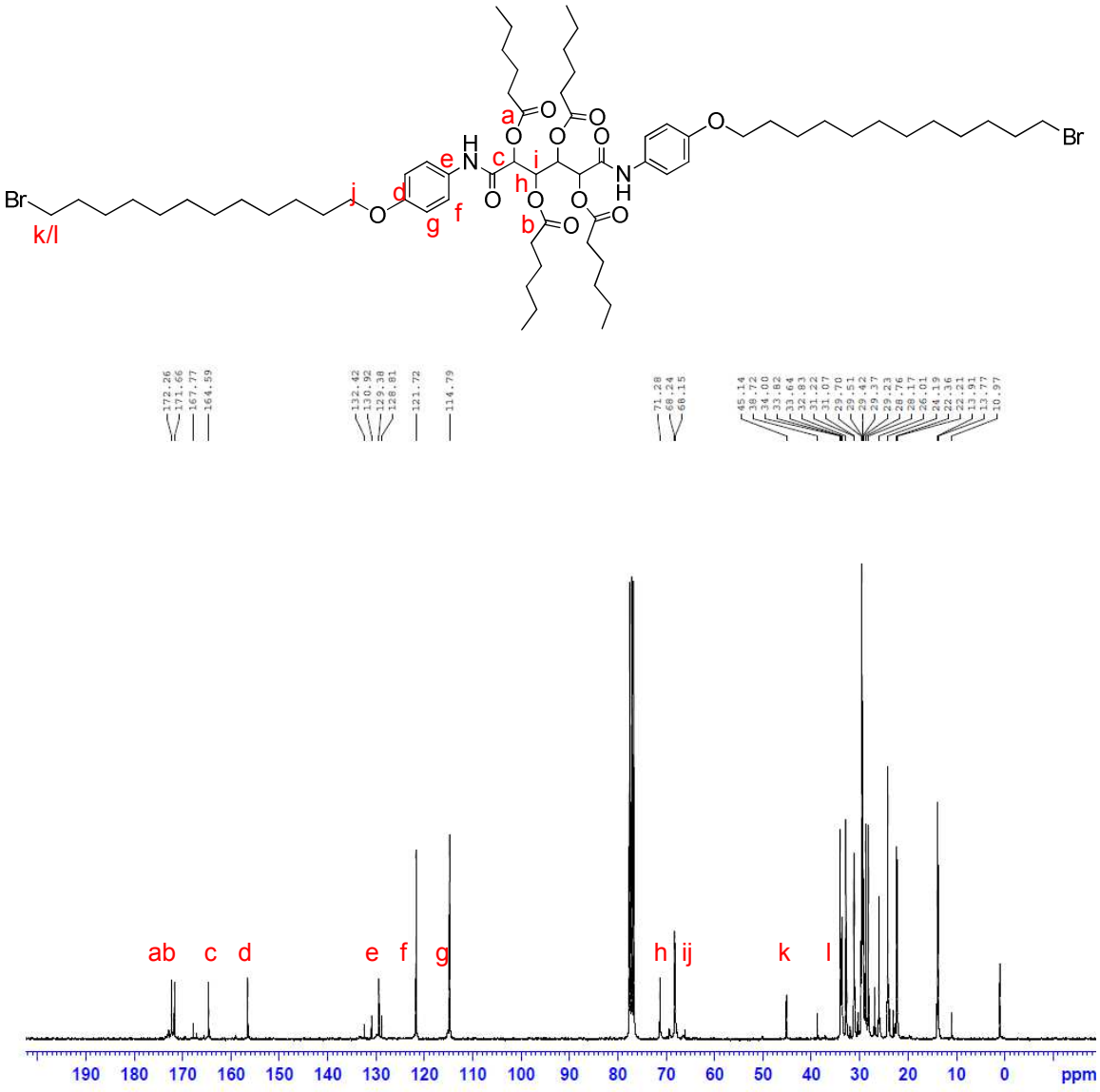

A 8. ^{13}C NMR spectrum of Compound (11) in $CDCl_3$ (300 MHz).

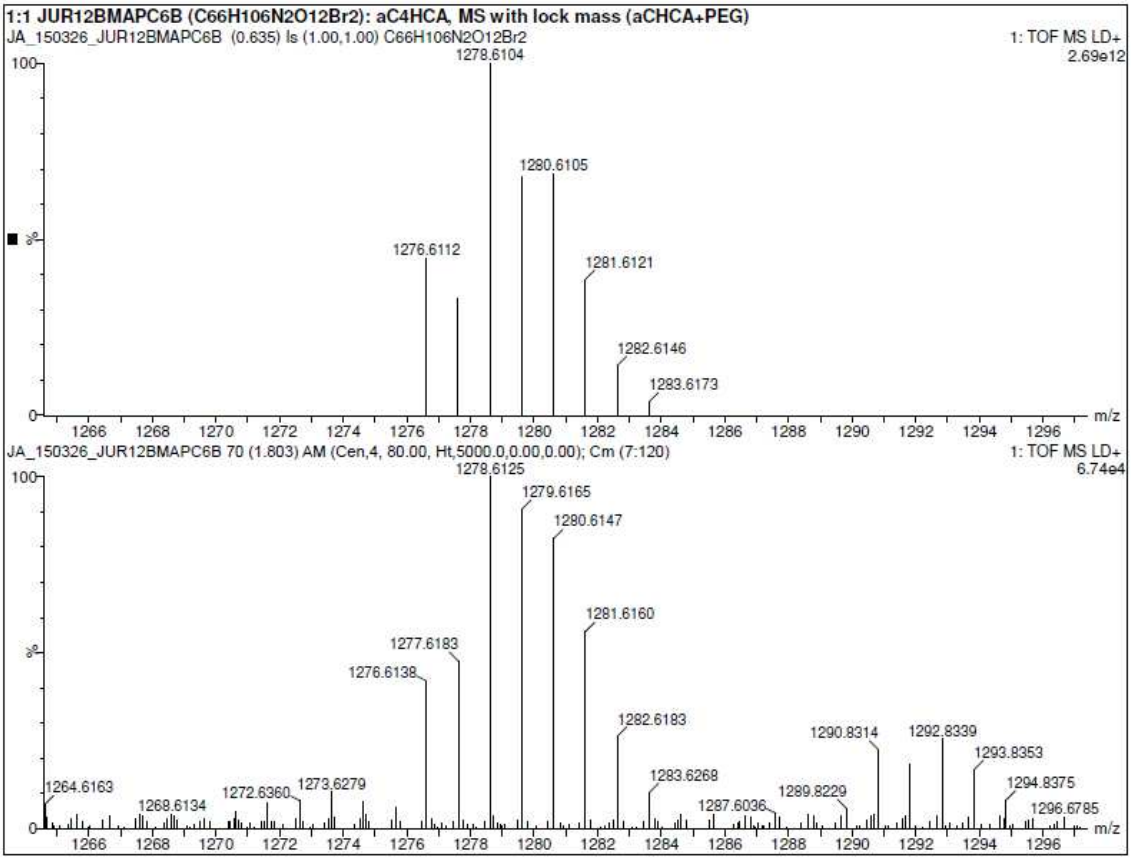

A 9. MALDI MS spectrum for Compound (11). m/z calculated (MH^+) = 1278.6104. Found (MH^+)= 1278.6125. Top panel is the theoretical spectrum. Lower panel is the experimental spectrum.

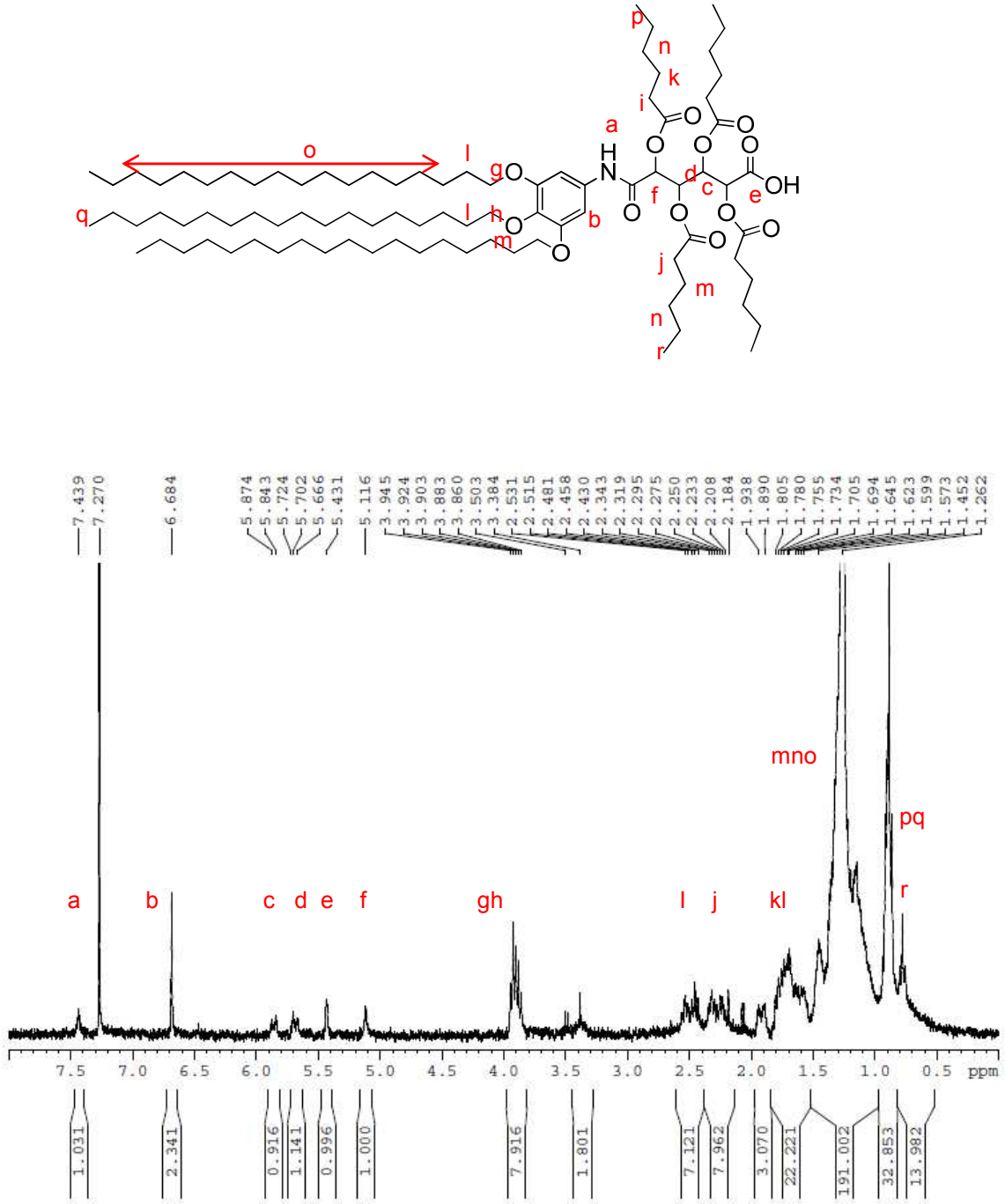

A 10. ^{1}H NMR spectrum of Compound (12) in $CDCl_3$ (300 MHz).

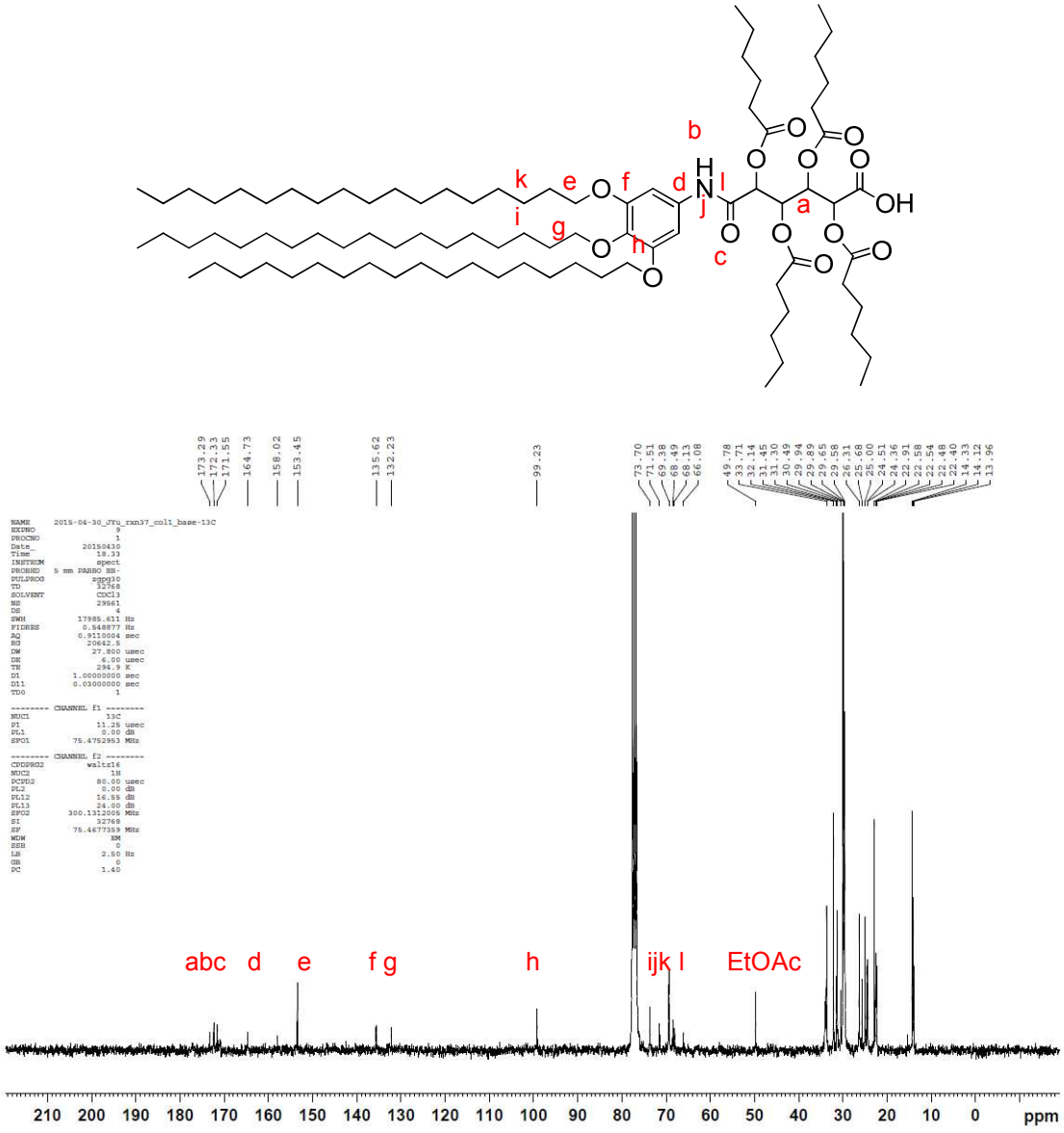

A 11. ^{13}C NMR spectrum of Compound (12) in $CDCl_3$ (300 MHz).

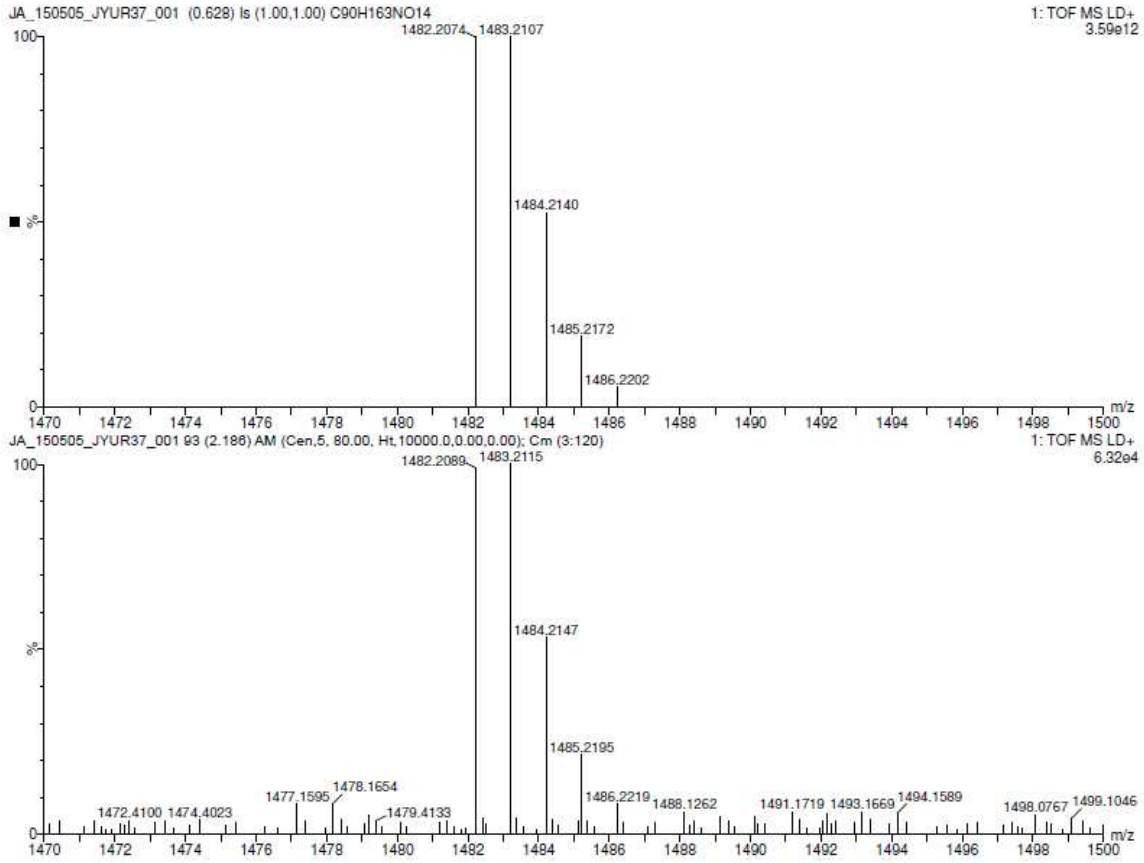

A 12. MALDI MS spectrum of Compound (12). m/z Calculated (M^+) = 1483.21463 (100.0%). Founded (M^+) = 1482.2089. Top panel is the theoretical spectrum. Bottom panel is the experimental spectrum.

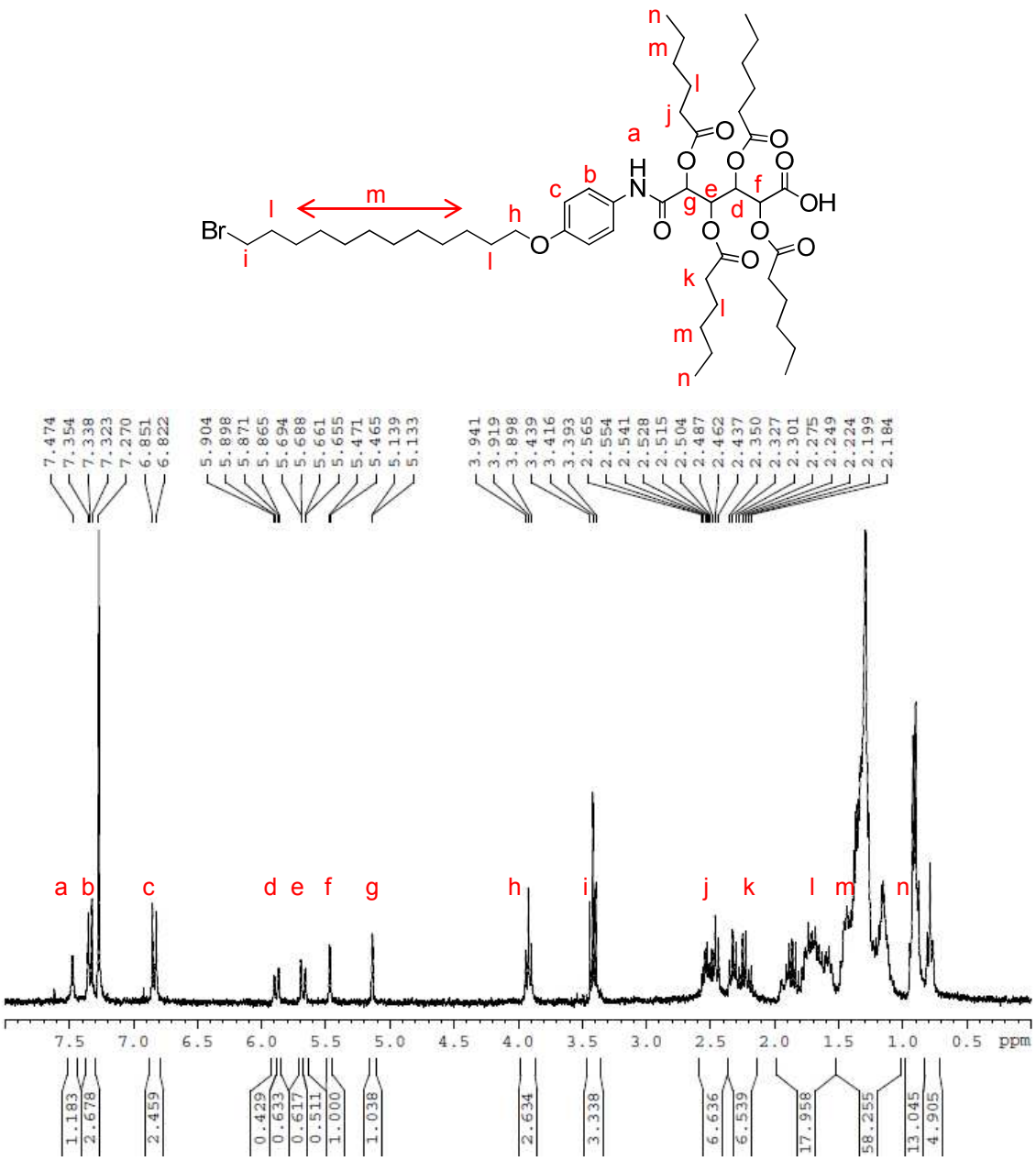

A 13. ^{1}H NMR spectrum of Compound (13) in $CDCl_3$ (300 MHz).

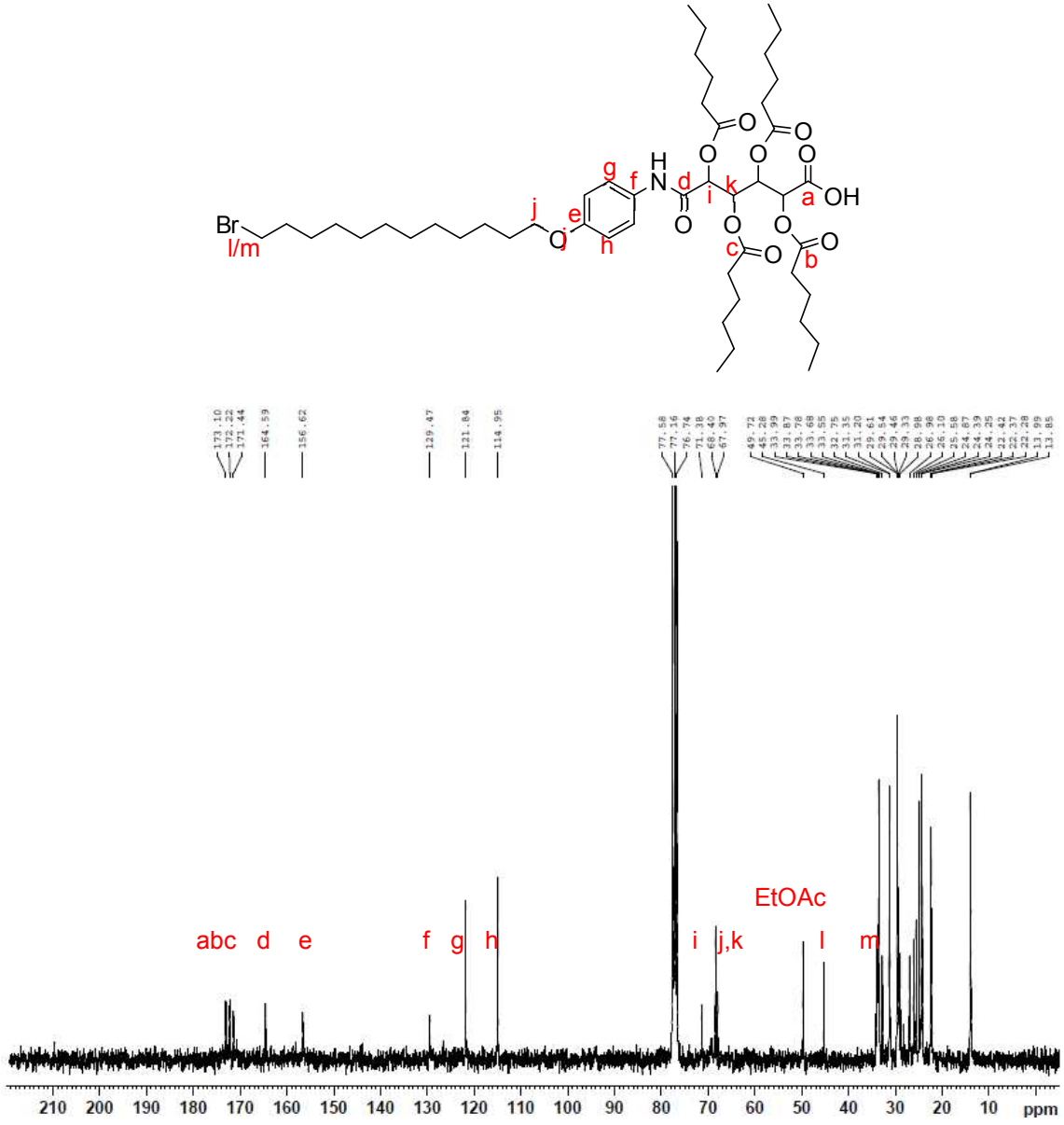

A 14. ^{13}C NMR spectrum of Compound (13) in $CDCl_3$ (300 MHz).

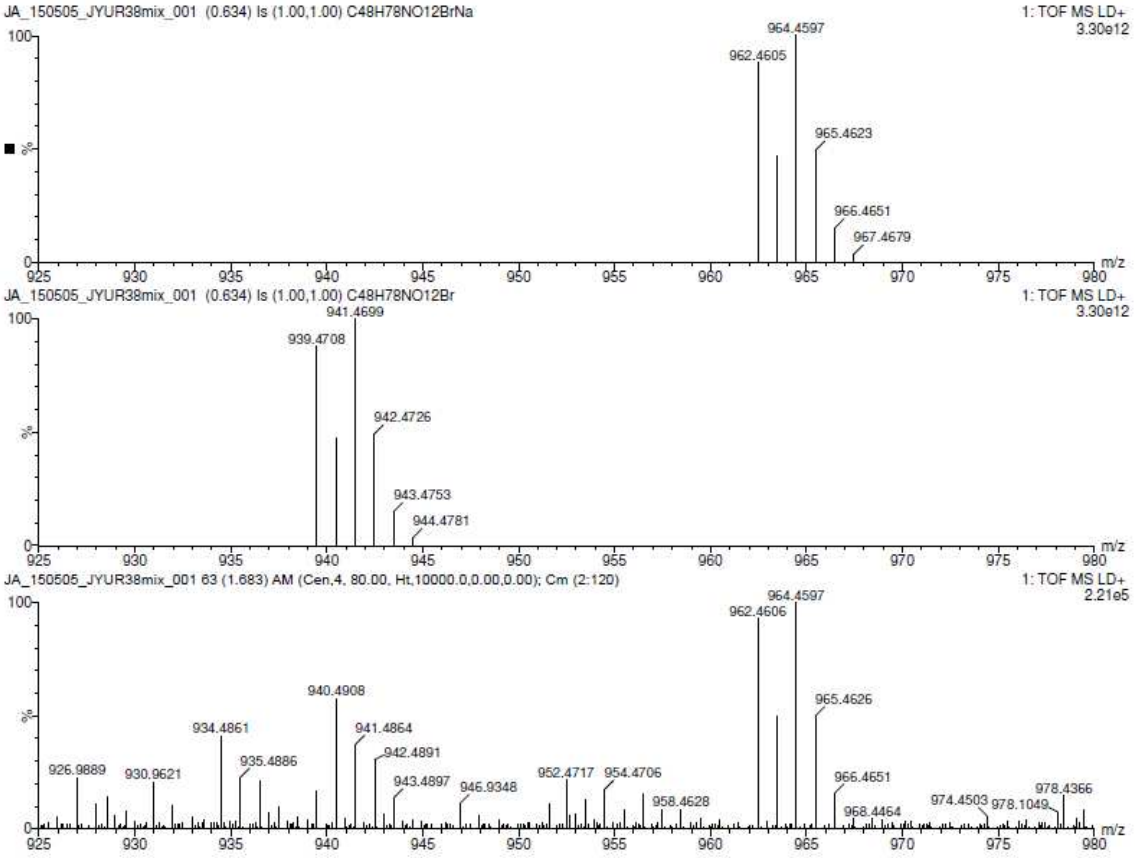

A 15. MALDI MS spectrum of Compound (13). m/z Calculated (MNa^+) = 961.45268 (100%). Founded (MNa^+) = 962.4606. Top panel is the theoretical spectrum. Bottom panel is the experiment spectrum.

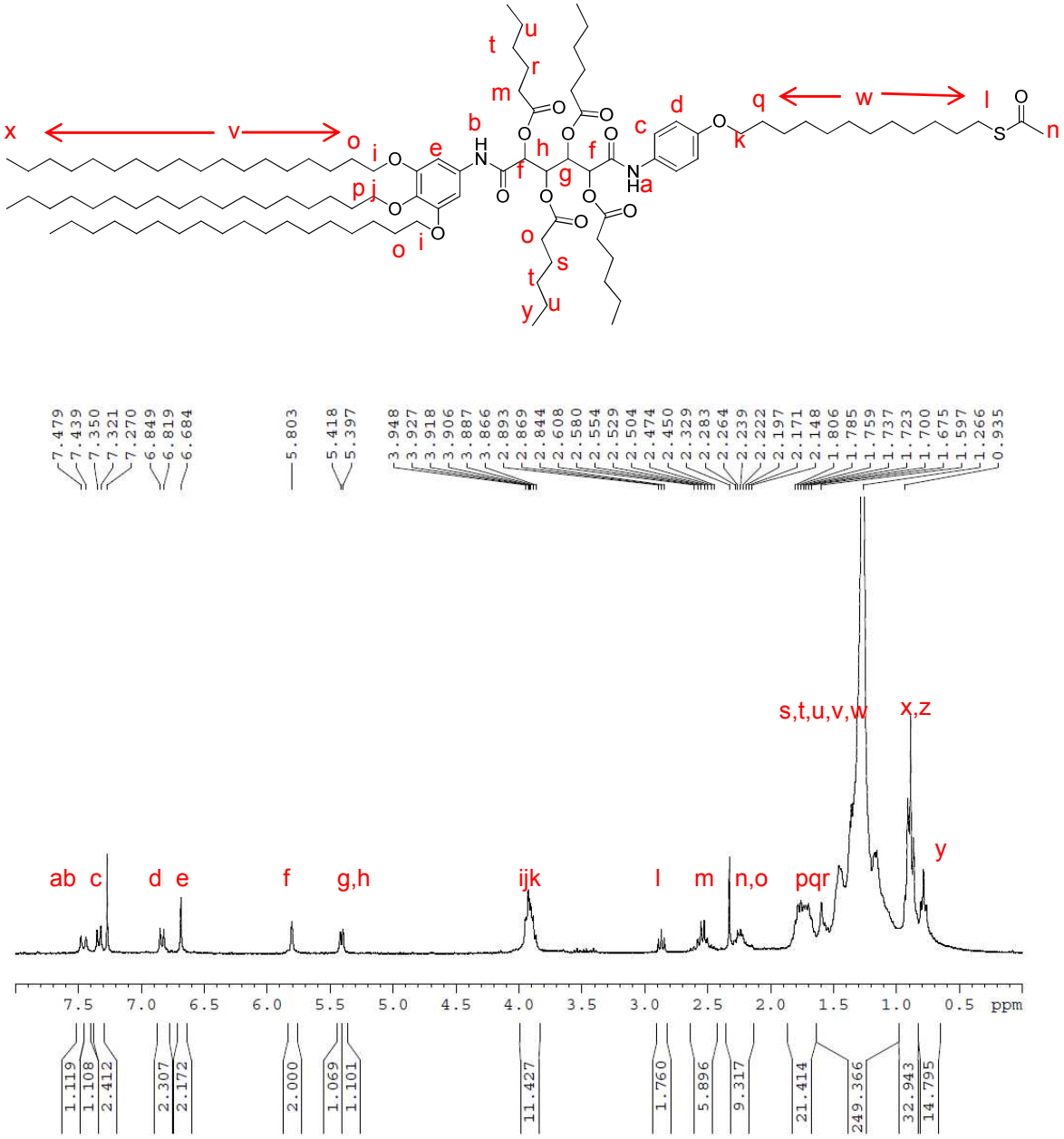

A 16. ^{1}H NMR spectrum of (14) in $CDCl_3$ (300 MHz).

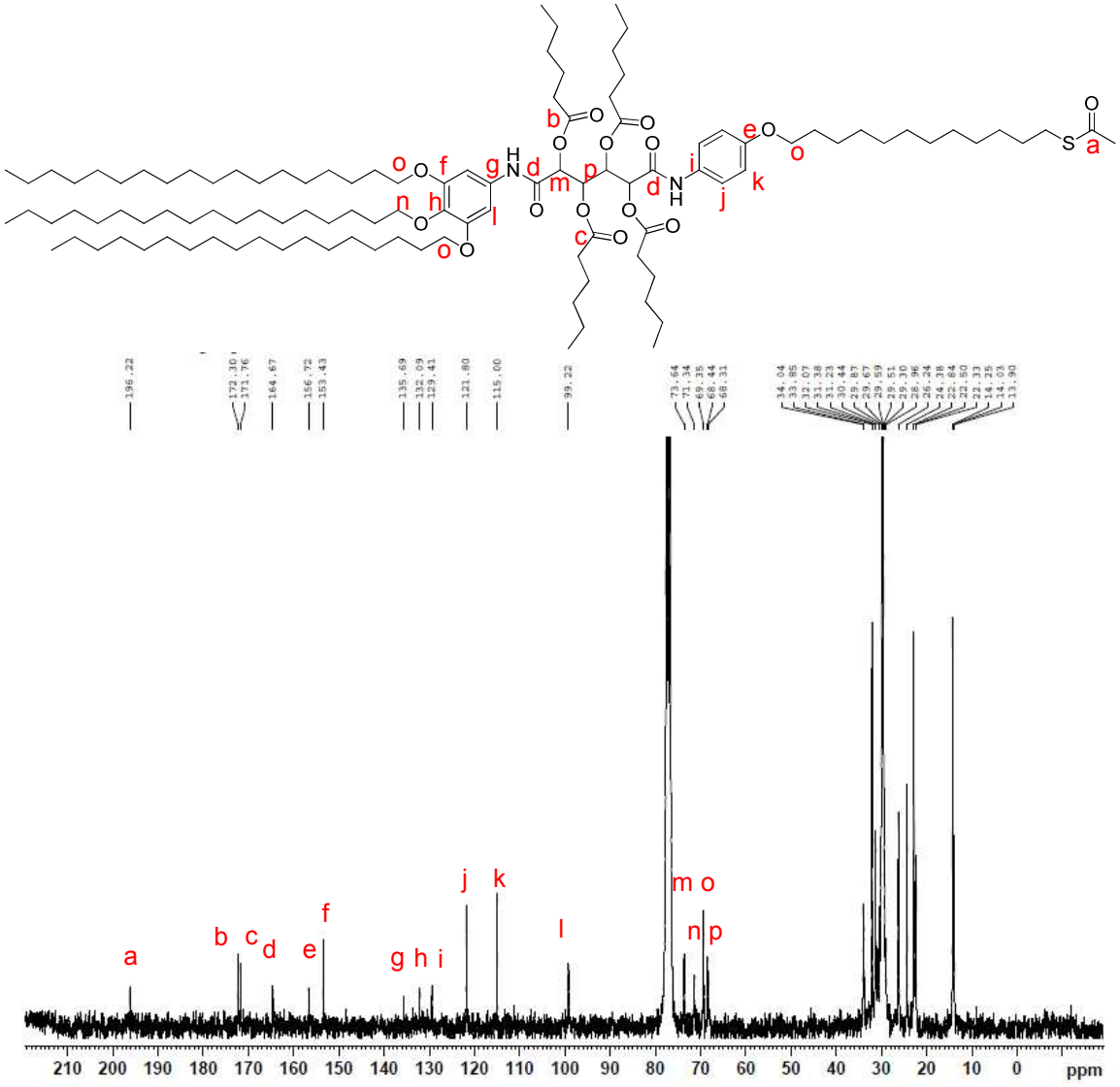

A 17. ^{13}C NMR spectrum of (14) in $CDCl_3$ (300 MHz).

APPENDIX B. Polarized Optical Microscopy Images

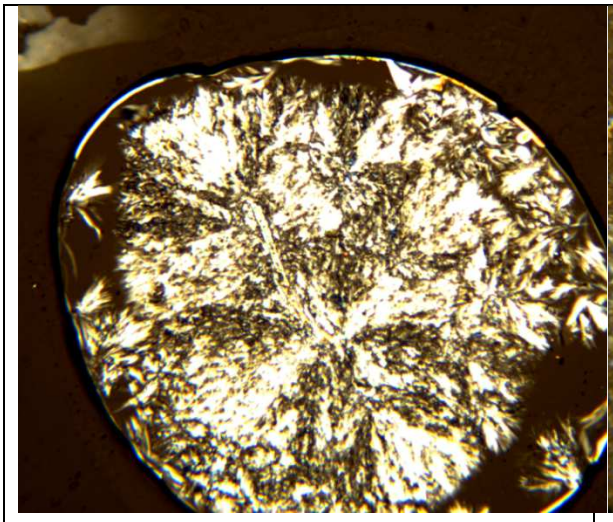

B 1. Compound 13, Cooling at 10 °C /min, 10, 10X, 85.8 °C

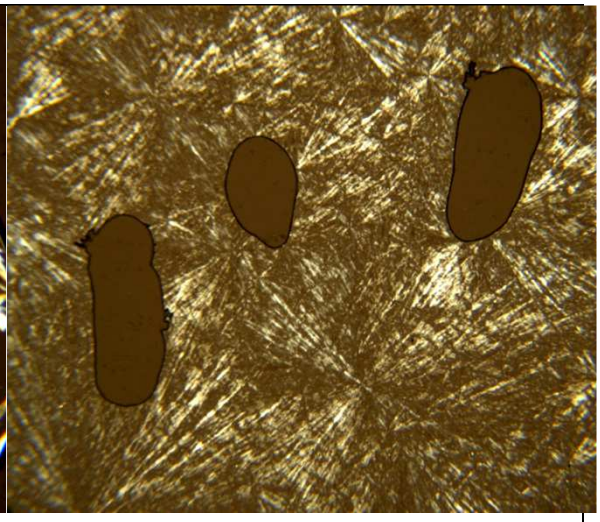

B 2. Compound 11, Cooling at 10 °C/min, 170.3 °C, 10X, 10 polarizer

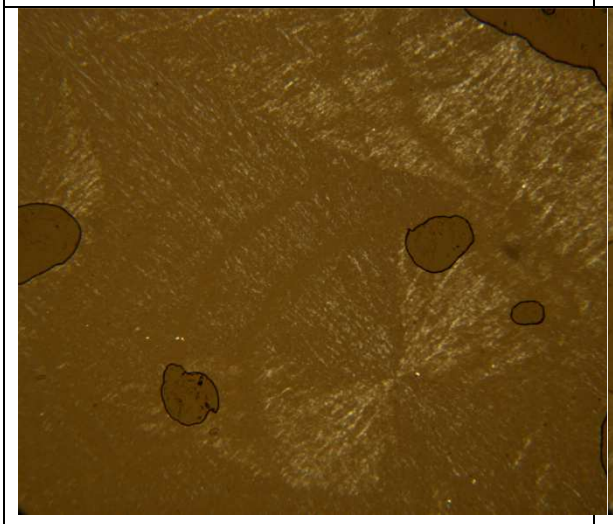

B 3. Compound 11.

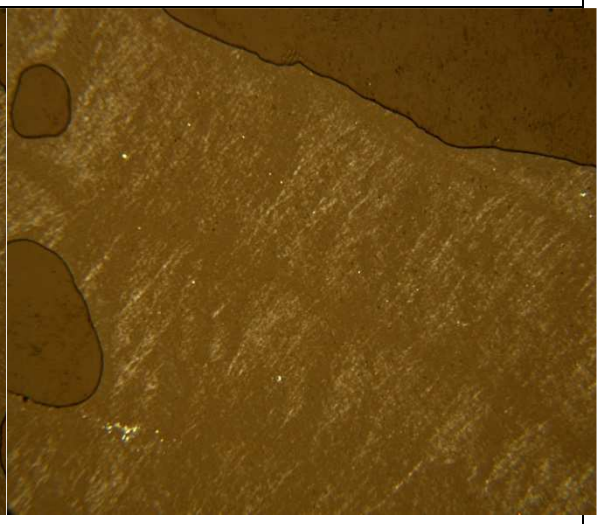

B4. Compound 11, Cooling at 1 °C /min, 173.0 °C

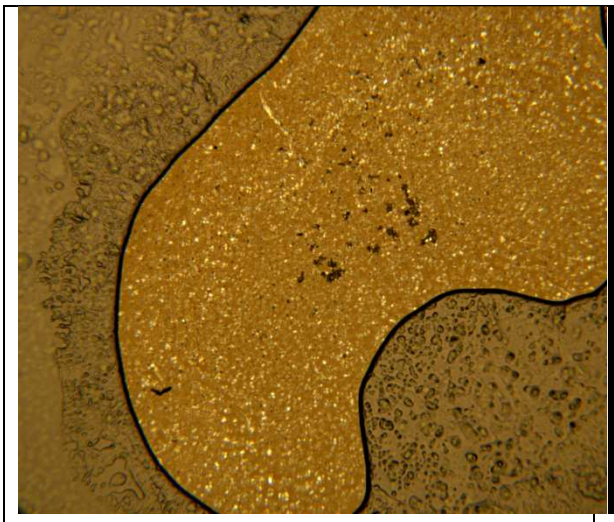

B5. Compound 10, Cooling at 20 °C/min, 156.2 °C, 10X, 20 polarizer.

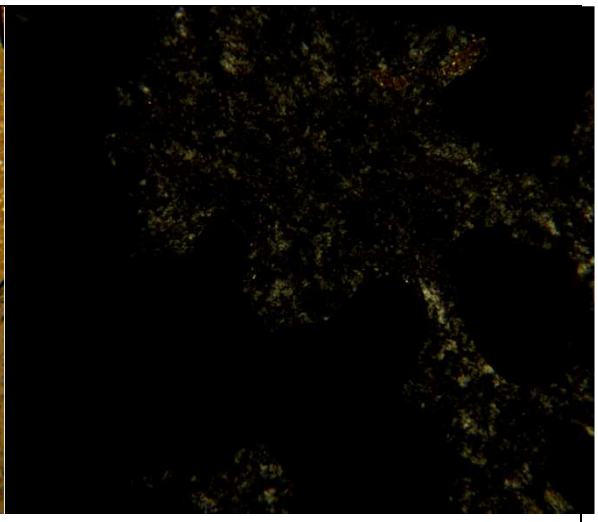

B6. Compound 10, Melting at 20 °C/min, 152.6 °C.

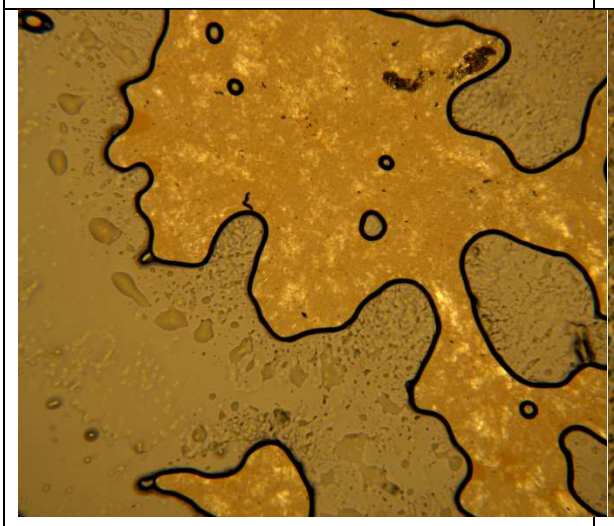

B 7. Compound 10, Melting at 20 °C/min, 152.8 °C.

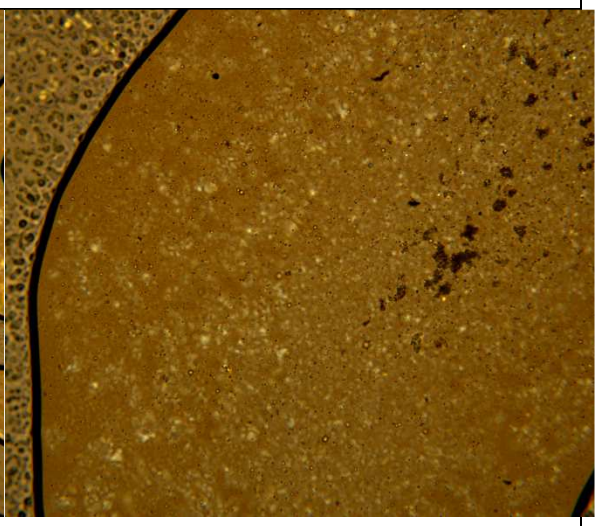

B 8. Compound 10, Cooling at 20 °C/min, 156.8 °C, 20X, 30 polarizer.

APPENDIX C. Copyright Permissions

Jonathan Yu <jonathankwyu@gmail.com>

Permission for Reuse of Thesis
1 message

Omar Zghal <omar.zghal@yahoo.com> Tue, Aug 11, 2015 at 12:43 PM
To: Jonathan Yu <jonathankwyu@gmail.com>

Hello Jon,

I hereby grant you permission to reuse "Design and Synthesis of Ligands for Preparation of Amphiphilic Nanoparticles" for Chapter 2.8 of "Advanced Organic Ligands for Protecting Metal Nanoparticles".

I wish you the best as you continue with your writing.

Take care,
Omar Zghal

Title: Size matters: why nanomaterials are different
Author: Emil Roduner
Publication: Chemical Society Reviews
Publisher: Royal Society of Chemistry
Date: May 4, 2006

Order Completed

Thank you very much for your order.

This is a License Agreement between University of Windsor -- Jonathan Yu ("You") and Royal Society of Chemistry. The license consists of your order details, the terms and conditions provided by Royal Society of Chemistry, and the payment terms and conditions.

Get the printable license.

License Number	3683181416262
License date	Aug 06, 2015
Licensed content publisher	Royal Society of Chemistry
Licensed content publication	Chemical Society Reviews
Licensed content title	Size matters: why nanomaterials are different
Licensed content author	Emil Roduner
Licensed content date	May 4, 2006
Volume number	35
Issue number	7
Type of Use	Thesis/Dissertation
Requestor type	non-commercial (non-profit)
Portion	figures/tables/images
Number of figures/tables/images	5
Distribution quantity	100
Format	print and electronic
Will you be translating?	no
Order reference number	None
Title of the thesis/dissertation	Advanced Organic Ligands for Protecting Metal Nanoparticles
Expected completion date	Aug 2015
Estimated size	90
Total	0.00 CAD

ORDER MORE... CLOSE WINDOW

License Details

This Agreement between University of Windsor ("You") and John Wiley and Sons ("John Wiley and Sons") consists of your license details and the terms and conditions provided by John Wiley and Sons and Copyright Clearance Center.

Get the printable license.

License Number	3683191155186
License date	Aug 06, 2015
Licensed Content Publisher	John Wiley and Sons
Licensed Content Publication	Wiley eBooks
Licensed Content Title	On the Size-Induced Metal-Insulator Transition in Clusters and Small Particles
Licensed Content Author	Peter P. Edwards,Roy L. Johnston,C.N.R. Rao
Licensed Content Date	Mar 26, 2008
Licensed Content Pages	28
Type of Use	Dissertation/Thesis
Requestor type	University/Academic
Format	Print and electronic
Portion	Figure/table
Number of figures/tables	1
Original Wiley figure/table number(s)	-
Will you be translating?	No
Title of your thesis / dissertation	Advanced Organic Ligands for Protecting Metal Nanoparticles
Expected completion date	Aug 2015
Expected size (number of pages)	90
Requestor Location	University of Windsor 401 Sunset Avenue None None Windsor, ON N9B 3P4 Canada Attn: Jonathan Yu
Billing Type	Invoice
Billing address	University of Windsor 401 Sunset Avenue None None Windsor, ON N9B 3P4 Canada Attn: Jonathan Yu
Total	0.00 CAD

BACK

Title: Why gold nanoparticles are more precious than pretty gold: Noble metal surface plasmon resonance and its enhancement of the radiative and nonradiative properties of nanocrystals of different shapes

Author: Susie Eustis,Mostafa A. El-Sayed

Publication: Chemical Society Reviews

Publisher: Royal Society of Chemistry

Date: Dec 16, 2005

Order Completed

Thank you very much for your order.

This is a License Agreement between University of Windsor -- Jonathan Yu ("You") and Royal Society of Chemistry. The license consists of your order details, the terms and conditions provided by Royal Society of Chemistry, and the payment terms and conditions.

Get the printable license.

License Number	3683200805013
License date	Aug 06, 2015
Licensed content publisher	Royal Society of Chemistry
Licensed content publication	Chemical Society Reviews
Licensed content title	Why gold nanoparticles are more precious than pretty gold: Noble metal surface plasmon resonance and its enhancement of the radiative and nonradiative properties of nanocrystals of different shapes
Licensed content author	Susie Eustis,Mostafa A. El-Sayed
Licensed content date	Dec 16, 2005
Volume number	35
Issue number	3
Type of Use	Thesis/Dissertation
Requestor type	non-commercial (non-profit)
Portion	figures/tables/images
Number of figures/tables/images	1
Distribution quantity	100
Format	print and electronic
Will you be translating?	no
Order reference number	None
Title of the thesis/dissertation	Advanced Organic Ligands for Protecting Metal Nanoparticles
Expected completion date	Aug 2015
Estimated size	90
Total	0.00 CAD

ORDER MORE... CLOSE WINDOW

Title: Universal relation for size dependent thermodynamic properties of metallic nanoparticles

Author: Shiyun Xiong,Weihong Qi,Yajuan Cheng,Baiyun Huang,Mingpu Wang,Yejun Li

Publication: Physical Chemistry Chemical Physics

Publisher: Royal Society of Chemistry

Date: Apr 26, 2011

Order Completed

Thank you very much for your order.

This is a License Agreement between University of Windsor -- Jonathan Yu ("You") and Royal Society of Chemistry. The license consists of your order details, the terms and conditions provided by Royal Society of Chemistry, and the payment terms and conditions.

Get the printable license.

License Number	3683201295427
License date	Aug 06, 2015
Licensed content publisher	Royal Society of Chemistry
Licensed content publication	Physical Chemistry Chemical Physics
Licensed content title	Universal relation for size dependent thermodynamic properties of metallic nanoparticles
Licensed content author	Shiyun Xiong,Weihong Qi,Yajuan Cheng,Baiyun Huang,Mingpu Wang,Yejun Li
Licensed content date	Apr 26, 2011
Volume number	13
Issue number	22
Type of Use	Thesis/Dissertation
Requestor type	non-commercial (non-profit)
Portion	figures/tables/images
Number of figures/tables/images	1
Distribution quantity	100
Format	print and electronic
Will you be translating?	no
Order reference number	None
Title of the thesis/dissertation	Advanced Organic Ligands for Protecting Metal Nanoparticles
Expected completion date	Aug 2015
Estimated size	90
Total	0.00 CAD

ORDER MORE... CLOSE WINDOW

Title: Enhanced Catalytic Activity of Self-Assembled-Monolayer-Capped Gold Nanoparticles

Author: Tomoya Taguchi,Katsuhiro Isozaki,Kazushi Miki

Publication: Advanced Materials

Publisher: John Wiley and Sons

Date: Sep 12, 2012

Order Completed

Thank you for your order.

This Agreement between University of Windsor -- Jonathan Yu ("You") and John Wiley and Sons ("John Wiley and Sons") consists of your license details and the terms and conditions provided by John Wiley and Sons and Copyright Clearance Center.

Your confirmation email will contain your order number for future reference.

Get the printable license.

License Number	3683211293897
License date	Aug 06, 2015
Licensed Content Publisher	John Wiley and Sons
Licensed Content Publication	Advanced Materials
Licensed Content Title	Enhanced Catalytic Activity of Self-Assembled-Monolayer-Capped Gold Nanoparticles
Licensed Content Author	Tomoya Taguchi,Katsuhiro Isozaki,Kazushi Miki
Licensed Content Date	Sep 12, 2012
Licensed Content Pages	6
Type of use	Dissertation/Thesis
Requestor type	University/Academic
Format	Print and electronic
Portion	Figure/table
Number of figures/tables	1
Original Wiley figure/table number(s)	Figure 1a
Will you be translating?	No
Title of your thesis / dissertation	Advanced Organic Ligands for Protecting Metal Nanoparticles
Expected completion date	Aug 2015
Expected size (number of pages)	90
Requestor Location	University of Windsor 401 Sunset Avenue Windsor, ON N9B 3P4 Canada Attn: Jonathan Yu
Billing Type	Invoice
Billing address	University of Windsor

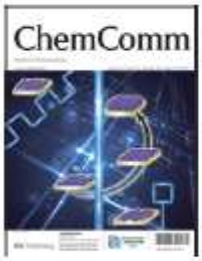

Title: A novel approach to fingerprint visualization on paper using nanotechnology: reversing the appearance by tailoring the gold nanoparticles' capping ligands

Author: Sanaa Shenawi,Nimer Jaber,Joseph Almog,Daniel Mandler

Publication: Chemical Communications (Cambridge)

Publisher: Royal Society of Chemistry

Date: Mar 18, 2013

Order Completed

Thank you very much for your order.

This is a License Agreement between University of Windsor -- Jonathan Yu ("You") and Royal Society of Chemistry. The license consists of your order details, the terms and conditions provided by Royal Society of Chemistry, and the payment terms and conditions.

Get the printable license.

License Number	3683220964827
License date	Aug 06, 2015
Licensed content publisher	Royal Society of Chemistry
Licensed content publication	Chemical Communications (Cambridge)
Licensed content title	A novel approach to fingerprint visualization on paper using nanotechnology: reversing the appearance by tailoring the gold nanoparticles' capping ligands
Licensed content author	Sanaa Shenawi,Nimer Jaber,Joseph Almog,Daniel Mandler
Licensed content date	Mar 18, 2013
Volume number	49
Issue number	35
Type of Use	Thesis/Dissertation
Requestor type	non-commercial (non-profit)
Portion	figures/tables/images
Number of figures/tables/images	1
Distribution quantity	100
Format	print and electronic
Will you be translating?	no
Order reference number	None
Title of the thesis/dissertation	Advanced Organic Ligands for Protecting Metal Nanoparticles
Expected completion date	Aug 2015
Estimated size	90
Total	0.00 CAD

ORDER MORE... CLOSE WINDOW

Title: N-Heterocyclic carbene coated metal nanoparticles

Author: Eleanor C. Hurst,Karen Wilson,Ian J. S. Fairlamb,Victor Chechik

Publication: New Journal of Chemistry

Publisher: Royal Society of Chemistry

Date: Jul 30, 2009

Order Completed

Thank you very much for your order.

This is a License Agreement between University of Windsor -- Jonathan Yu ("You") and Royal Society of Chemistry. The license consists of your order details, the terms and conditions provided by Royal Society of Chemistry, and the payment terms and conditions.

Get the printable license.

License Number	3683221356544
License date	Aug 06, 2015
Licensed content publisher	Royal Society of Chemistry
Licensed content publication	New Journal of Chemistry
Licensed content title	N-Heterocyclic carbene coated metal nanoparticles
Licensed content author	Eleanor C. Hurst,Karen Wilson,Ian J. S. Fairlamb,Victor Chechik
Licensed content date	Jul 30, 2009
Volume number	33
Issue number	9
Type of Use	Thesis/Dissertation
Requestor type	non-commercial (non-profit)
Portion	figures/tables/images
Number of figures/tables/images	1
Distribution quantity	100
Format	print and electronic
Will you be translating?	no
Order reference number	None
Title of the thesis/dissertation	Advanced Organic Ligands for Protecting Metal Nanoparticles
Expected completion date	Aug 2015
Estimated size	90
Total	0.00 CAD

ORDER MORE... CLOSE WINDOW

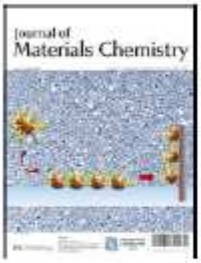

Title: Structural control of the monolayer stability of water-soluble gold nanoparticles

Author: Sarit S. Agasti,Chang-Cheng You,Palaniappan Arumugam,Vincent M. Rotello

Publication: Journal of Materials Chemistry

Publisher: Royal Society of Chemistry

Date: Oct 15, 2007

Order Completed

Thank you very much for your order.

This is a License Agreement between University of Windsor -- Jonathan Yu ("You") and Royal Society of Chemistry. The license consists of your order details, the terms and conditions provided by Royal Society of Chemistry, and the payment terms and conditions.

Get the printable license.

License Number	3683240800706
License date	Aug 06, 2015
Licensed content publisher	Royal Society of Chemistry
Licensed content publication	Journal of Materials Chemistry
Licensed content title	Structural control of the monolayer stability of water-soluble gold nanoparticles
Licensed content author	Sarit S. Agasti,Chang-Cheng You,Palaniappan Arumugam,Vincent M. Rotello
Licensed content date	Oct 15, 2007
Volume number	18
Issue number	1
Type of Use	Thesis/Dissertation
Requestor type	non-commercial (non-profit)
Portion	figures/tables/images
Number of figures/tables/images	1
Distribution quantity	100
Format	print and electronic
Will you be translating?	no
Order reference number	None
Title of the thesis/dissertation	Advanced Organic Ligands for Protecting Metal Nanoparticles
Expected completion date	Aug 2015
Estimated size	90
Total	0.00 CAD

ORDER MORE... CLOSE WINDOW

VITA AUCTORIS

NAME:	Jonathan Ka-Wing Yu
PLACE OF BIRTH:	Windsor, ON
YEAR OF BIRTH:	1991
EDUCATION:	University of Windsor, B.Sc. Honours Chemistry with Thesis, Windsor, ON, 2013
	University of Windsor, M.Sc. in Chemistry and Biochemistry, Windsor, ON, 2015